1-1-1997

Polymer surface modification : chemical surface modification, layer-by-layer adsorption, and surface reconstruction.

Wei, Chen
University of Massachusetts Amherst

POLYMER SURFACE MODIFICATION: CHEMICAL SURFACE MODIFICATION, LAYER-BY-LAYER ADSORPTION, AND SURFACE RECONSTRUCTION

A Dissertation Presented

by

WEI CHEN

Submitted to the Graduate School of the
University of Massachusetts Amherst in partial fulfillment
of the requirements for the degree of

DOCTOR OF PHILOSOPHY

September 1997

Polymer Science and Engineering

POLYMER SURFACE MODIFICATION: CHEMICAL SURFACE MODIFICATION, LAYER-BY-LAYER ADSORPTION, AND SURFACE RECONSTRUCTION

A Dissertation Presented

by

WEI CHEN

Approved as to style and content by:

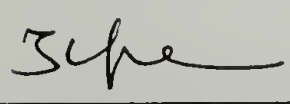

Thomas J. McCarthy, Chair

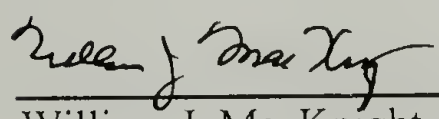

William J. MacKnight, Member

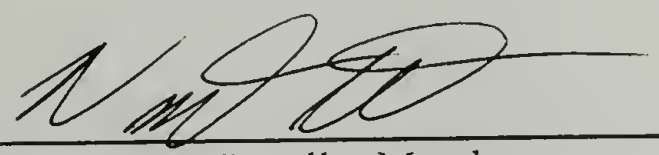

Vincent M. Rotello, Member

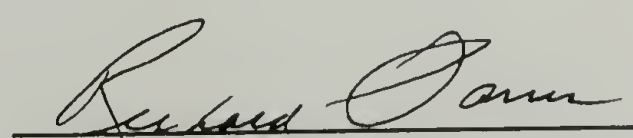

Richard J. Farris, Department Head
Polymer Science and Engineering

To my grandmothers and my parents

ACKNOWLEDGMENTS

There are many people who made my graduate school experience very enjoyable and memorable. My advisor, professor Thomas J. McCarthy, deserves special mention. He is a good teacher, not only in science, but also in life. I am grateful for his knowledge, intelligence, unique personality, and for giving me the freedom to do what I was most interested in. Having him as my Ph.D. advisor was one of the best decisions I ever made. Professors MacKnight and Rotello deserve my gratitude, as well, for the advice and time that they have given me in the last year.

I would like to thank the past and current McCarthy group members for their friendship both in and outside the lab. I want to thank all of them, especially Vipavee, Padma, Juha, Raul, Tak, Bob, Jim, Gene, Meng, Heather, Rick and Jack.

Most of all, I want to thank my husband, BaoBao, for being so caring, patient and supportive both emotionally and technically all through my four years in graduate school.

Finally, I want to thank my grandmothers and my parents for their unconditional love and support on the other side of the earth. I appreciate very much the sacrifice that they have made by letting me go to another country to pursue my education when I was at a young age. I thank my sister, Wen, for all the fun we had together.

ABSTRACT

POLYMER SURFACE MODIFICATION: CHEMICAL SURFACE MODIFICATION, LAYER-BY-LAYER ADSORPTION, AND SURFACE RECONSTRUCTION

SEPTEMBER 1997

WEI CHEN, B.A., SMITH COLLEGE

M.S., YALE UNIVERSITY

Ph.D., UNIVERSITY OF MASSACHUSETTS AMHERST

Directed by: Professor Thomas J. McCarthy

The three projects, chemical modification (Chapter 1), layer-by-layer deposition (Chapter 2), and surface reconstruction (Chapter 3),.that constitute this Ph.D. thesis are closely related in their overall objectives: using polymer surface modification to manipulate microscopic surface structures and control macroscopic properties.

Alcohol functionality can be introduced to the surface of poly(ethylene terephthalate) (PET) using either reduction or glycolysis; both of which cleave the PET chain. Both of these modified surfaces (PET-OH^R and PET-OH^G) and hydrolyzed PET (PET-OH/COOH) can be prepared using conditions that optimize surface functional group concentration, but minimize sample degradation. The surface alcohol density is higher on PET-OH^G than on PET-OH^R by a factor of ~2. The concentration of alcohols on reduced surfaces is increased by solvent annealing of the PET film prior to reduction. Reactivities of PET-OH^R and PET-OH^G samples were assessed and compared.

Layer-by-layer deposition of polyelectrolytes (poly(allylamine hydrochloride) and poly(sodium styrenesulfonate)) has been used to build up multilayer films on three organic polymer substrates: PET, PET-CO_2^- and PET-NH_3^+. XPS and contact angle data indicate that the layers are stratified and the wettability of the multilayer

assemblies is largely controlled by the identity of the outermost polyelectrolyte layer. The layer thickness and the stoichiometry of the deposition process (ammonium ion:sulfonate ion ratio) are affected by the substrate surface chemistry and can be controlled by adjusting the ionic strength of the polyelectrolyte solutions. Peel tests indicate that the multilayer assemblies show good mechanical integrity.

A perfluorohexylated-C_{60} (fullerene) was prepared and its surface activity and mobility were studied as a function of bulk concentration, annealing temperature, and annealing time in a polymer matrix (polystyrene). Perfluorohexylated-C_{60} is extremely surface-active in the polystyrene matrix and occupies 95% - 85% of the outermost 10 Å - 40 Å (XPS results), and renders a surface that is similar to a monolayer containing -CF_3 groups (hexadecane contact angle data). Surface reconstruction studies were carried out via either spin-casting or transferring a free standing polystyrene film over the composite materials (the surface-active agent and polystyrene). Both approaches show similar behavior of migration of perfluorohexylated-C_{60} from the bulk to the surface.

TABLE OF CONTENTS

LIST OF TABLES

LIST OF FIGURES

LIST OF SCHEMES

CHAPTER 1

CHEMICAL SURFACE MODIFICATION OF POLY(ETHYLENE TEREPHTHALATE)

Introduction

Reactions at polymer surfaces and interfaces are central to many polymer materials applications.[1,2] Many methods, such as corona discharge treatment, plasma modification and surface graft polymerization, have been successfully applied as surface modification methods for a variety of polymers.[3] They work to control the technologically significant properties of adhesion, wettability, biocompatibility and gas permeability. These surface modification methods, however, cannot be well controlled and usually result in topographically and chemically heterogeneous surfaces. We (McCarthy's research group) have been developing synthetic routes to chemically modified polymer surfaces with the objective of preparing substrates with controllable surface chemical structures and topographies so that we can control macroscopic surface properties and relate them to surface chemical structures.

We have focused on chemically resistant polymer film samples as substrates and have devised methods to introduce versatile organic functional groups at their surfaces. The surface-functionalized film samples could thus be converted to a range of samples having the same inert bulk but different surface-chemical structures. We have focused primarily on fluoropolymers, such as poly(tetrafluoroethylene) (PTFE),[4] poly(tetrafluoroethylene-co-hexafluoropropylene) (FEP),[5-7] poly(chlorotrifluoroethylene) (PCTFE),[7-14] poly(vinylidene fluoride) (PVF_2),[7, 15, 16] and non-fluorinated chemically resistant polymers, such as PEEK.[17] The advantages of these materials as model substrates have been discussed in the referred papers. More recently, we have turned our attention to the surface modification of less chemically resistant (more

reactive) polymers and studied chemical surface modification of poly(ethylene terephthalate) (PET).

In some senses it is more straight-forward to modify a reactive polymer than a chemically resistant one: the ester moiety in PET clearly suggests more chemical strategies than do the perfluoroalkane chains in PTFE. There are, however, equally challenging issues to address in preparing modified substrates that are suitable for further chemical modification; we point out five of these issues as they apply to PET: (1) Modification of PET through ester reactivity involves chain cleavage that leads to surface functionality at new chain ends, but also causes the degradation of the polymer sample. Reaction conditions have to be tuned to optimize functional group concentration and minimize degradation. (2) The sequence of ester cleavage reactions on PET can determine the relative concentration of surface functionality. In the hydrolysis of PET (Scheme 1.1), for example, the first reaction yields one alcohol and one carboxylic acid. If the modification reaction involves only initial chain cleavage, then the surface will contain an equal concentration of alcohols and carboxylic acids. If, however, the reaction proceeds near the initial hydrolysis sites, the relative surface functional group concentrations will depend on the relative rates of different hydrolyses. The second reaction near an initial hydrolysis site can yield (Scheme 1.1) two carboxylic acids (2a), two alcohols (2b), or one alcohol and one acid (2c). (3) The surface functional group density will depend on the

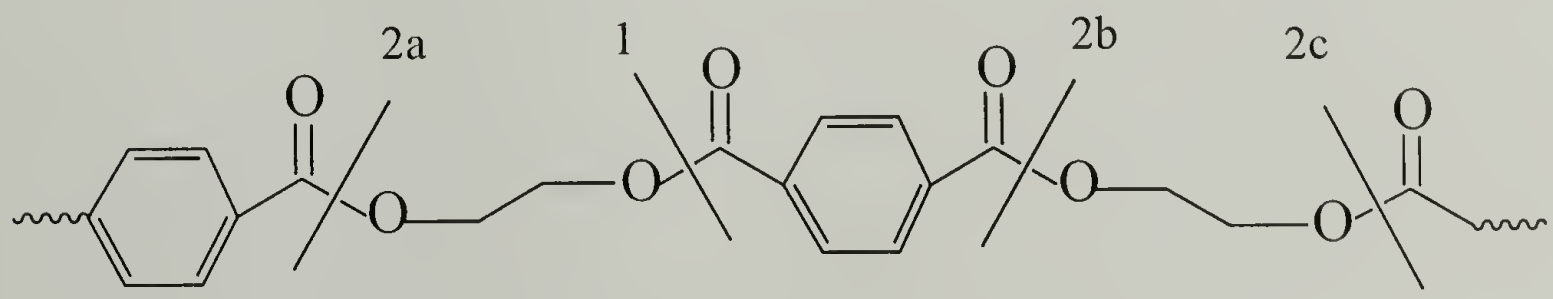

Scheme 1.1. Sequential hydrolytic cleavage sites on PET.

morphology of the polymer near the surface, and, in particular, on the orientation of chains relative to the plane of the surface. This is described pictorially (using the reduction of PET to alcohols as an example) in Scheme 1.2: If chains are oriented more perpendicular to the plane of the surface, then surface functional group density will be higher than if chains are oriented more parallel. If the chain orientation varies with depth, surface functional group composition will change with extent of reaction due to the change in chain orientation. (4) The surface-functionalized PET samples prepared by initial modification reactions will still contain reactive ester functionality. Conditions for subsequent functional group transformations have to be selective against ester chemistry. (5) Surface functional groups on PET may react differently because of structural differences. For example,

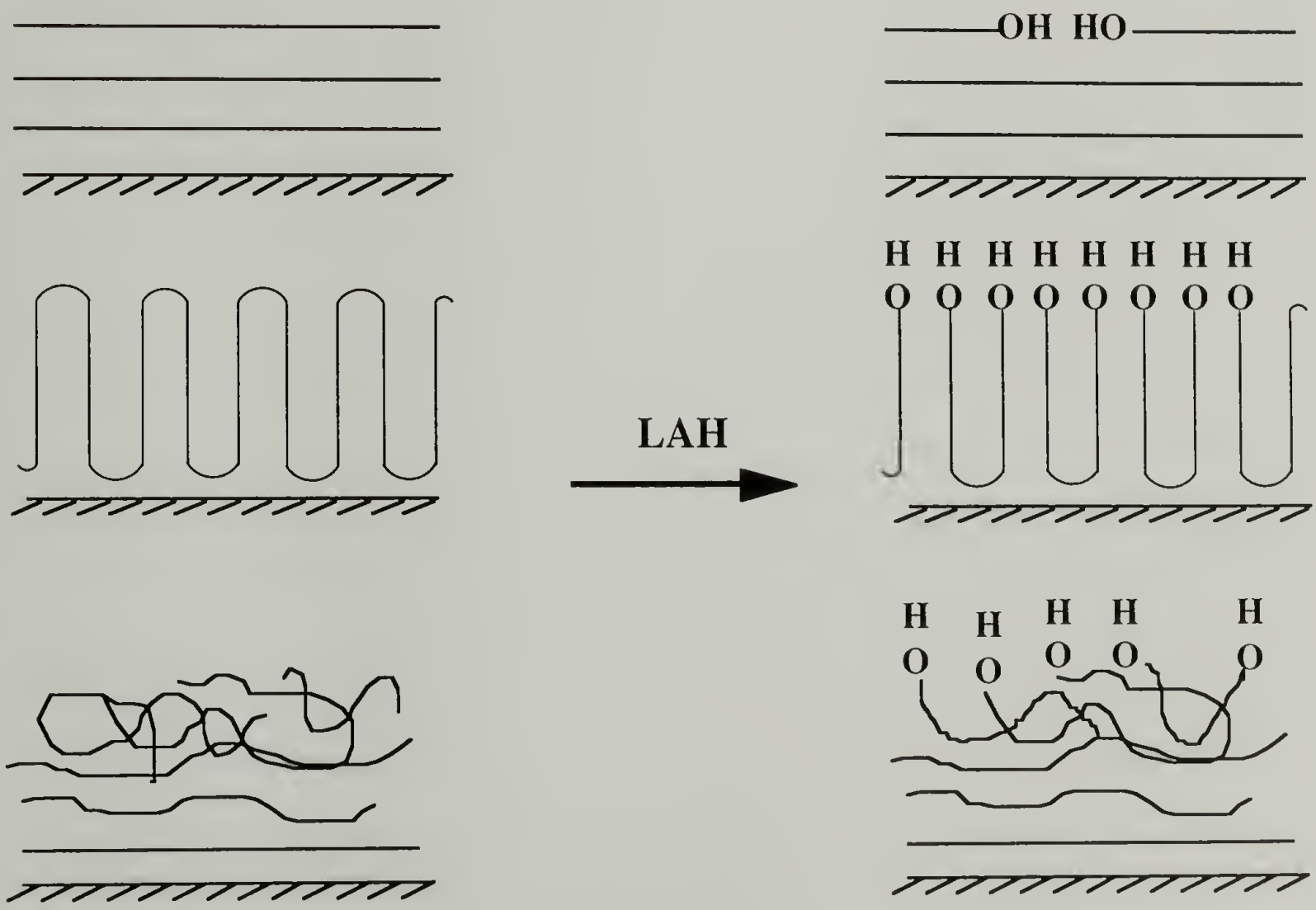

Scheme 1.2. Conformations of PET surface chains.

an alcohol-containing PET surface prepared by reduction will contain both hydroxyethyl groups and benzylic alcohols as reactive species and these may react at different rates or yield different products with some reagents.

These issues were the focus of this study. Our initial objectives were to prepare and study the reactivities of alcohol-functionalized PET surfaces prepared by three routes (reduction, transesterification with ethylene glycol - glycolysis, and hydrolysis followed by selective reduction of the carboxylic acid), acid-functionalized surfaces prepared by hydrolysis followed by reaction with succinic anhydride and mixed surfaces prepared by hydrolysis. We were not very successful in preparing a surface containing only carboxylic acids or in selectively reducing acids on the polyester surface. The control of functionality and degradation with hydrolysis conditions and the preparation and reactivity of alcohol-functionalized PET surfaces prepared by two different routes (reduction with lithium aluminum hydride and transesterification with ethylene glycol) are discussed here.

Polymer Surface Analytical Techniques

Samples of PET and its derivatives were characterized by x-ray photoelectron spectroscopy (XPS), contact angle measurements, and attenuated total reflectance infrared (ATR IR). Among the three techniques, ATR IR is the least surface-sensitive and assesses functionality at depths on the order of microns. ATR IR spectra did not reveal any changes in the films. This indicates that all the modification reactions on PET occurred within the outer couple of hundred angstroms. Due to the lack of utility of ATR IR, we decided not to include it in the following discussion.

X-ray Photoelectron Spectroscopy (XPS)

XPS, also referred to as Electron Spectroscopy for Chemical Analysis (ESCA), is one of the most powerful techniques for polymer surface analysis. It provides not only

atomic composition but also qualitative information concerning the functional groups of the outermost 10 - 100 Å.[18] The physical basis for the analysis is the photoelectric effect, where a beam of monoenergetic soft x-rays (most commonly Al K_α or Mg K_α) is focused on the sample, ejecting core shell electrons. The detector analyzes the kinetic energy, E_k, of the ejected electrons. The binding energy, E_b, of the electron in an atomic orbital of the source element can then be calculated using eq. 1.1, where hν is the energy

$$E_b = h\nu - E_k - \phi \qquad (1.1)$$

of the x-ray photons and ϕ is the work function of the spectrometer. The number of electrons emitted are then counted as a function of their energy. Each element has a unique set of core electrons and hence a unique spectrum. Atomic composition is calculated from peak areas and atomic sensitivity factors obtained from samples with known composition. The energy states of the core electrons are also influenced by the valence states, so qualitative information concerning the functional groups at the surface can also be provided.

The surface sensitivity of XPS is due to the finite escape depth of the ejected core electrons even though the x-ray beam passes deep into the sample. Equation 1.2 relates the number of electrons detected (N) to the number of electrons ejected (No) at sampling depth t as where λ is the electron mean free path and θ is the angle to the detector from

$$N = N_0 e^{-(\frac{t}{\lambda \sin\theta})} \qquad (1.2)$$

the plane of the sample surface.[19] This exponential relationship indicates that the functional groups in the outermost surface layer are more heavily weighed in the XPS data. Values for λ in organic polymers are somewhat controversial ranging from the low

values reported by Clark[18,20] to higher values reported by others.[21,22] Ashley and coworkers have developed a theoretical approach to the problem[23-26] and calculate mean free paths based on the kinetic energy of the electron, bulk density, and molecular structure. For XPS analysis of film samples carried out for this dissertation, both Mg K_α and Al K_α anodes were used and 14 Å[18] was used as mean free path for C_{1s} electrons unless otherwise specified.

According to eq. (1.2), variable take-off angle (the angle between the sample surface and the detector) XPS data should yield a depth profile near the surface . Scheme 1.3 depicts the sample/detector geometry. At smaller take-off angles, electrons have to travel through a greater distance in the solid before they can reach the detector so only those ejected from the outermost surface are analyzed. Therefore, XPS data at smaller take-off angles are more surface-selective. All samples in this dissertation were analyzed at 15° and 75° take-off angles. Eq. (1.2) indicates that 95% of detected photoelectrons originate in the outermost $3\lambda\sin\theta$. If we use λ = 14 Å, 15° and 75° take-off angles assay the outer ~ 10 Å and ~ 40 Å, respectively. About 54 % of the photoelectrons measured at 75° originate in the top 10 Å.

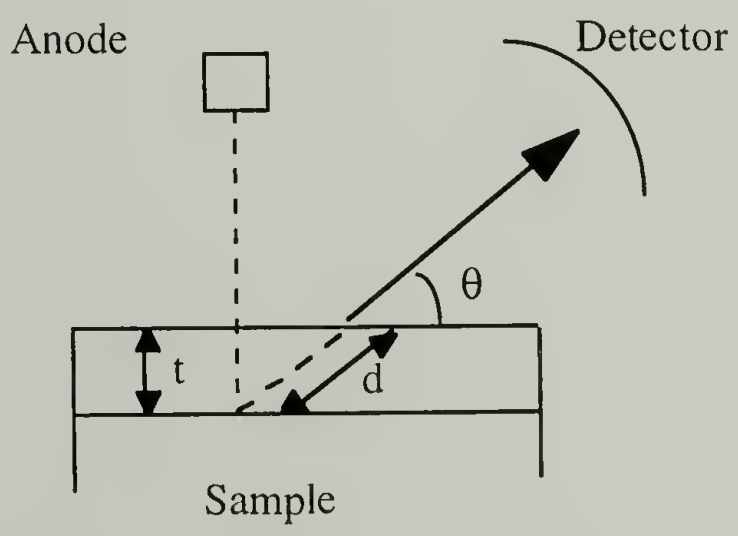

Scheme 1.3. Sample/detector geometry in variable angle XPS.

Contact Angle Analysis

Contact angle is the most surface-sensitive technique used in this research and probes the outermost few angstroms near the surface. The surface tension of a material can be determined using contact angle measurements. Young's equation[27] describes the

$$\gamma^{SV} - \gamma^{SL} = \gamma^{LV} \cos\theta \qquad (1.3)$$

angle (θ) formed by the probe fluid on the material as a result of the balance of the three surface tensions, γ^{SV} of the solid-vapor interface, γ^{SL} of the solid-liquid interface, and γ^{LV} of the liquid-vapor interface, as shown in Scheme 1.4. Both water and hexadecane were used as probe fluids. We measured both advancing contact angles (θ_A) and receding contact angles (θ_R) as probe fluid was added to or withdrawn from the drop.

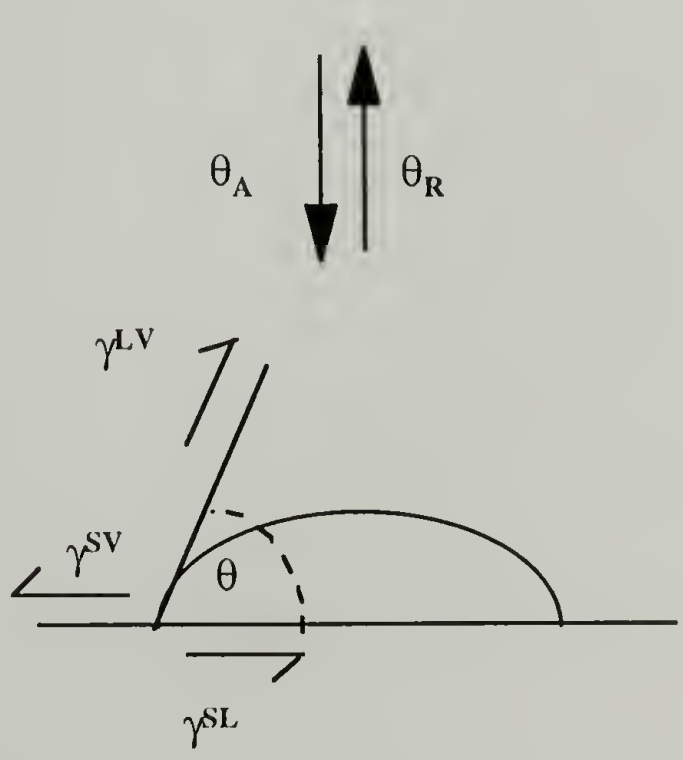

Scheme 1.4. Dynamic contact angle measurement.

With a surface that is smooth, immobile, nondeforming, chemically homogeneous, and does not interact with the probe fluid, advancing contact angle and receding contact angle should have equal values.[28] In reality, however, they always differ due to the violation of one or more of the above criteria. The difference between θ_A and θ_R is termed hysteresis.

PET and Approaches to PET Surface Modification

Physical Properties of PET

PET films used for this study were DuPont Mylar with a thickness of 5 mil. $CaSiO_3$ is added to the film as an antiblocking agent. The films are biaxially orientated during processing, and as a result, PET film has a uniplanar structure: the molecular chain segments are oriented nearly randomly about an axis normal to the film plane. The crystallinity obtained from density measurements is about 40 - 45 % ($d = 1.333$ g/cm^3 for amorphous region and $d = 1.455$ g/cm^3 for crystalline region). It has a glass transition temperature of about 69 °C (thermal analysis method) to 115 °C (dynamic mechanical testing methods) and a high crystalline melting temperature of 265 °C. It has good mechanical strength, toughness, and fatigue resistance at elevated temperatures.[29] That it can be (and is being) recycled is an advantage.[30-32] PET is an economically important thermoplastic that is used as photographic film, magnetic recording tape, packaging material and electronic insulation.[29] Its intrinsic low surface energy, however, results in poor adhesion, wettability, and biocompatibility - it is an ideal candidate for surface modification.

Poly(ethylene terephthalate) recycled from soft-drink bottles is depolymerized by glycolysis in excess ethylene glycol (EG) at 190 °C in the presence of a metal acetate.[30] Of the four metal acetates (lead, zinc, cobalt, and manganese) studied, zinc acetate gave the highest extent of depolymerization, i.e. the relative amount of monomer formed. The

glycolyzed products consist mostly of bis(hydroxyethyl) terephthalate and its dimer. After long reaction time (> 8 h), no higher oligomers were detected.

Glycolysis of PET in EG at high temperature under pressure without catalyst has also been investigated.[31] It was found that the rate of depolymerization goes up as temperature, pressure, and concentration ratio of EG to PET increase.

Approaches to PET Surface Modification

PET has been surface modified by a variety of techniques including plasma,[33] corona discharge,[34] ion beam,[35] laser treatment,[36] entrapment of poly(ethylene oxide),[37] swelling-assisted modification by methacrylic acid,[38] photoinitiated graft polymerization,[39] hydrolysis,[40-42] aminolysis,[43-45] reduction,[44,46] and carboxylation.[47] Of the different approaches to surface modification, only flame treatment, corona discharge treatment, plasma modification and surface graft polymerization are practical techniques.[3] They have the advantage that they work to control the technologically significant properties of adhesion, wettability, biocompatibility and gas permeability, but the disadvantage that chemically well-defined surfaces cannot be designed and prepared. The chemical surface modifications of PET, however, aim to introduce discrete surface functional groups such as -COOH, -OH, and $-NH_2$ to increase PET surface tension for various applications.

Hydrolysis. Most often, hydrolysis of PET fiber/film is carried out in alkaline solution (usually NaOH aqueous solution) to produce both -COOH and -OH groups on the surface.[40-42] The reaction appears to be autocatalytic: in the early stage of reaction, attack of OH^- ions occurs randomly on the polymer chains. Further attack of OH^- ions occurs mostly on already cleaved chains. Therefore, in the later stages, reaction is primarily of the "unzipping" type. The observed steep rise in mass loss with further increases in concentration of alkali (> 1M) and temperature (> 70 °C) is due to the

increased frequency of the hydrolytic attack and enhanced dissolution of polymer chains with increasing severity of the treatment. The relative effectiveness of the reaction parameters is in the order of: treatment time < alkaline concentration < treatment temperature.[40]

Scanning electron micrographs of the treated samples show that the surfaces become rougher as reaction conditions (longer reaction time, higher reaction temperature, higher reagent concentration) becomes more severe.[40,41]

Contact angle, a measure of hydrophilicity, shows significant improvement (lowering) after hydrolysis. More severe reaction conditions did not result in lower contact angle.[41]

In an attempt to quantify the number of -COOH groups on the hydrolyzed surface, neutron activation analysis (NAA) was used to measure the amount of cesium - tagged carboxylated groups on CsOH-treated woven PET fabric and absorption spectrophotometry measured the affinity of negatively charged carboxylate groups on the surface for methylene blue, a cationic dye. The cesium method and the dye method yielded $0.8 \sim 1.0 \times 10^{14}$ and $1.9 \sim 2.4 \times 10^{14}$ COO^-/cm^2, respectively.[42]

Aminolysis. Reaction of an amine with an ester group of PET leads to chain scission at the reaction site, and to amide and alcohol formation.[43-45]

In contrast to PET hydrolysis which is confined to the fiber surface, amines are reported to diffuse into PET fibers leading to reaction throughout the fibers. In order to limit the reaction to the surface, high molecular weight multifunctional amines were used to decrease their diffusion into the bulk and reduce the amount of scission needed to achieve the desired amine concentration on the surface.[43]

The reactions of PET with multifunctional amines, diethylenetriamine (DETA), triethylenetetramine (TETTA), and tetraethylenepentamine (TTEPA), revealed that

amination could be confined to the periphery (~ 4 μm) and was found to be uniform on the fiber surface after aminated fibers were stained with an acid dye at low pH.[43]

The rate of the reactions, as revealed by acid dye staining, was in the order of DETA > TETTA > TTEPA. The extent of the incorporation of amine groups was found to be similar for the three amines studied and resulted in amine density of ~ 1.8×10^{-8} mol/cm^2.[43]

Incorporation of a hydrophilic amine at the PET surface resulted in a significant improvement in water wettability. Most of the change in wettability was achieved early on in the reaction, and the wettability of the treated PET did not change much at longer reaction times.[43]

Another study showed that amination of PET with 3-aminopropyltriethoxysilane (APTES) resulted in a 100 % surface coverage of APTES on the surface according to XPS data. It was proposed that the initial reaction occurs via nucleophilic attack on the ester linkage of PET by the amino group. However, unlike other aminolysis reactions, no degradation was observed on prolonged exposure to pure APTES. It is believed that the alkoxide group generated after the initial reaction can react with the silyl end of the same or another APTES in the vicinity. The reacted APTES would then cross-link with other APTES molecules to form a film on the surface. Films modified by this method have been shown to be stable in most chemical environments.[44]

Bergbreiter et. al.[45] showed that the use of lithiated α,ω-diaminopoly(alkene oxide) oligomers as reagents for modification of polyesters via aminolysis is a viable method to surface modify these polymers and to incorporate reactive amino groups. Metalation significantly activates these amino-group containing oligomers under the reaction condition (60 °C, mixed THF-heptane solvent). Contact angle measurements indicated that the modified surface have greatly enhanced hydrophilicity. The predominant species present, based on XPS and ATR IR results, were α,ω-diaminopoly(alkene oxide) oligomers attached via a single amide bond.

Reduction. The ester moiety of PET can be reduced and cleaved to give two alcohol groups.[44,46] Reduction has been carried out almost exclusively using $LiAlH_4$ in ether solution. A significant decrease in hydrophobicity was observed for the reduced surface, with water contact angle decreased significantly. This is consistent with the fact that there is a increase in the number of polar functionalities on the surface after reduction. The percentages of carbonyl and ether carbons, however, did not differ significantly from the unmodified PET according to data obtained from the XPS C_{1s} region. It was thought to be because reduction is also a degradative process. Extensive degradation was observed when the reduction time was extended to longer times, indicating that the reduction may have only served to strip away the top layer of the PET surface, exposing a fresh layer of PET.[44]

Carboxylation. A sequence of reactions was designed to introduce -COOH to PET surface.[47] The procedure involves (1) hydrolysis with 0.25 M NaOH H_2O - CH_3CN (1/1; v/v) for 18 h at 60 °C; (2) oxidation with 5 % $KMnO_4$ in 1.2 N H_2SO_4 for 1 h at 60 °C; (3) activation by 0.1 % water soluble carbodiimide at pH 3.5 for 1 h at 23 °C; (4) coupling to amino acid (0.001 M) at pH 8.2 for 2 h at 23 °C. Radiochemical assays, in which ^3H-labeled lysine were used , gave the number of -COOH function groups present on the polymer surface. XPS analysis was also used to quantify the number of functional groups introduced to the surface. Values of about 30 - 50 pmol/cm^2 were found, corresponding to the functionalization of 1-2 % of PET repeat units. Weight loss was observed under these experimental conditions.

Experimental

Materials

PET film (duPont Mylar, 5 mil) was cleaned by rinsing with distilled water and methanol and then refluxing in hexane for 2 h. All materials were obtained from Aldrich unless otherwise specified. Tetrahydrofuran was distilled from sodium benzophenone dianion; pyridine and hexadecane were distilled from calcium hydride at reduced pressure; anhydrous ethylene glycol was further dried under vacuum (0.02 mm, room temp., > 1 h) after addition of ~1 % of benzene; distilled water was further purified by reverse osmosis (Milli-RO 6 plus, Millipore). Thionyl chloride was purified by distillation; heptafluorobutyryl chloride and acetyl chloride were purified by freeze-pump-thaw cycles and trap-to-trap distillation; stearoyl chloride was distilled at reduced pressure. Acetone (Fisher), 1 M borane in THF, 1,1'-carbonyldiimidazole, concentrated HCl (Fisher), dibutyltin dilaurate, 1,6-diisocyanatohexane, hexane (Fisher), 1M lithium aluminum hydride in THF, lithium diisopropylamide, methanol (Fisher), phenyl isocyanate, potassium *tert*-butoxide, Red-Al® (65+ wt. % solution of sodium bis(2-methoxyethoxy)aluminum hydride in toluene), sodium hydroxide (Fisher), succinic anhydride, *p*-toluenesulfonic acid, tolylene-2,4-diisocyanate, trichloroacetyl isocyanate, and zinc acetate were used as received. Air-sensitive materials were stored under dry nitrogen. All reactions except hydrolysis and those with HCl were carried out under dry nitrogen in Schlenk flasks; reagents were transferred via either cannulae or syringes; reactions with films were not stirred.

Methods

X-ray photoelectron spectra (XPS) were obtained with a Perkin-Elmer-Physical Electronics 5100 with AlK_{α} excitation (400 W, 15.0 kV). Spectra were taken at two different take-off angles, 15° and 75° from the plane of the surface to the entrance lens of

the detector optics. Contact angle measurements were made with a Ramè-Hart tclescopic goniometer and a Gilmont syringe with a 24-gauge flat-tipped needle. Probe fluids were Milli-Q water and hexadecane. Dynamic advancing (θ_A) and receding angles (θ_R) were recorded while the probe fluid was added to and withdrawn from the drop. The values reported are averages of five measurements made on different areas of the film sample surface. Attenuated total reflectance infrared (ATR IR) spectra were obtained under dry air by using an IBM 38 FTIR spectrometer and a germanium internal reflection element (45°). Scanning electron microscopy (SEM) was performed using a JEOL 100CX STEM. Gravimetric measurements were made with a Sartorius 1612MP-1 analytical balance.

Hydrolysis of PET (PET-OH/COOH)

A cleaned PET film sample (1 x 5 cm) was introduced to a flask containing 25 mL of 1 M NaOH that had been equilibrated to the desired temperature in a constant temperature bath for at least 1 h. After the desired reaction time, the film sample was removed with tweezers and rinsed sequentially with 0.1 M HCl, two aliquots of water, methanol, and hexane, and then dried at reduced pressure (0.02 mm, room temp., 24 h).

Acid catalyzed (HCl, zinc acetate, p-toluenesulfonic acid) hydrolysis was also carried out and will be discussed in the Results and Discussion section below.

Reduction of PET (PET-OH^R)

To a nitrogen-purged Schlenk tube containing a cleaned PET film sample (1 x 5 cm), 25 mL THF was added. After 4.5 h at room temperature, the solvent was removed and the film was dried (0.02 mm, room temp., 24 h). A THF solution (25 mL) of $LiAlH_4$ (at the desircd concentration) was added. After the desired reaction time at the desired reaction temperature, the film was washed sequentially with THF (two aliquots), water,

0.1 M HCl, water (two aliquots), methanol, and hexane, and then dried (0.02 mm, room temp, 24 h).

Glycolysis of PET (PET-OH^G)

To a nitrogen-purged Schlenk tube containing a cleaned PET film sample (1 x 5 cm), 25 mL of 0.60 M potassium *tert*-butoxide in ethylene glycol was introduced. After the desired reaction time at room temperature, the film was rinsed sequentially with ethylene glycol (two aliquots), water, 0.1 M HCl, water (two aliquots), methanol, and hexane, and then dried (0.02 mm, room temp., 24 h).

Labeling Reactions

-OH Group Labeling (PET-$OC(O)C_3F_7$). To a nitrogen-purged Schlenk tube containing the film (1 x 5 cm) under study, a solution of heptafluorobutyryl chloride (1.6 g, 6.7 mmol) in THF (25 mL) was added. After reaction for 2 h at room temperature, the film was removed, rinsed sequentially with THF (three aliquots), methanol and hexane, and then dried (0.02 mm, room temp., 24 h).

-COOH Group Labeling (PET-$C(O)C_3H_3N_2$). To a nitrogen-purged Schlenk tube with a film already labeled with heptafluorobutyryl chloride, a solution of 1,1'-carbonyldiimidazole (0.5 g, 3 mmol) in THF (25 mL) was introduced. After 4 h at room temperature, the film was rinsed sequentially with THF (four aliquots) and hexane, and dried (0.02 mm, room temp., 24 h).

Reactivities of PET-OHs

Reaction with Thionyl Chloride (PET-Cl/O_2SO). PET-OH film samples (1 x 5 cm) were allowed to react under nitrogen with thionyl chloride (1.6 g, 14 mmol) in THF (25 mL) at room temperature for 24 h. The film samples were rinsed with THF (four aliquots) and then dried (0.02 mm, room temp., 24 h).

Reaction with Acid Chlorides (Acetyl Chloride, Stearoyl Chloride) (PET-OC(O)R). To a nitrogen-purged Schlenk tube containing PET-OH film samples (1 x 5 cm), THF (25 mL) was added via cannula, and then the acid chloride (6-14 mmol) followed by 0.10 mL of pyridine were introduced via syringe. The reactions were allowed to proceed at room temperature for 24 h. The films were rinsed sequentially with THF (three aliquots), methanol, and hexane, and then dried (0.02 mm, room temp., 24 h).

Reaction with Isocyanates (Phenyl Isocyanate, Trichloroacetyl Isocyanate, 1,6-Diisocyanatohexane, Tolylene-2,4-Diisocyanate) (PET-OC(O)NHR-NCO/$(OC(O)NH)_2R$). PET-OH film samples (1 x 5 cm) were allowed to react under nitrogen with isocyanate (6-9 mmol) and 0.10 mL of dibutyltin dilaurate in THF (25 mL) at room temperature for 24 h. The film samples were rinsed sequentially with THF (three aliquots) and hexane, and then dried (0.02 mm, room temp., 24 h).

Attempted Reactions

Reaction of PET-OH with HC1 (PET-Cl). PET-OH film samples (1 x 5 cm) were reacted with conc. HC1 (25 mL) catalyzed by $ZnCl_2$ (2 g) at 45 °C for 24 h. The film samples were washed with water (x2), and then dried (0.02 mm, room temp., 24 h).

Reduction of Hydrolyzed PET (PET-OH^H). Hydrolyzed PET and control PET film samples (1 x 5 cm) were reacted with 25 mL of 0.1 M borane in THF at room temp. for up to 48 h under nitrogen. The samples were washed with THF (x2), water, 0.1 M HC1, water (x2), methanol, and hexane, and dried (0.02 mm, room temp., 24 h).

Preparation of PET-COOH. PET-OH film samples (1 x 5 cm) were reacted with lithium diisopropylamide (0.01 g, 0.09 mmol) in THF (25 mL) at room temperature for 15 min under nitrogen. All but ~1 mL of the solution was removed via cannula. A solution of succinic anhydride (0.25 g, 2.5 mmol) in THF (25 mL) was added via cannula and reacted with the film samples for up to 6 h at room temperature under nitrogen. A clean PET film sample was also reacted with lithium diisopropylamide (0.01 g, 0.09 mmol) in THF (25 mL) at room temperature for 5 h under nitrogen. All of the film samples were washed with THF (x2), water, 0.1 M HC1, water (x2), methanol, and hexane, and dried (0.02 mm, room temp., 24 h).

Results and Discussion

Commercial PET film samples were cut to appropriate size, cleaned with water, methanol, and then refluxing hexane and dried to constant mass. Tared samples lost ~0.18% mass over 24 h at reduced pressure and room temperature and no further mass loss was observed upon additional drying. After this procedure, PET surfaces exhibit advancing/receding contact angles (θ_A/θ_R) of 77°/55° and are free of impurities as assessed by both ATR IR and XPS analyses. SEM analysis indicates the presence of ~0.1 μm diameter filler particles spaced by ~0.5 μm that are present in the commercial samples as antiblocking agents. These are sub-surface since they are not detected by XPS and the surface roughness that they impart does not affect contact angle analysis. We have carried out a series of reactions on PET film samples, each of which involves exposing the film samples to reactive solutions in Schlenk tubes for various lengths of

time at controlled temperature; the reactions were not stirred. For each reported reaction, a number of experiments were performed to maximize conversion. In cases where careful kinetics are not reported, the conditions given represent those that gave the highest reproducible yields. The initial modification reactions were directed at the ester functionality to yield alcohol and alcohol/carboxylic acid functionalized surfaces (equations 1.4-1.6).

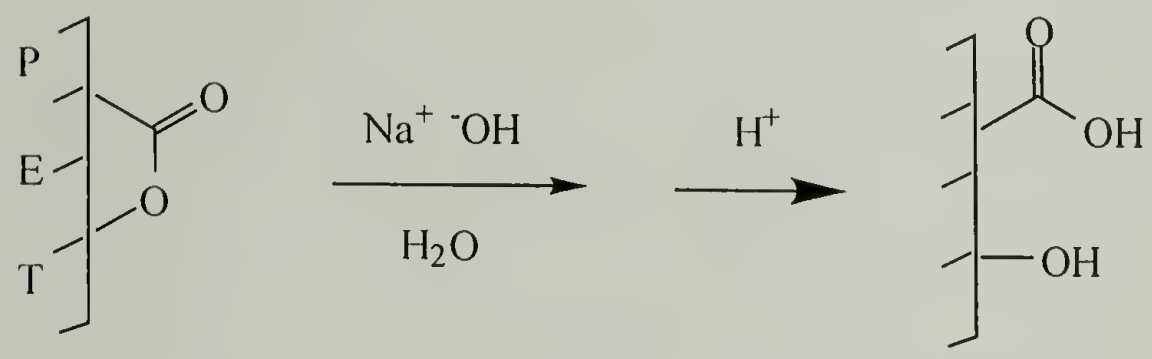

(1.4)

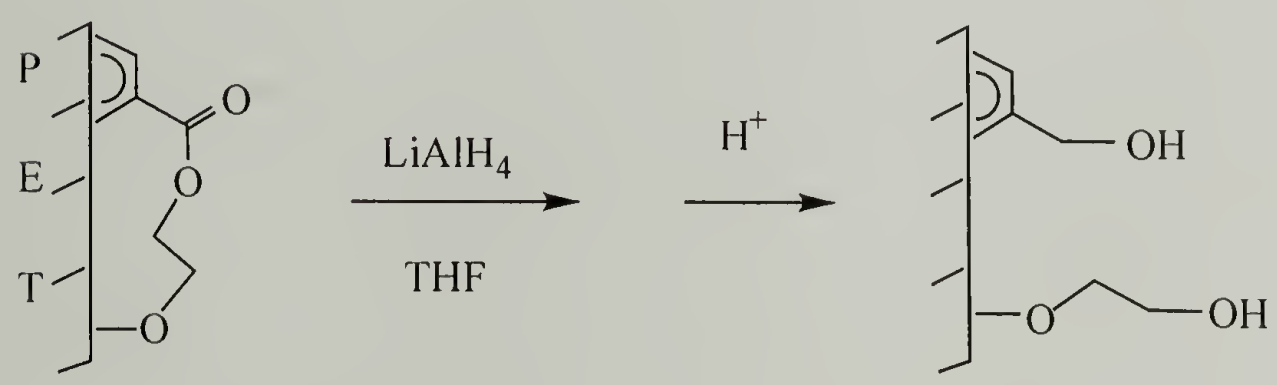

(1.5)

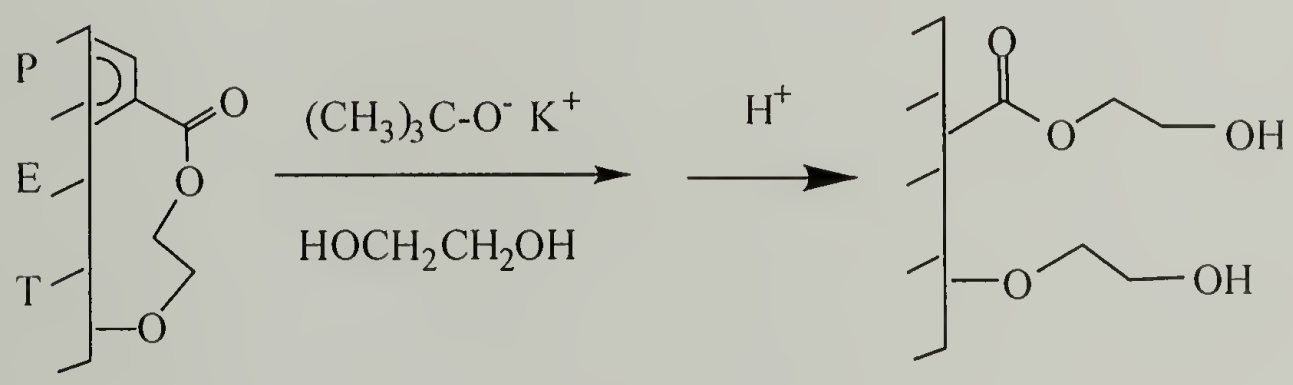

(1.6)

The surface concentration of functionality was assessed by XPS labeling reactions that are specific for alcohol and carboxylic acid groups. The reactivity of the alcohol functionality on different modified substrates was then assessed by converting PET-OH

film samples to a range of samples using reagents that do not react with PET in control experiments. The resulting samples thus have different surface-chemical structures, but identical interiors. Each of the reactions was monitored by contact angle, XPS, ATR IR, and gravimetric analysis.

Hydrolysis

A range of hydrolysis conditions was surveyed in preliminary experiments that were monitored by gravimetric analysis and contact angle. Acid-catalyzed hydrolysis conditions that were studied include 1 M HCl at elevated temperatures, $(CH_3CO_2)_2Zn$ at room temperature, and *p*-toluenesulfonic acid in water and acetone/water mixtures at elevated temperatures. The gravimetric analysis and contact angle data for the acid-catalyzed hydrolysis is given in Table 1.1. Base-catalyzed hydrolysis studies used sodium hydroxide in various concentrations (0.2 - 4 M) in water and water/methanol mixtures at various temperatures as shown in Table 1.2. The base-catalyzed reactions were clearly more effective than those catalyzed by acid and were chosen for further

Table 1.1. Acid catalyzed hydrolysis of PET.

Catalyst	Conc. (M)	Solvent	Temp. (°C)	Time (min)	Wt. gain (%)	θ_A (deg.)	θ_R (deg)
HCl	1	H_2O	73	16	-0.06	72	42.2
	1	H_2O	73	60	0.01	71.2	41.2
	1	H_2O	100	30	-0.14	72	38.8
$(CH_3CO_2)_2Zn$	0.0018	H_2O	25	1020	0	76.5	50
p-toluenesulfonic acid	0.0256	H_2O	100	60	-0.2	66.3	42.4
					-0.1	69.8	42.8
	0.179	H_2O	60	60	0	70.5	36.5
	0.0256	Acetone/H_2O 50:50	70	60	0.5	73.6	46.2

study. Wettability improved significantly with no measurable mass loss in base-catalyzed reactions, but this was not the case for acid-catalyzed reactions. One of our objectives (described above - Scheme 1.1) was to control the alcohol:carboxylic acid ratio and we suspected that acid versus base catalysis may be one method to do this. Acid catalysis was abandoned, however, due to the corrosive behavior of the reactions. It seems that the addition of methanol to base-catalyzed reactions significantly increases the rate of reactions, but does not improve wettability over aqueous sodium hydroxide solutions (Table 1.2).

Reaction kinetics for hydrolysis of PET in 1 M aqueous NaOH at 25 °C, 40 °C, 60 °C, 65 °C, and 70 °C were determined using both contact angle and gravimetric analysis of the film samples (Table 1.2). At each temperature, the water contact angles of the hydrolyzed surfaces decreased and reached constant values before any degradation was detectable by gravimetric analysis. Longer reaction times resulted in surfaces of identical wettability, but mass loss of the film samples became measurable (Table 1.2). These observations agree with previous findings.[40-42] The disappearance of filler particles from the surface was also observed by SEM at longer reaction times. Hydrolyzed film samples (PET-OH/-COOH) for further study were prepared at each temperature using a reaction time that gave leveled contact angles and no measurable mass loss. Reaction times of 4 h, 30 min, 16 min, 16 min, and 8 min were chosen for hydrolysis temperatures at 25 °C, 40 °C, 60 °C, 65 °C, and 70 °C, respectively. Water contact angles of each of these PET-OH/-COOH surfaces were indistinguishable (θ_A/θ_R = 62° ± 2°/16° ± 1°).

The rationale for choosing a range of hydrolysis temperatures was that the total surface functional group density and the ratio of -OH and -COOH groups may be a function of hydrolysis temperature. Different activation energies for cleavage at different sites (Scheme 1.1) would result in a temperature-dependent surface composition.

Table 1.2. Base (NaOH) catalyzed hydrolysis of PET.

Temp (°C)	Conc. (M)	Solvent	Time (min)	Wt. gain (%)	θ_A (deg)	θ_R (deg)
25	1	H_2O	120	0	64	16.2
			240	-0.006	63.5	16.8
			480	-0.04	63.5	16
			1530	-0.46	63.4	16.2
	1	H_2O/MeOH 50:50	8	0	60.9	17
			16	0	60.8	16.8
			24	-0.1	61.5	18
			32	-0.25	59.7	15
	0.2	MeOH	8	-0.01	65	35.4
			20	-0.03	64.4	34
40	1	H_2O	8	-0.05	70	25
			24	0	66.4	26
			30	0.006	63	16
			60	-0.06	62.6	15.4
			90	-0.17	63.7	17
			270	-0.34	63.4	17
60	1	H_2O	8	-0.05	59.2	16.5
			16	0.1	60	16
			24	0.06	60	20
			32	-0.09	61	22
	4	H_2O	5	-0.05	68.8	19.4
			8	-0.26	63.3	21
			12	-0.4	61.6	22
			16	-0.5	60.8	22
	4	MeOH	2.5	-8.3	69	23
			4.5	-14.1	64	18.6
			6.5	-22.8	65.6	23
			10	-31.1	65	17
65	1	H_2O	2	-0.02	64.2	20
			8	0.01	64.2	18.2
			16	-0.01	63.2	15.8
			60	-0.4	61.8	16
70	1	H_2O	2	0.03	64.8	18
			8	-0.02	65	18.8
			16	-0.1	60.4	16
			30	-0.2	58.3	15.4

Surface functional group densities were determined by an XPS labeling scheme that distinguishes between alcohols and carboxylic acids (equation 1.7). Heptafluorobutyryl chloride reacts selectively with alcohols in the presence of carboxylic acids and

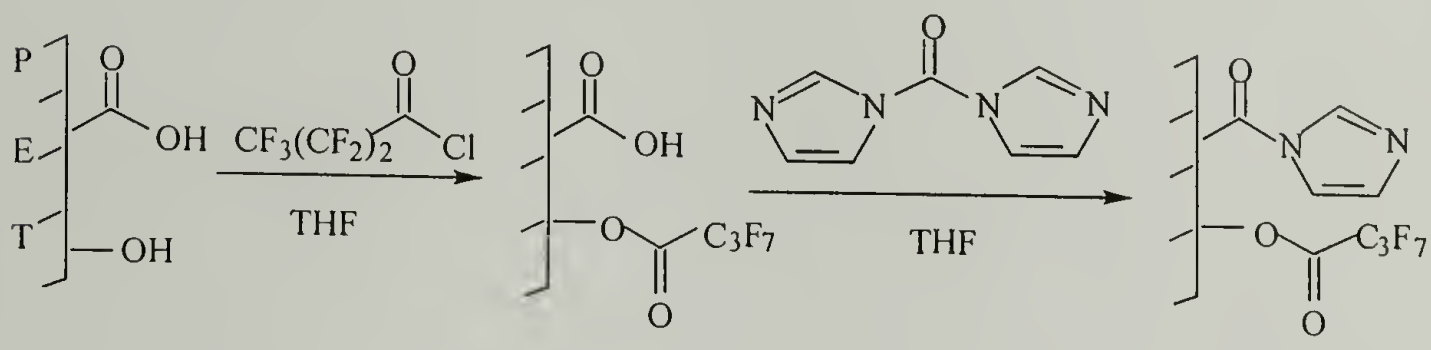

(1.7)

1,1'-carbonyldiimidazole reacts with carboxylic acids.[48] These reactions introduce fluorine and nitrogen that can be quantified by XPS to determine the relative number of alcohol and carboxylic acid functional groups as well as the total functional group density relative to PET repeat units in the XPS sampling depth. The atomic composition of the PET repeat unit is, $C_{10}O_4$ (XPS does not detect hydrogen); if n and m are the numbers of -OH and -COOH groups per PET repeat unit, respectively, the labeled surfaces have atomic compositions of $(C_{10}O_4)(C_4F_7O_2)_n(C_3N_2O)_m$. The values for n and m can be directly determined from the XPS data. The 15° take-off angle data (that assess the composition of the outermost ~10 Å of the samples[49]) indicate that the surfaces contain ~0.1 -OH groups per PET repeat unit and ~0.06 -COOH groups per repeat unit within the XPS sampling region. This data, along with the total surface functional group concentrations, is plotted versus hydrolysis temperature in Figure 1.1. The 75° take-off angle data, that assess the outer ~40 Å of the samples,[49] indicate ~0.06 -OH and ~0.04 -COOH groups per repeat unit. Both fluorine and nitrogen atomic composition data at both 15° and 75° take-off angles show no dependence on hydrolysis temperature. The take-off angle dependence indicates that the thickness of the modified layers (depth of the hydrolysis reactions) is less than 40 Å, and in particular that the functional group density

is higher in the outermost 10 Å than in the region beneath this. This is consistent with the gravimetric analysis and also the fact that no changes in ATR IR spectra are observed for these reactions. The lack of changes in the infrared spectra indicate a modification depth of less than 200 Å (we would expect to see changes if the depth were greater than this value because the sampling depth[50] under the conditions employed is ~0.2 - 0.5 μm for 3000 - 1500 cm^{-1}). These labeling reactions were the only chemistry of PET-OH/COOH studied in any detail.

The functional group concentrations determined by XPS can be used to estimate surface densities (functional groups/cm^2). There are 4.2 x 10^{14} PET repeat units/cm^2 in the outermost 10 Å of virgin PET (assuming a density of 1.375).

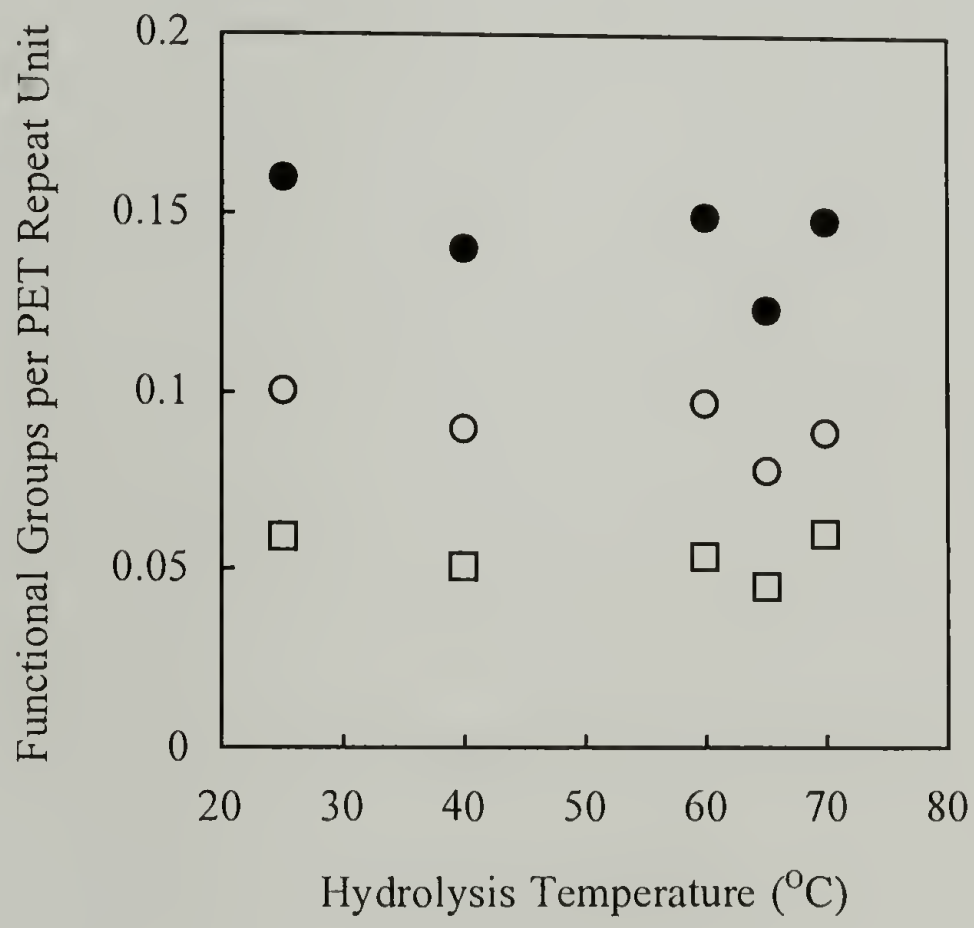

Figure 1.1. Number of functional groups per PET repeat unit as a function of hydrolysis temperature, determined from XPS analysis of labeled PET-OH/COOH surfaces: alcohols (○), carboxylic acids (□), total functional groups(●).

The ratios determined from the 15° take-off angle XPS data thus indicate that there are ~4 x 10^{13} alcohols/cm^2 and ~2.5 x 10^{13} carboxylic acids/cm^2. As mentioned earlier, a hydrolyzed PET film catalyzed by CsOH at 60 °C contains 0.8 ~ 1.0 x 10^{14} and 1.9 ~ 2.4 x 10^{14} COO^-/cm^2 from the cesium method and the dye method, respectively.[42] These numbers are slightly higher than that calculated from XPS data. The alcohol and carboxylic acid densities are only estimates and are calculated only for comparison with data described below. The alcohol:carboxylic acid ratio (4:2.5) is likely biased high, and should not be construed to indicate that hydrolysis at particular sites is favored: the perfluoroalkyl groups likely stratify above the acyl imidazolide groups to lower surface energy. We conclude that base-catalyzed hydrolysis consistently yields surface mixtures of alcohols and carboxylic acids and that the surface density and relative numbers of -OH and -COOH groups have no dependence on the hydrolysis temperature in the range studied.

Reduction

Initial experiments to screen conditions for reducing PET to an alcohol-containing surface (PET-OH^R) used lithium aluminum hydride and bis(2-methoxyethoxy)aluminum hydride in THF and toluene solutions; contact angle and XPS analysis of heptafluorobutyryl chloride - labeled samples were used to assess conversions. During the course of these studies we noted that if the PET samples were soaked in THF prior to exposure to the reducing agent, then the yield of surface alcohols was improved significantly; thermal annealing above the T_g of PET prior to reduction did not increase the number of alcohols introduced to the surface (Tables 1.3 and 1.4). We believe that the solvent anneals the surface and changes the average chain orientation to render the increased yields; this is described in Scheme 1.2 above and below to a further extent. The PET used for all of the experiments described below as substrates for reduction was solvent-annealed for 4.5 h in THF at room temperature prior to reaction.

Table 1.3. Effect of annealing (thermal and solvent) on the number of functional groups introduced to the PET surface using $LiAlH_4$ as the reducing agent.

	Reduction			Labeling with HFBC after reduction			
Conc. (M)	Wt. gain (%)	θ_A (deg)	θ_R (deg)	F (15°) (%)	F (75°) (%)	θ_A (deg)	θ_R (deg)
Without annealing							
0.074	-0.2	76.5	34	4.89	3.11	84	40.5
Annealing 0.5 h at 128°C							
0.074	-0.17	68.4	31.8	4.75	3.21	84.2	42
Annealing in THF for 4.5 hr at room temp.							
0.074	0.04	75.8	38.2	5.77	3.95	82	49.4

Table 1.4. Effect of annealing (thermal and solvent) on the number of functional groups introduced to PET surface using Red-Al as the reducing agent.

	Reduction				Labeling with HFBC after reduction			
Conc. (M)	Time (min)	Wt. gain (%)	θ_A (deg)	θ_R (deg)	F (15°) (%)	F (75°) (%)	θ_A (deg)	θ_R (deg)
Without annealing								
0.13	60	-1.8	72	32	4.18	2.73	79	41.5
Annealing in THF for 4.5 hr at room temp.								
0.03	30	-0.3	72	31.5	6.14	4.14	83.4	46.6

These conditions were chosen somewhat arbitrarily and a careful study was not made to optimize yield. Reduction using $LiAlH_4$ was chosen for further studies as they gave the most consistent results.

Three reaction parameters were studied to optimize the yield of surface alcohol functionality: reducing agent concentration, reaction time, and reaction temperature. These variables are not independent and they were optimized sequentially to maximize alcohol density on the modified surface. For the first parameter studied, $LiAlH_4$ concentration, the reaction time and temperature were kept constant, at 30 min and 25 °C. Water contact angles of the reduced surfaces are shown as a function of reducing agent concentration in Figure 1.2.

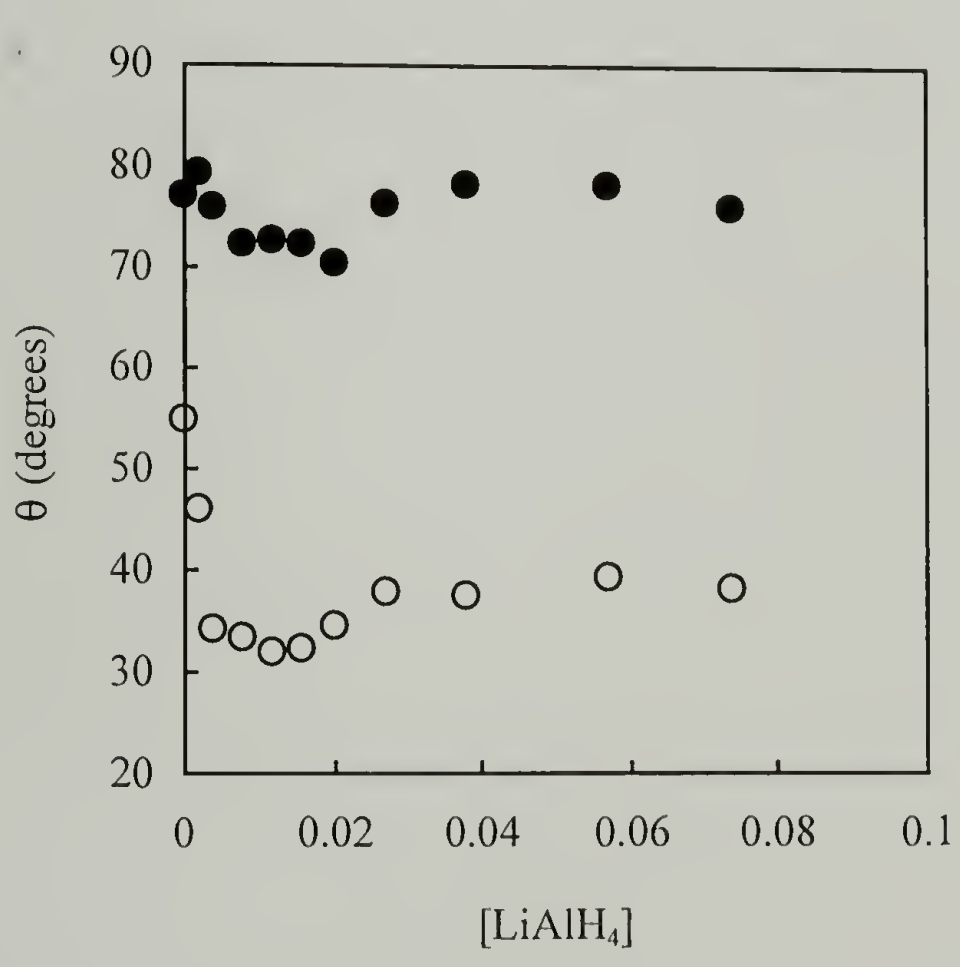

Figure 1.2. Water contact angle of PET-OH^R surfaces as a function of reducing agent ($LiAlH_4$) concentration: θ_A (●), θ_R (○).

The U-shaped curves observed in both the advancing and receding angle data were confusing, but reproducible. The initial increase in wettability with increasing reagent concentration to a maximum is expected for reaction at a solution-solid interface, but the subsequent drop in wettability upon further increase of the reducing agent concentration puzzled us for sometime. A plausible explanation follows: In virgin PET the chains tend to be parallel to the surface due to the processing conditions (biaxial orientation). With this initial chain conformation, small chain segments produced during reduction leave the surface and dissolve in the solution. This leads to surfaces with low alcohol density as was observed in PET samples that were reduced prior to annealing in THF (see Scheme 1.2). At the other extreme, if all the chains near the interface were perpendicular to the surface, a high alcohol density surface would result from reduction. We believe that the solvent annealing allows chains near the surface to relax and adopt a more random conformation, that is between these two extremes. Accordingly, reduction of solvent-annealed PET gives higher alcohol density than that of unannealed PET. The increase in contact angle observed with increasing reducing agent concentration can be ascribed to the removal of this randomized layer and exposure of parallel oriented chains. The same type of behavior (a maximum in alcohol concentration) is observed with the variables of temperature and reaction time (discussed below).

The reduced film samples were labeled with heptafluorobutyryl chloride and 1,1'-carbonyldiimidazole for XPS analysis to quantify the number of -OH and -COOH groups on the surface. No nitrogen was detected indicating the absence of carboxylic acids. Figure 1.3 shows plots of fluorine content of PET-OH^R versus $LiAlH_4$ concentration. Both the 15° and 75° take-off angle data show maximum modification in the same concentration region as contact angle analysis indicates maximum wettability. That the fluorine content observed at 15° is considerably higher than that observed at 75° indicates that the reduction is surface-selective. No mass loss was observed at any of the concentrations studied; this confirms the surface selectivity and also indicates that the

region of the surface that is reoriented during the solvent annealing is very thin. SEM indicates that the filler particles are not disturbed by this procedure.

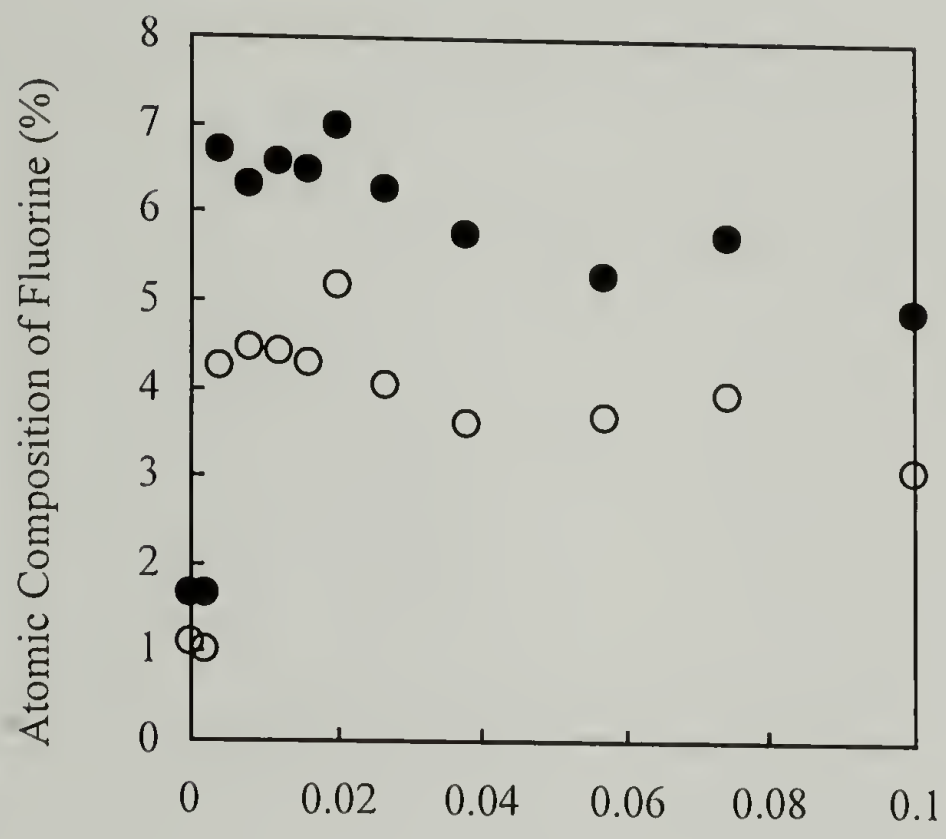

Figure 1.3. XPS fluorine atomic concentration of PET-OH^R as a function of reducing agent concentration after labeling with heptafluorobutyryl chloride: 15° take-off angle data (●), 75° take-off angle data (○).

We chose the midpoint of the maximum modification region, $[LiAlH_4]$ = 0.012 M, as the concentration to use for studying reaction time (at 25 °C); reaction time was varied from 5 to 60 min (Table 1.5). Water contact angles of different film samples were insensitive to the variation of reaction time in the range studied. XPS indicated, based on fluorine content of heptafluorobutyryl chloride - labeled samples that the surface alcohol concentration increased over the first ~30 min of reaction and decreased subsequently.

Table 1.5. Effect of reaction time with solvent annealing prior to reduction ([LAH] = 0.012 M, reaction temperature = room temp.).

	Reduction		Labeling with HFBC after reduction			
Time (min)	θ_A (deg)	θ_R (deg)	F (15°) (%)	F (75°) (%)	θ_A (deg)	θ_R (deg)
5	75	38.2	5.22	3.48	81.8	46.8
10	72.6	32.4	5.93	4.1	84.2	48.5
30	72.6	32	6.57	4.41	83.4	53.8
60	73.4	35.6	6.34	4.23	83.5	48.5

The fluorine atomic concentration for a 30 min reacted sample was: 6.6% / 4.4% (15° / 75° take-off angle).

The effect of reaction temperature was studied with $LiAlH_4$ concentration and reaction time at the determined optimum values, 0.012 M and 30 min. Reactions were carried out at 0 °C, 25 °C, 35 °C, and 45°C (Table 1.6). The contact angles of film

Table 1.6. Effect of reaction temperature with solvent annealing prior to reduction ([LAH] = 0.012 M, reaction time = 30 min).

	Reduction		Labeling with HFBC after reduction			
Temp. (deg)	θ_A (deg)	θ_R (deg)	F (15°) (%)	F (75°) (%)	θ_A (deg)	θ_R (deg)
0	71.8	30.5	5.14	3.53	80.4	46.4
25	72.6	32	6.57	4.41	83.4	53.8
35	72.2	33.2	6.77	4.42	82.2	51.6
45	73.8	34.6	6.04	4.18	82.6	51.2

samples were again not sensitive to the variation of reaction temperature. XPS analysis of labeled samples indicated a maximum in alcohol concentration for the sample prepared at 35 °C; the fluorine atomic concentration for this sample was 6.8% / 4.4% (15° / 75° take-off angle). This alcohol concentration is essentially identical to that of samples prepared at 25 °C so we chose 25 °C (for experimental simplicity), 0.012 M $LiAlH_4$ and 30 min as the conditions for further studies. The 15° take-off angle data indicate that the surfaces prepared under these conditions contain ~0.15 -OH groups per PET repeat unit. This corresponds, using the assumptions discussed above, to ~6.3 x 10^{13} alcohols/cm^2. The PET-OH^R surface thus has approximately the same density of alcohol functionality as the total functional group density of PET-OH/COOH.

Glycolysis

Transesterification using ethylene glycol was the other method used to prepare alcohol-functionalized PET. We realized from the reduction studies just discussed that the reaction parameters (reagent concentration, reaction time, and reaction temperature) that affect the extent of modification are dependent variables and arbitrarily chose a fixed reagent concentration and a fixed reaction temperature and optimized the reaction by studying the kinetics under these conditions. Glycolysis was carried out in 0.60 M potassium *tert*-butoxide in ethylene glycol at room temperature. The water contact angles decreased upon reaction from θ_A/θ_R = 77°/55° to θ_A/θ_R = 63°/30° over the first 30 min of reaction. The advancing contact angle remained at 63° until 6 h reaction time (the longest time studied), while the receding contact angle decreased further to 25° after 4 h reaction, where it remained until 6 h reaction time. Gravimetric analysis of glycolyzed film samples indicated no detectable mass loss upon reaction; the scatter in the data suggested a slight mass gain, if anything. SEM indicates that the filler particles are still present after this procedure. Glycolyzed film samples were labeled with heptafluorobutyryl chloride (for -OH groups) and 1,1'-carbonyldiimidazole (for -COOH

groups). No nitrogen was detected indicating that no carboxylic acids are present. Figure 1.4 shows the XPS results (fluorine content versus reaction time) for this series of labeled samples. The results mirror the contact angle data, indicating that the alcohol density levels after 4 hours of reaction. Both the XPS and contact angle data suggest that the reaction may stop after ~4 hours, but this may not be the case. The glycolysis may continue and degrade the sample leaving a steady state concentration of alcohols. The gravimetric data (no mass loss) suggests that under these conditions, degradation is negligible and a thin modified layer is formed. The take-off angle dependence of the fluorine content (Figure 1.4) as well as the ATR IR spectra (only PET absorbances) support this conclusion.

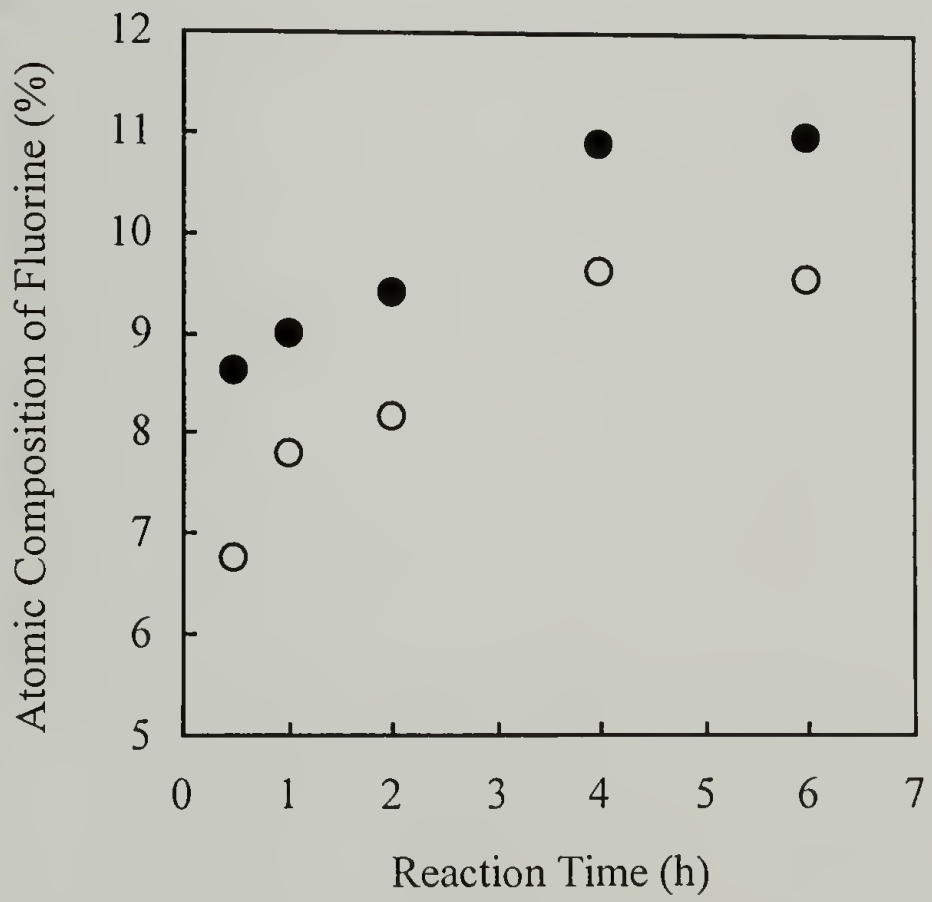

Figure 1.4. Kinetics of PET-OH^G formation as assessed by XPS fluorine concentration of heptafluorobutyryl chloride - labeled samples: 15° take-off angle data (●), 75° take-off angle data (○).

The 15° take-off angle data indicate PET-OH^{G} prepared under these conditions (4 h, 0.60 M potassium *tert*-butoxide, 25 °C) contains ~0.27 surface alcohol groups per PET repeat unit. From this ratio a surface alcohol density of ~1.3×10^{14} alcohols/cm^2 is calculated using the assumptions described above. The PET-OH^{G} surface contains about twice the alcohol concentration as the PET-OH^{R} surface and twice the total functional group density of PET-OH/COOH surfaces.

PET-OH Chemistry

The reactivity of surface alcohols was assessed using two film samples, PET-OH^{R} and PET-OH^{G}, prepared using the optimized conditions described above. These two surfaces differ chemically in two respects: (1) the PET-OH^{R} surface contains both hydroxyethyl groups and benzylic alcohols and the PET-OH^{G} surface contains only hydroxyethyl groups, (2) the density of alcohols on the PET-OH^{G} surface is about twice as high as on PET-OH^{R}. Reactions with thionyl chloride, acid chlorides and isocyanates were studied (equation 1.8). The water contact angle and XPS atomic composition data

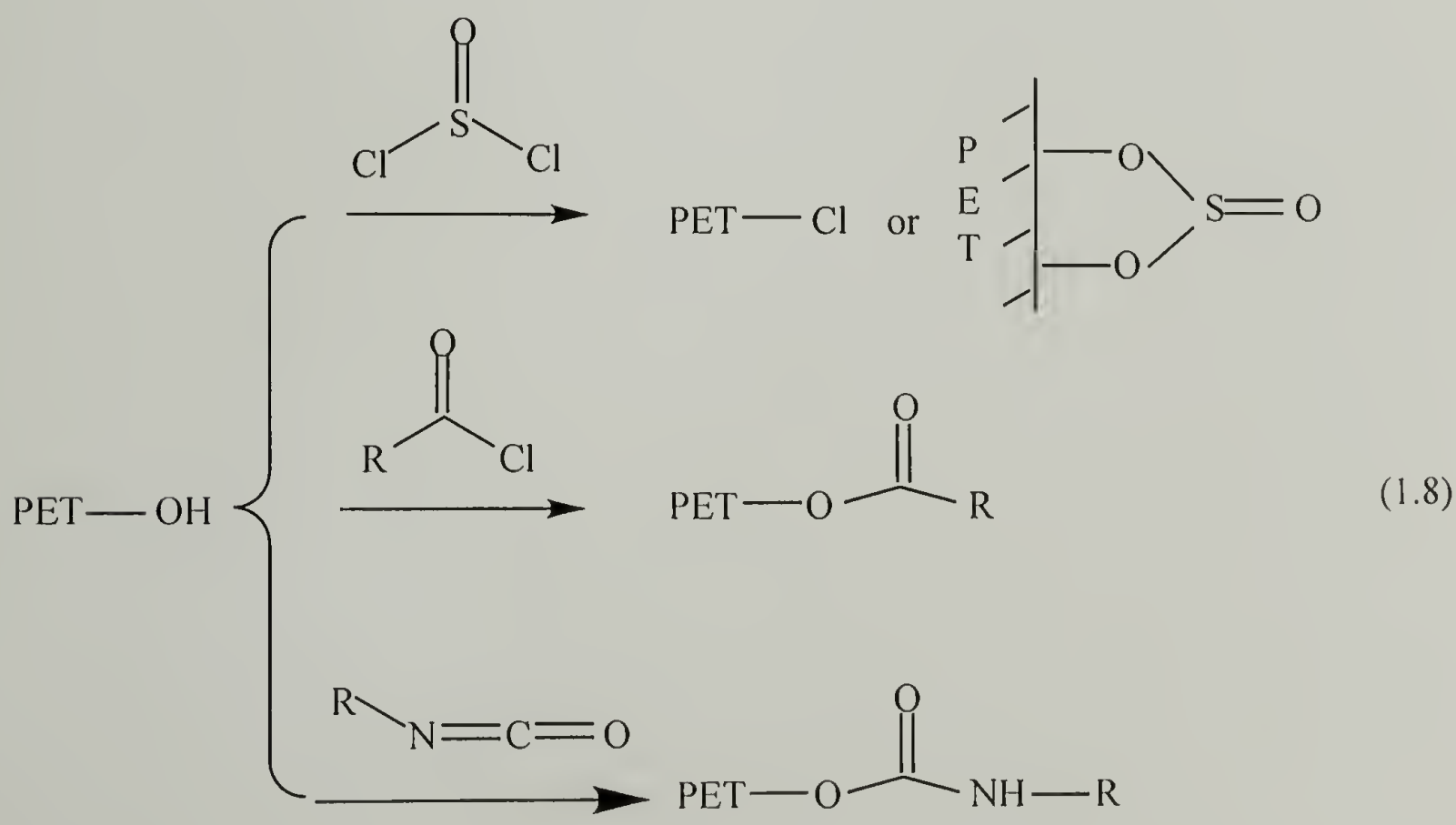

(1.8)

(15° take-off angle) for all of the PET derivatives are given in Tables 1.7 and 1.8, respectively. We assessed the reactivity of the surface alcohols in general and the

Table 1.7. Advancing and receding contact angles (water) for PET derivatives.

Film Sample	θ_A	θ_R
PET	77°	55°
PET-OH/PET-COOH	62°	16°
PET-OH^R	72°	32°
PET-OH^G	63°	25°
PET-Cl/PET-$(O)_2SO^R$	78°	44°
PET-Cl/PET-$(O)_2SO^G$	69°	32°
PET-$OC(O)C_3F_7{}^R$	83°	54°
PET-$OC(O)C_3F_7{}^G$	106°	46°
PET-$OC(O)CH_3{}^R$	77°	43°
PET-$OC(O)CH_3{}^G$	73°	32°
PET-$OC(O)(CH_2)_{16}\ CH_3{}^R$	88°	54°
PET-$OC(O)(CH_2)_{16}\ CH_3{}^G$	101°	52°
PET-$OC(O)NH\phi^R$	81°	43°
PET-$OC(O)NH\phi^G$	82°	28°
PET-$OC(O)NHCCl_3{}^R$	79°	34°
PET-$OC(O)NHCCl_3{}^G$	75°	21°
PET-$OC(O)NH(CH_2)_6NCO$/ PET-$(OC(O)NH)_2(CH_2)_6{}^R$	73°	41°
PET-$OC(O)NH(CH_2)_6NCO$/ PET-$(OC(O)NH)_2(CH_2)_6{}^G$	76°	34°
PET-$OC(O)NH\phi(CH_3)NCO$/ PET-$(OC(O)NH)_2\phi CH_3{}^R$	84°	42°
PET-$OC(O)NH\phi(CH_3)NCO$/ PET-$(OC(O)NH)_2\phi CH_3{}^G$	80°	29°

Table 1.8. XPS atomic composition data (15° take-off angle) for PET derivatives.

Film Sample	C	O	N	Cl	S or F
PET	71.50	28.50			
PET-OH/PET-COOH	69.90	30.10			
PET-OH^R	70.68	29.32			
PET-OH^G	69.10	30.90			
PET-Cl/PET-$(O)_2SO^R$	69.56	30.02		0.26	0.16^S
PET-Cl/PET-$(O)_2SO^G$	68.27	31.22		0.16	0.35^S
PET-$OC(O)C_3F_7{}^R$	66.47	26.96			6.57^F
PET-$OC(O)C_3F_7{}^G$	62.43	26.69			10.88^F
PET-$OC(O)CH_3{}^R$	68.08	31.92			
PET-$OC(O)CH_3{}^G$	67.93	32.07			
PET-$OC(O)(CH_2)_{16}\ CH_3{}^R$	70.84	29.16			
PET-$OC(O)(CH_2)_{16}\ CH_3{}^G$	73.51	26.49			
PET-$OC(O)NH\phi^R$	69.03	30.18	0.79		
PET-$OC(O)NH\phi^G$	68.23	30.48	1.29		
PET-$OC(O)NHCCl_3{}^R$	67.04	30.44	0.92	1.60	
PET-$OC(O)NHCCl_3{}^G$	63.15	31.66	1.57	3.61	
PET-$OC(O)NH(CH_2)_6NCO$/ PET-$(OC(O)NH)_2(CH_2)_6{}^R$	67.87	31.04	1.08		
PET-$OC(O)NH(CH_2)_6NCO$/ PET-$(OC(O)NH)_2(CH_2)_6{}^G$	67.53	30.59	1.88		
PET-$OC(O)NH\phi(CH_3)NCO$/ PET-$(OC(O)NH)_2\phi CH_3{}^R$	67.70	31.10	1.20		
PET-$OC(O)NH\phi(CH_3)NCO$/ PET-$(OC(O)NH)_2\phi CH_3{}^G$	67.23	30.38	2.39		

differences in reactivity of the two alcohol surfaces. The XPS spectra of all surfaces exhibited a take-off angle (15° and 75°) dependence indicating that unreacted PET is

present in the outer ~40 Å of film samples. The 15° data reported here is more representative of the composition of the portions of the samples that have been modified.

Reactions of PET-OH with Thionyl Chloride. Both PET-OH^R and PET-OH^G were allowed to react with thionyl chloride. After the reactions, contact angles of film samples increased (Table 1.7), and both sulfur and chlorine were observed by XPS (Table 1.8), indicating the formation of both alkyl chloride and sulfite functionality (PET-Cl/O_2SO). We have studied this reaction previously with two different alcohol surfaces, PEEK-OH[17] and PCTFE-OH.[10] In the case of PEEK-OH, only PEEK-Cl is formed and in the case of PCTFE-OH, only the sulfite forms. We ascribe this reactivity difference to three factors: surface alcohol concentration, functional group flexibility and chemical structure. PEEK-OH contains a relatively low concentration of secondary doubly benzylic alcohols attached directly to the PEEK backbone; each of these factors favors alkyl chloride formation rather than sulfite formation; we suspect that this reaction proceeds by an S_N1 mechanism. On the other hand, the PCTFE-OH structure contains a high concentration of primary alcohols attached to the polymer chain by a flexible 3-methylene spacer, favoring sulfite formation.

The presence of both sulfur and chlorine in the reaction products of PET-OH^R and PET-OH^G indicates competitions between alkyl chloride and sulfite formation. The relative amount of sulfur and chlorine is, however, different on the two PET-OH - derived surfaces (Table 1.8), indicating different reactivities: chlorine is present in higher concentration than sulfur on PET-OH^R and the ratio is the reverse on PET-OH^G. This difference in reactivities can be ascribed to the different alcohol structures and densities on the two surfaces. PET-OH^R contains both a lower alcohol concentration (more greatly spaced) as well as benzylic alcohols favoring alkyl chloride formation and PET-OH^G contains a more dense array of primary alkyl groups favoring the sulfite. The reaction yields were determined by labeling unreacted alcohols with heptafluorobutyryl chloride

after the reaetions. The 15° take-off angle XPS data indicate yields (basecd on fluorinc atomic eomposition) of 69.4% for PET-OH^R and 59.2% for PET-OH^G.

Reactions of PET-OH with Acid Chlorides (PET-OC(O)R). We have uscd heptafluorobutyryl ehloride extensively as a labeling reagent for surfaec alcohols both in this study and several othcrs. The kinctics of this reaction was studied with PET-OH^G and indieates that esterifieation is rapid. After 10 min of reaetion with 1.556 g (6.69 mmol) heptafluorobutyryl ehloride in 25 mL THF at room tcmpcraturc, PET-OH^G (now PET-$OC(O)C_3F_7{}^G$) exhibits water eontaet angles of θ_A/θ_R = 106°/46° and XPS data indistinguishable from samples reaeted for longer times (up to 4 h). We assume that this reaction is quantitative (rcaetion times of 2 h were used for all labcling studics) and the reaetion yields and eompositions indieated in this paper are based on this assumption. We note that the advaneing eontaet angle of PET-$OC(O)C_3F_7{}^R$ is signifieantly lowcr than that of PET-$OC(O)C_3F_7{}^G$ indieating the expected lower eoneentration of perfluoropropyl groups.

PET-OH^R and PET-OH^G were allowed to reaet with aeetyl ehloridc and unrcacted -OH groups were labeled with heptafluorobutyryl ehloride to determinc yicld. Without the addition of pyridine to the rcaetions, the yields wcrc ~60% aftcr 24 h. The lower reaction rates of aeetyl ehloride eompared to heptafluorobutyryl chloridc arc duc to eleetronic differenecs. With pyridine catalysis, acetyl chloride reaets rapidly. From labeling studies, there were essentially no rcsidual aleohol groups on PET-OH surfaces after reactions. Yields calculatcd from XPS data are ~100% for both PET-OH^R, and PET-OH^G surfaces.

Reaetions with stearoyl ehloride werc cvcn slower than with acetyl chloridc due to sterics. Yields were ~20% aftcr 24 h without pyridine. With the prcscncc of pyridinc, the yields improved signifieantly to 93.0% for PET-OH^R and 90.8% for PET-OH^G. Longer reaction times did not improve the yields. Water eontact angles of thc ester

surfaces were high (Table 1.7), especially the stearate surface derived from PET-OH^G (with higher ester group density). There is, however, no change in hexadecane contact angles of the film samples after the reaction (θ_A/θ_R = ~10°/0°). If the closely packed long hydrocarbon chains crystallized on the surface, we would expect to see an increase in hexadecane contact angle; this is the case for the reaction of stearoyl chloride with PCTFE-OH.[51] The low hexadecane contact angles indicate relatively low -OH density on both PET-OH surfaces resulting in loosely packed hydrocarbon chains that do not crystallize.

Reactivity of PET-OH surfaces toward the three acid chlorides studied are in the order of heptafluorobutyryl chloride >> acetyl chloride > stearoyl chloride due to electronic and steric reasons. Reaction yields reached >90% in all cases. Both PET-OH^R and PET-OH^G surfaces show similar reactivity (nucleophilicity) in these reactions.

Reactions of PET-OH with Isocyanates. PET-OH samples were reacted with both monoisocyanates (trichloroacetyl isocyanate and phenyl isocyanate) and diisocyanates (1,6-diisocyanatohexane - HDI and tolylene-2,4-diisocyanate - TDI) using dibutyltin dilaurate catalysis. For the reactions with monoisocyanates, reaction yields could be calculated directly by XPS (nitrogen content) analysis of the urethane surfaces. For the reactions with phenyl isocyanate, yields were 84.2% for PET-OH^R, and 83.0% for PET-OH^G (15° take-off angle data). Yields for the reactions with trichloroacetyl isocyanate were ~100% for both PET-OH film samples. The higher reaction yields may be due to sterics or the higher reactivity of trichloroacetyl isocyanate (kinetics were not determined). We note (Table 1.8) that the chlorine atomic concentration is low relative to nitrogen (there should be 3 Cl atoms per N) on the PET-OC(O)NHCOCCl$_3$ surfaces. This is due to the fact that chlorine is lost as a result of X-ray damage; no special precautions (reduced X-ray power or minimized acquisition time) were taken in analysis.

The situation is more complicated with reactions of diisocyanates. The diisocyanates, $R(NCO)_2$, can couple with two adjacent -OH groups to form PET-$(OC(O)NH)_2R$ or react with only one alcohol to form PET-OC(O)NHRNCO. The ratios of these two products can be determined using XPS (nitrogen content) in conjunction with the labeling of unreacted alcohols with heptafluorobutyryl chloride to determine overall reaction yield. For the reaction with HDI, reaction yields were calculated to be 79.7% for PET-OH^R and 75.6% for PET-OH^G (15° take-off angle data). Yields of reactions with TDI were calculated to be 84.5% for PET-OH^R and 80.3% for PET-OH^G. The ratio of surface alcohols on PET-OH^R that react with HDI and form diurethane (coupled product) to surface alcohols that react with a single site on the diisocyanate (to form a half urethane/half isocyanate) is 73:37. The same ratio for reaction of PET-OH^R with TDI is 49:51. The results for PET-OH^G, expressed as the same ratio, are 27:73 for HDI and 8:92 for TDI (Table 1.9). The result that HDI reacts bifunctionally to a greater

Table 1.9. Percent of -OH coupled in reactions of PET-OHs with diisocyanates.

Diisocyanates	PET-OH^R	PET-OH^G
1,6-diisocyanatohexane	73.1 %	26.5 %
tolylene-2,4-diisocyanate	48.6 %	7.8 %

extent than TDI with both surfaces is readily explained: The two isocyanate groups on the former have the same reactivity while those on the latter have different reactivity and furthermore, the former is more flexible. The observation that alcohol groups on PET-OH^R are more likely to form diurethane than those on PET-OH^G is counter to what we expected from relative surface alcohol concentrations and is difficult to explain. Perhaps

the partitioning of the diisocyanates between bulk solution and the solution/solid interface is different for the two PET-OH surfaces and there is lower local concentrations of diisocyanates at the PET-OH^R surface. We cannot offer a clearer explanation.

Failed Reactions

PET-Cl. Synthesis of PET-Cl was attempted by allowing PET-OHs to react with concentrated HCl catalyzed by $ZnCl_2$. Similar chlorine atomic concentrations were observed on both PET-OHs and virgin PET after reactions. HCl does not only act as chlorination agent but also serves as a hydrolysis catalyst.

PET-OH^H. Selective reduction of the -COOH group of the hydrolyzed film sample was attempted using 0.1 M borane THF at room temperature. Film samples were labeled with heptafluorobutyryl chloride and 1,1'-carbonyldiimidazole to monitor the change of number of -OH and -COOH as a function of reaction time. From both 15° and 75° take-off angle XPS data, there was a ~ 30 % increase in the number of -OH groups and a 30 % decrease of the number of -COOH functionality on the surface after 48 h. However, there was also an increase of -OH group on the surface of a control PET film sample which was reacted under the same conditions. This indicates that borane reduces not only the -COOH group but also the ester moiety of PET.

PET-COOH. We attempted to prepare PET-COOH from PET-OH. The strategy was to deprotonate the alcohols on the surface using a non-nucleophilic base, such as lithium diisopropylamide, and react the PET-O^- with succinic anhydride to form PET-$OC(O)CH_2CH_2COOH$. However, LDA not only deprotonates -OH, but also attacks the ester moiety of PET, even when a very low concentration of LDA (0.01 g in 25 mL THF) is used. After reaction for 5 h, contact angle values of the PET film sample

dropped from 77°/55° to 71° /31° , and small amount of nitrogen was observed in the XPS spectrum of the film sample. In a second attempt, we deprotonated the surface -OH first by reacting PET-OH with LDA (0.01 g) in THF (25 mL) for 15 min. The LDA/THF solution was then transferred out and succinic anhydride/THF solution was added. According to labeling results, the conversion from -OH to -COOH reached as high as 70 %. However, the conversion was not reproducible, presumably due to the high susceptibility of PET-O^- to proton containing species during transferring. The failed reactions indicate the challenging aspect of surface modification of a chemically less resistant polymer.

Conclusions

Alcohol functionality can be introduced to the surface of PET using either reduction or glycolysis, both of which cleave the PET chain. The surface density of alcohols is higher on PET-OH samples prepared by glycolysis than on those prepared by reduction by a factor of ~2. The concentration of alcohols on reduced surfaces is increased by solvent annealing of the PET film prior to reduction; we believe that this is due to a reorientation of chains near the surface. Both of these modified surfaces (PET-OH^R and PET-OH^G) and hydrolyzed PET (PET-OH/COOH) can be prepared using conditions that minimize sample degradation. Conditions that optimize surface functional group concentration were determined. PET-OH^R and PET-OH^G samples react with alcohol-selective reagents (thionyl chloride, acid chlorides, and isocyanates) and their reactivity differs due to their chemical differences and their different surface alcohol densities.

Notes and References

1. Clark, D. T.; Feast, W. J. "Polymer Surfaces"; Wiley-Interscience: New York, 1978.

2. Feast, W. J.; Munro, H. S.; Richards, R. W. "Polymer Surfaces and Interfaces"; John Wiley and Sons: New York, 1993.

3. Ward, W.; McCarthy, T. J. In *Encyclopedia of Polymer Science and Engineering*, 2nd ed; Mark, H. F., Bikales, N. M.,Overberger, C. G., Menges, G.,Kroschwitz, J. I., Eds.; John Wiley and Sons: New York, 1989; suppl. vol., p 674.

4. Costello, C. A.; McCarthy, T. J. *Macromolecules*, **1987**, *20*, 2819.

5. Costello, C. A.; McCarthy, T. J. *Macromolecules*, **1990**, *23*, 2648.

6. Shoichet, M. S.; McCarthy, T. J. *Macromolecules*, **1991**, *24*, 1441.

7. Shoichet, M. S.; McCarthy, T. J. *Macromolecules*, **1991**, *24*, 982.

8. Dias, A. J.; McCarthy, T. J. *Macromolecules*, **1985**, *18*, 1826.

9. Dias, A. J.; McCarthy, T. J. *Macromolecules*, **1985**, *20*, 2068.

10. Lee, K.-W.; McCarthy, T. J. *Macromolecules*, **1988**, *21*, 2318.

11. Lee, K.-W.; McCarthy, T. J. *Macromolecules*, **1988**, *21*, 3353.

12. Kolb, B. U.; Patton, P. A.; McCarthy, T. J. *Macromolecules*, **1990**, *23*, 366.

13. Cross, E. M.; McCarthy, T. J. *Macromolecules*, **1990**, *23*, 3916.

14. Bee, T. G.; McCarthy, T. J. *Macromolecules*, **1992**, *25*, 2093.

15. Dias, A. J.; McCarthy, T. J. *Macromolecules*, **1984**, *17*, 2529.

16. Iyengar, D. R.; Brennan, J. V.; McCarthy, T. J. *Macromolecules*, **1991**, *24*, 5886.

17. Franchina, N. L.; McCarthy, T. J. *Macromolecules*, **1991**, *24*, 3045.

18. Clark, D.T.; Thomas, H.R. J. *Polym. Sci., Polym. Chem. Ed.* **1977**, *15*, 2843.

19. Andrade, J. D. *Surface and Interfacial Aspects of Biomedical Polymers,Surface Chemistry and Physics;* Plenum Press: New York, 1985; Vol. 1, Ch. 5.

20. Clark, D.T.; Thomas, H.R.; Shuttleworth, D. *J. Polym. Sci., Polym. Lett. Ed.* **1978**, *16*, 465.

21. Hall, S.M.; Andrade, J.D.; Ma, S.M.; King, R.N. *J. Electron Spectroscopy* **1979**, *17*, 181.

22. Clark, D.T.; Adams, D.B.; Dilks, A.; Peeling, J.; Thomas, H.R. *J. Electron Spectroscopy* **1976**, *8*, 51.

23. Ashley, J.C. *IEEE Trans. Nucl. Sci.* **1980**, *NS-27*, 1454.

24. Ashley, J.C.; Williams, M.W. *Rad. Res.* **1980**, *81*, 364.

25. Ashley, J.C. *J. Electron Spectroscopy* **1982**, *28*, 177.

26. Ashley, J.C.; Tung, C.J. *Surf. Interfac. Anal.* **1982**, *4*, 52.

27. Zisman, W. A. *Adv. Chem. Ser.* **1964**, *43*, 1, and references therein.

28. Reference 19, Ch. 7.

29. Werner, E.; Janocha, S.; Hopper, M. J.; Mackenzie, K. J. In *Encyclopedia of Polymer Science and Engineering*, 2nd ed; Mark, H. F., Bikales, N. M., Overberger, C. G., Menges, G., Kroschwitz, J. I., Eds.; John Wiley and Sons: New York, 1989; Vol 12, p 193.

30. Baliga, S.; Wong, W. T. *J. Polym. Sci.: Polym. Chem.*, **1989**, *27*, 2071.

31. Chen, J. Y.; Ou, C. F.; Hu, Y. C.; Lin, C. C. *J. Appl. Polym. Sci.* **1991**, *42*, 1501.

32. Campanelli, J. R.; Kamal, M. R.; Cooper, D. G. *J. Appl. Polym. Sci.* **1994**, *54*, 1731.

33. Wang, J.; Feng, D.; Wang, H.; Rembold, M.; Fritz, T. *J. Appl. Polym. Sci.* **1993**, *50*, 585.

34. Strobel, M.; Lyons, C. S.; Strobel, J. M.; Kapaun, R. S. *J. Adhes. Sci. Technol.* **1992**, *6*, 429.

35. Bertrand, P.; DePuydt, Y.; Beuken, J. M.; Lutgen, P.; Feyder, G. *Nucl. Instrum. Methods Phys. Res., Sect. B.* **1987**, *B19-20*, 887.

36. Arenolz, E.; Heitz, J.; Wagner, M.; Baeuerle, D.; Hibst, H.; Hagemeyer, A. *Appl. Surf. Sci.* **1993**, *69*, 16.

37. Desai, N. P.; Hubbell, J. A. *Macromolecules* **1992**, *25*, 226.

38. Xue, J.; Wilkie, C. A. *J. Polym. Sci.: Part A: Polym. Chem.* **1995**, *33*, 1019

39. Yao, Z. P.; Rånby, B. *J. Appl. Polym. Sci.* **1990**, *41*, 1459.

40. Dave, J.; Kumar, R.; Srivastava, H. C. *J. Appl. Polym. Sci.* **1987**, *33*, 455.

41. Solbrig, C. M.; Obendorf, S. K. *J. Appl. Polym. Sci.: Appl. Polym. Sym.*, **1991**, *47*, 437.

42. Solbrig, C. M. *Dissertation Abstracts International* **1991**, *51, 12*, 5899-B.

43. Avny, Y.; Reubenfeld, L. *J. Appl. Polym. Sci.* **1986**, *32*, 4009.

44. Bùi, L. N.; Thompson, M.; McKeown, N. B.; Romaschin, A. D.; Kalman, P. G. *Analyst* **1993**, *118*, 463.

45. Xu, G.-F.; Bergbreiter, D. E.; Letton, A. *Chem. Mater.* **1992**, *4*, 1240.

46. Collin, R. J. U.S. Pat. 2,955,954, **1964**.

47. Marchand-Brynaert, J.; Deldime, M; Dupont, I.; Dewez, J.-L.; Schneider, Y.-J. *J. Coll. Interfac. Sci.* **1995**, *173*, 236.

48. Carbonyl diimidazole reacts with alcohols as well as carboxylic acids, thus the labeling reaction with heptafluorobutyryl chloride was carried out first. That heptafluorobutyryl chloride does not react with carboxylic acids (to form anhydrides) under these conditions was determined using PMP-COOH (poly(4-methyl-1-pentene) containing surface carboxylic acids).[52]

49. The values are calculated using 14 Å as the mean free path of C_{1s} electrons ejected using Al K_α irradiation. This value was measured in poly(p-xylylene).[18]

50. Harrick, N. J. Internal Reflection Spectroscopy, Wiley Interscience: New York, 1967.

51. Bee, T. G., Ph.D. dissertation, University of Massachusetts, 1993.

52. Leväsalmi, J.-M.; McCarthy, T. J. *Macromolecules*, **1997**, *30*, 1752.

CHAPTER 2

LAYER-BY-LAYER DEPOSITION ON POLY(ETHYLENE TEREPHTHALATE): A TOOL FOR POLYMER SURFACE MODIFICATION

Introduction

Over the past several years, Decher and others[1-12] have developed layer-by-layer deposition as a simple and versatile method for preparing supported multilayer thin films. This process is driven by electrostatic attraction between opposite charges. These and other types of organic thin films show promise in applications such as sensors, friction reducing coatings, integrated optics and electronic device fabrication.[13] This method has several important advantages over other techniques for preparing ordered multilayer thin films: the assembly is based on spontaneous adsorptions, the substrate can have, in principle, any size, shape, topography or topology, no stoichiometric control is necessary to maintain surface functionality - defects don't propagate.

We have been involved in a program directed at controlling solid polymer surface properties through chemical manipulation of surface functionality (see Chapter 1).[14-21] This type of modification has the advantage that chemically well-defined surfaces are prepared which are amenable to fundamental surface structure - surface property correlations. The clear disadvantage of this approach is that it is rarely practical. The practical approaches to polymer surface modification include flame treatment, corona discharge treatment, plasma modification and surface graft polymerization.[22] These have the disadvantage that chemically well-defined surfaces cannot be designed and prepared, but the advantage that they work to control the technologically significant properties of adhesion, wettability, biocompatibility and gas permeability. Multistep chemical reactions will certainly not replace the more simple and practical approaches for most applications - even if they are more well understood.

Layer-by-layer deposition may offer the advantages of both these approaches as a surface modification technique for polymers. It is a simple, relatively fast, environmentally benign and potentially economical process. Surface functionality can be controlled directly by choosing appropriate polyelectrolytes.

We chose poly(ethylene terephthalate) (PET) to assess the layer-by-layer deposition technique as an alternative for surface modification for several reasons: (1) It contains carbonyl groups that are capable of hydrogen bonding. (2) The surface can be readily hydrolyzed to introduce carboxylic acid (as well as alcohol) functionality that can support negative charge (PET-CO_2^-) in sufficiently basic solution. (3) The surface can react with polyamines to incorporate amine functionality that can support positive charge (PET-NH_3^+) in non-basic solution.

Polymer Adsorption at Interfaces

Much effort has been put into theoretical and experimental work to understand the adsorption of polymers at interfaces.[23-29] The adsorption behavior of neutral polymers and polyelectrolytes onto surfaces has become clear. The adsorption is influenced by different factors, such as surface charge density, adsorption time, polymer concentration, polymer molecular weight, pH, and ionic strength of the solution.

Adsorption of Neutral Polymers

Adsorption of uncharged polymers has been reviewed by Fleer and Lyklema.[23] One generally finds thick adsorbed layers with long tails and many segments of the adsorbed polymers in loops. Charging the surface has a very minor effect on the adsorption behavior of an uncharged polymer. The adsorbed amount on a charged surface is less than on an uncharged surface if the number of available sites for adsorption decreases (occupied by the counter ion). In good solvent conditions, the adsorbed amount is very low and only weakly dependent on the molecular weight of the polymer.

However, in poor solvent conditions, the adsorbed amount depends linearly on the logarithm of the molecular weight. When the ionic strength of the solvent increases, the adsorption amount should increase because the solvent quality decreases as a result of increasing salt concentration.[24]

Adsorption of Strong Polyelectrolytes

Van der Schee et. al.[25-27] extended the mean-field theory for the adsorption of neutral polymers to include electrostatic interactions for the adsorption of polyelectrolytes. For strong polyelectrolytes, adsorption is not dependent on the pH of the solution, but strongly dependent on whether the surface is charged or not.

For adsorption onto a neutral surface, for example the adsorption of polystyrene sulfonate (PSS) from aqueous solution to polyoxymethylene (POM) single crystals,[28] the adsorption isotherms (Figure 2.1) have a rounded shape as a consequence of the low affinity of the polyelectrolyte segments for the surface. It is found that a roughly linear relationship exists between adsorbed amount and NaCl concentration, as a result of enhanced screening of segment-segment electrostatic repulsion at high salt concentration. Since the energetic effect is small, the adsorption entropy determines the adsorption to a large extent, and many segments should adsorb in the forms of loops and tails. Variation in adsorption entropy, in terms of molecular weight, will affect the adsorbed amount greatly.

When the surface is oppositely charged, high affinity between segments and substrate is expected, such as in the case of PSS on positively charged hematite surface.[28] As shown in Figure 2.2, the isotherms are less rounded because of the high affinity between the polyelectrolyte and the surface. The adsorbed amount is higher at high ionic strengths where segment-segment repulsion is screened, however, the dependence of adsorption on ionic strength is not as strong as in the case of an uncharged surface.

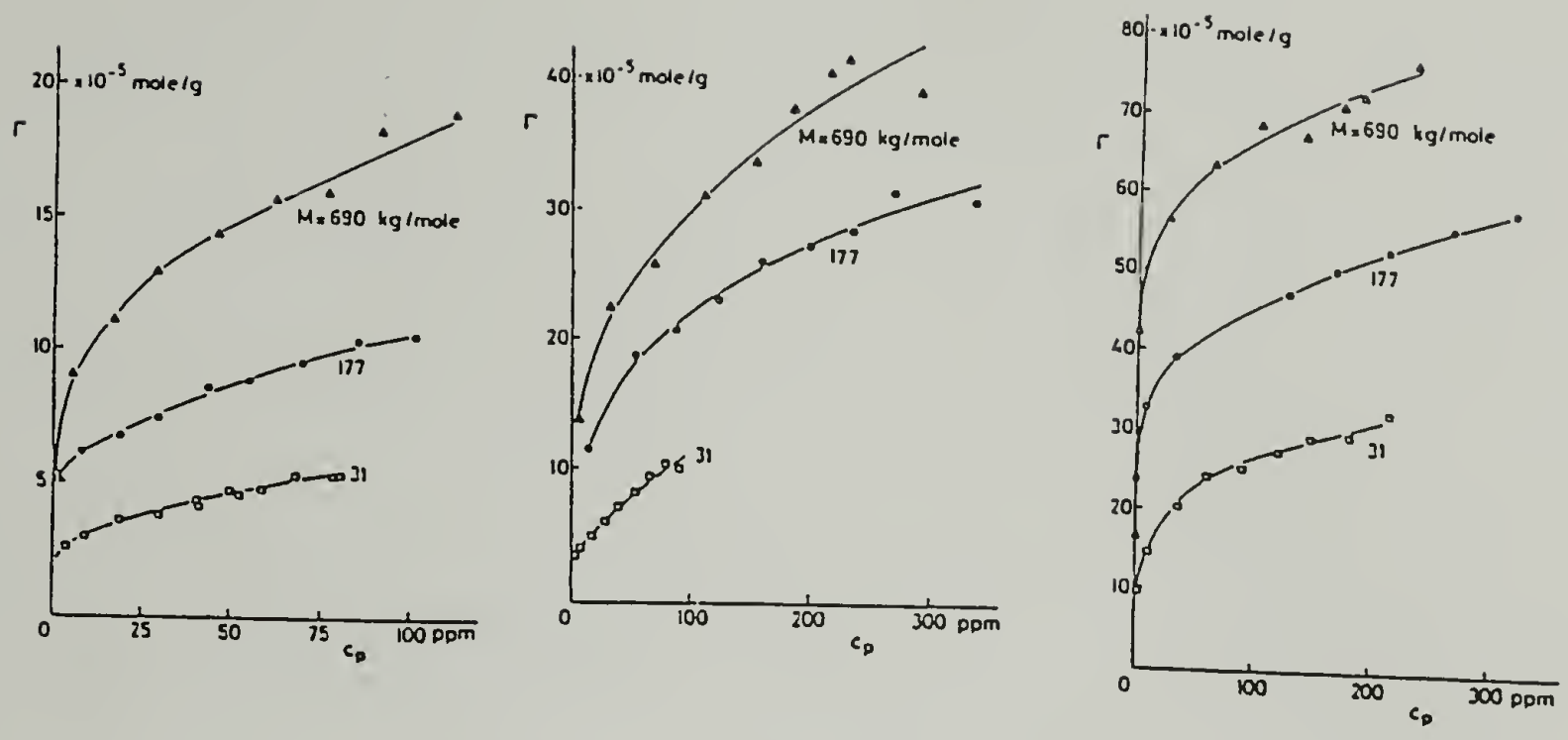

0.53 M NaCl 1.04 M NaCl 2.18 M NaCl

Figure 2.1. Adsorption isotherms of PSS on POM crystals in the presence of a) 0.53 M NaCl b) 1.04 M NaCl c) 2.18 M NaCl for three molecular weights.[28]

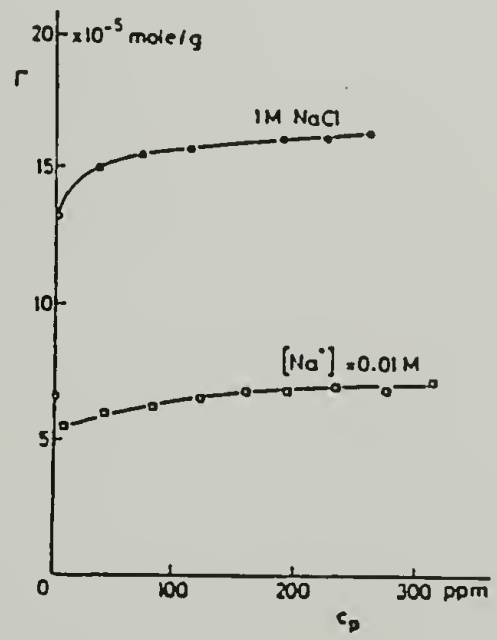

Figure 2.2. Adsorption isotherm of PSS (M=690 kg/mole) on hematite, at ionic strength 0.01 M and 1M.[28]

The polyelectrolyte adsorbs flatly on the surface in the case of high-affinity type behavior and the adsorbed amount has very little dependence on molecular weight of the polyelectrolyte.

Surface charge density should be another variable to consider. Based on Vincent et. al.'s work on adsorption of PSS onto positively charged polystyrene latex, the adsorbed amount decreases as a function of surface charge density due to a flatter adsorbed conformation at higher charge density.[29] However, Fleer et. al. suggest that the adsorbed amount should increase with higher surface charge density because of the more favorable electrostatic interaction.[24]

Adsorption of Weak Polyelectrolytes

For weak polyelectrolytes, the degree of dissociation depends on the pH of the solution. They behave either as neutral polymers or as strong polyelectrolytes when the pH is away from the pk_O of the polyelectrolytes. If the surface is oppositely charged, some recently developed theories, which are extensions of the Scheutjens-Fleer approach, predict a maximum in the adsorbed amount at a pH value below the pK_O of the polyacid as shown in Figure 2.3. The maximum is the result of two opposite trends, the favorable electrostatic attraction between the surface and the polyelectrolyte and the unfavorable repulsion between the segments on the polyelectrolyte.

Layer-by-Layer Adsorption

Layer-by-layer deposition is a simple and versatile method for preparing supported multilayer thin films. The basic process involves dipping a charged (e.g. cationic) substrate into a dilute aqueous solution of an anionic polyelectrolyte and allowing the polymer to adsorb and reverse the charge of the substrate surface. The negatively charged coated substrate is rinsed and dipped into a solution of cationic polyelectrolyte, which adsorbs and recreates a positively charged surface. Sequential

adsorptions of anionic and cationic polyelectrolytes allow the construction of multilayer films. The process is driven by electrostatic attraction between opposite charges.

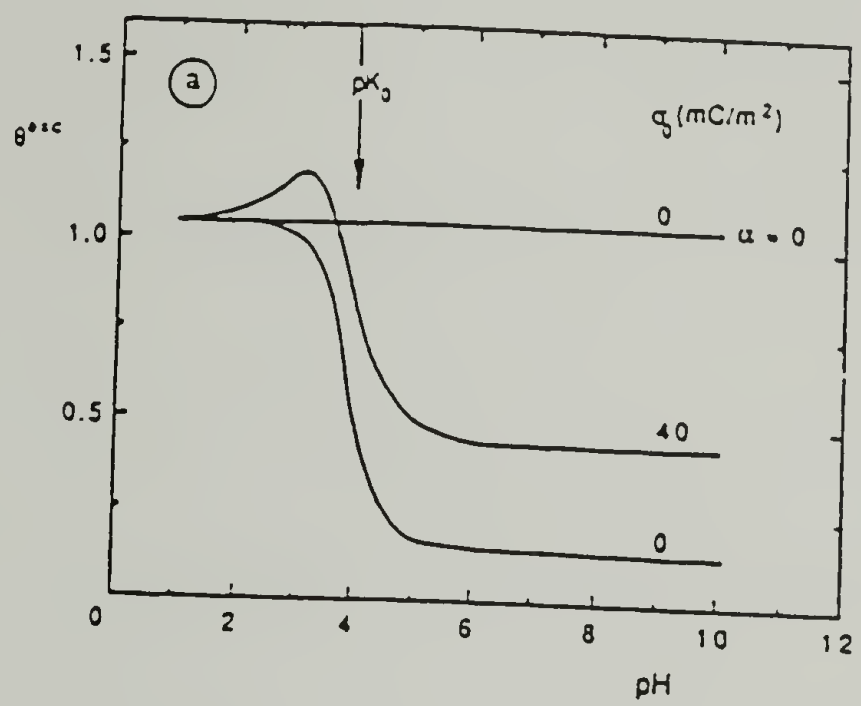

Figure 2.3. Excess adsorbed amount as a function of the pH for a neutral polymer ($\alpha = 0$) and a weak polyelectrolyte ($pK_0 = 4$) at different surface charge density ($\sigma_0 = 0$ or 40 mC/m^2).[24]

Substrates

The substrate can have, in principle, any size, shape, topography or topology. Layer-by-layer adsorption has been carried out on various types of surfaces, either neutral or charged. Clean and surface-modified inorganic substrates, such as fused quartz, silica, glass, and gold, are used most frequently. Glass slides have been used in the forms of hydrophilic (cleaned),[5] hydrophobic (plasma treatment with 1,1,1,3,3,3-hexamethyldisilazane),[5] positively charged (reaction with N-2-aminoethyl-3-aminopropyltrimethoxysilane),[5] and negatively charged (plasma treatment with CH_4 and O_2).[30]

Layer-by-layer depositions on organic substrates have recently been studied in this laboratory. In addition to the work presented here on PET and its derivatives, layer-by-layer deposition on PMP-COOH[10, 31] and PCTFE-OH[32] have also been assessed.

Polymer Solutions

Since the adsorption is driven by electrostatic attraction between opposite charges, any polymer that can be charged should be suitable for layer-by-layer deposition. Two oppositely charged polyelectrolytes can be deposited alternately to create an array of bilayers, or more than two polyelectrolytes can be used to obtain a desired heterostructure.

The most-studied system is poly(sodium styrenesulfonate) (PSS)[1,2,30] and poly(allylamine hydrochloride) (PAH).[1,2,5,30] Other polyelectrolytes, including polypeptides,[33] DNA,[34] viruses,[35] and conducting polymers (polyaniline),[6] have also been incorporated into the multilayer heterostructures to achieve desired properties.

Adsorption solutions consist of a polymer in a solvent, sometimes with a cosolvent to enhance the solubility of the polymer.[6] Most often, adsorption takes place from aqueous solution. Acid or base is usually added to adjust the pH of the solution. Ionic strength of the solution can be adjusted by incorporating a salt.

Control of Layer Thickness

In most cases, layer-by-layer adsorption fits in the domain of adsorption of polyelectrolytes (weak and strong) onto charged surfaces, where strong electrostatic interaction is the driving force. However, for the layer-by-layer deposition of polyaniline and poly(vinyl pyrrolidone) onto a charged glass substrate, hydrogen bonding is the driving force.[6] In any case, the adsorbed amount can be controlled by surface charge density, adsorption time, polymer concentration, polymer molecular weight, pH, and ionic strength of the solution, as discussed earlier.

Thermal Stability

The thermal stability of poly(vinyl sulfate) and poly(allylamine hydrochloride) deposited onto a glass slide showed that the layers are stable up to 150 °C. There is a 6 % deerease in layer thiekness upon heating, presumably due to loss of water. After the heated sample was cooled and kept at room temperature, the thickness inereased to its initial value. The roughness of the deposited layers did not change throughout the experiment.[2]

Characterization of Deposited Layers

Charaeterization of the layer-by-layer deposited films has emphasized the determination of layer thiekness and surfaee roughness. So far, small angle neutron and x-ray reflectivity,[1,2,4] ellipsometry,[3,4,5,7] UV-VIS spectroscopy,[1,3] profilometry,[5] light mieroseopy,[5,6] and AFM,[4,7,8] have been used to analyze the self-assembled multilayers.

Experimental

Materials and Methods

Poly(allylamine hydroehloride) (M_n = 50,000-65,000) and poly(sodium styrenesulfonate) (M_n = 70,000) were obtained from Aldrieh. Sodium chloride, $MnCl_2 . 4H_2O$, 1 M HCl, sodium hydroxide, methanol (HPLC grade), and hexane (HPLC grade) were purehased from Fisher. All materials were used as reeeived. Water was purified using a Millipore Milli-Q system that involves reverse osmosis followed by ion-exehange and filtration steps. Buffer solutions used for contaet angle measurement were CRC standard.[36] Solution pH for layer-by-layer adsorption studies was adjusted with either HCl or NaOH solution using a Fisher 825MP pH meter. X-ray photoeleetron speetra (XPS) were reeorded on a Perkin-Elmer-Physieal Eleetronies 5100 speetrometer with Al

K_α excitation (15 kV, 400 W). Spectra were taken and recorded at two different take-off angles, 15° and 75° between the plane of the sample surface and the entrance lens of the detector optics. Atomic concentration data were determined using sensitivity factors obtained from samples of known composition: C_{1s}, 0.201; O_{1s}, 0.540; N_{1s}, 0.385; S_{2p}, 0.440. Contact angle measurements were made with a Ramé-Hart telescopic goniometer and a Gilmont syringe with a 24-gauge flat-tipped needle. Probe fluids were either water (purified as described above) or buffer solutions. Dynamic advancing (θ_A) and receding angles (θ_R) were recorded while the probe fluid was added to and withdrawn from the drop, respectively. Scanning electron microscopy (SEM) was performed using a JEOL 100CX STEM. Peel tests were performed manually with an angle of 180° between the delaminated film surface and tape (3M #810).

Substrate Preparation

PET films (Mylar, 5 mil) were rinsed with distilled water and methanol, extracted in refluxing hexane for 2 h, and then dried (room temperature, 0.01 mm, >24 h). PET-CO_2^- was prepared by introducing clean PET to 1 M NaOH aqueous solution for 16 min at 60 °C. The film was subsequently rinsed with 0.1 M HCl, distilled water (twice), methanol, and then hexane, and dried at reduced pressure. PET-NH_3^+ was prepared by immersing clean PET film in PAH solution (167 mg PAH in 120 ml water, pH = 11.5) for 1 h at room temperature. The film was removed from the solution, rinsed with water three times and introduced to water adjusted to pH = 2.2 for 30 min. After rinsing with three aliquots of water, the PET-NH_3^+ film samples were dried at reduced pressure.

Layer-by-Layer Deposition

Adsorptions were carried out at room temperature in open beakers containing unstirred polyelectrolyte solutions that were prepared fresh every day. After every layer deposition, film samples were rinsed with water (purified as described above) three times.

After the desired number of layers had been deposited, films were dried at reduced pressure before characterization.

Results and Discussion

Substrate Preparation

Commercial poly(ethylene terephthalate) film (5 mil duPont Mylar) was used to prepare three substrates for layer-by-layer deposition. The film was rinsed with water and then methanol, extracted with hexane and dried to constant mass to prepare "unmodified polyester" (PET).

As discussed in Chapter 1, PET was hydrolyzed using 1 M aqueous NaOH for 16 min at 60 °C and subsequently protonated to prepare PET-CO_2H. This surface contains a mixture of carboxylic acid and alcohol functional groups and is negatively charged at sufficiently high pH. The conditions for hydrolysis were chosen to maximize surface carboxylic acid concentration and minimize polymer degradation (hydrolysis results in chain scission). Kinetics of the hydrolysis of PET at 60 °C were monitored by water contact angles, XPS, and gravimetric analysis. After reaction for 16 min, the contact angles reached a minimum value (θ_A/θ_R = 62°/16°), oxygen content as determined by XPS (15° take-off angle) was maximized (O, 30.1%; C, 69.9%) and no degradation (mass loss) was observed. PET exhibits contact angles of θ_A/θ_R = 77°/55° and XPS atomic concentrations of O, 28.5%; C, 71.5%. Longer hydrolysis times did not lead to lower contact angles or increased oxygen content. That PET-CO_2H is capable of supporting negative charge is indicated by the dependence of contact angle on the pH of the probe fluid. Figure 2.4 shows the advancing contact angles of buffered aqueous solutions on PET-CO_2H as well as on unmodified PET. The lower contact angles at higher pH values indicate the presence of -CO_2H that ionizes to -CO_2^- groups. The advancing contact angle data for PET are not completely independent of the pH of the probe fluid. Contact

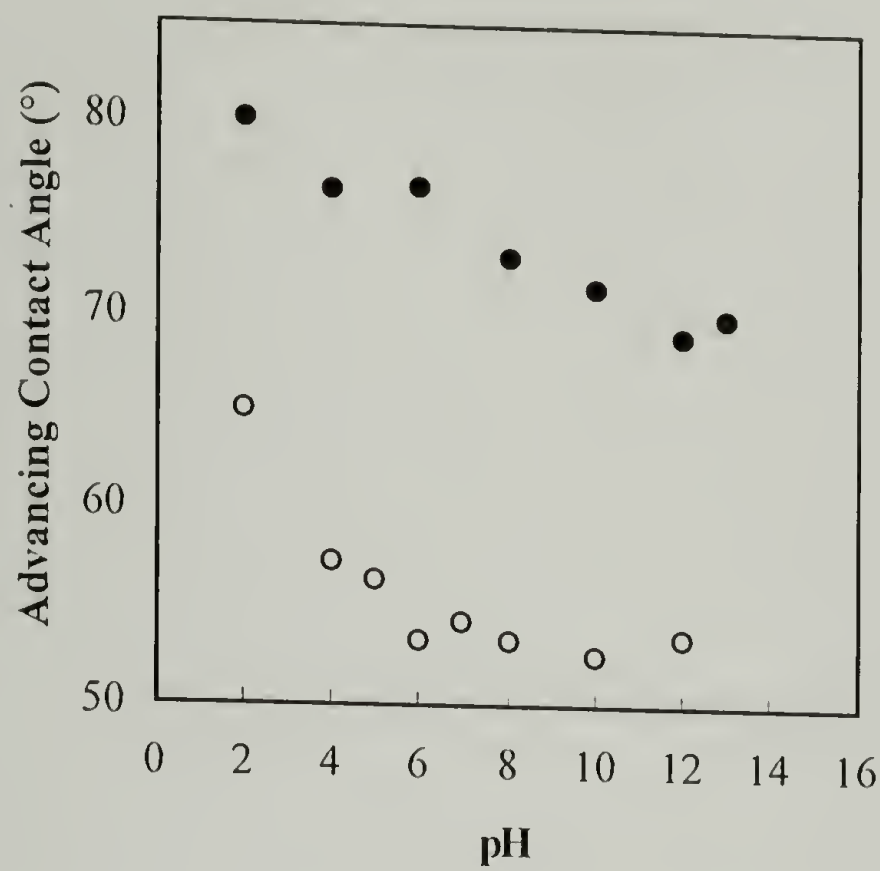

Figure 2.4. Contaet angles (θ_A) of buffered aqueous solutions on PET (●) and PET-CO_2H/PET-CO_2^- (○) film.

angles of higher pH solutions are slightly lower as hydrolysis of PET oecurs during eontact angle analysis. This is observed elearly in the receding eontact angle data. PET exhibits $\theta_R = 55°$ with water, $\theta_R = 42°$ with pH = 10 buffer and $\theta_R = 22°$ with pH = 12 buffer. Receding contact angles of fluids that are reaetive toward the substrate depend on the conditions (rate) of determining these dynamic values.

A PET substrate capable of supporting a positive eharge (PET-NH_3^+) was prepared by allowing poly(allylamine hydroehloride) (PAH) to adsorb to/reaet with PET at elevated pH (as the free base). PAH adsorbs to PET at low pH (see below), but reaets by amidation at high pH as the free base to form a covalently attached PAH layer. The adsorption/reaetion of PAH with PET was studied over the pH range of 1.87 to 11.84. Figure 2.5 shows XPS atomic eomposition data (nitrogen, 15° take-off angle) for PET samples treated with aqueous PAH (0.02 M repeat units) at room temperature for 1 h as

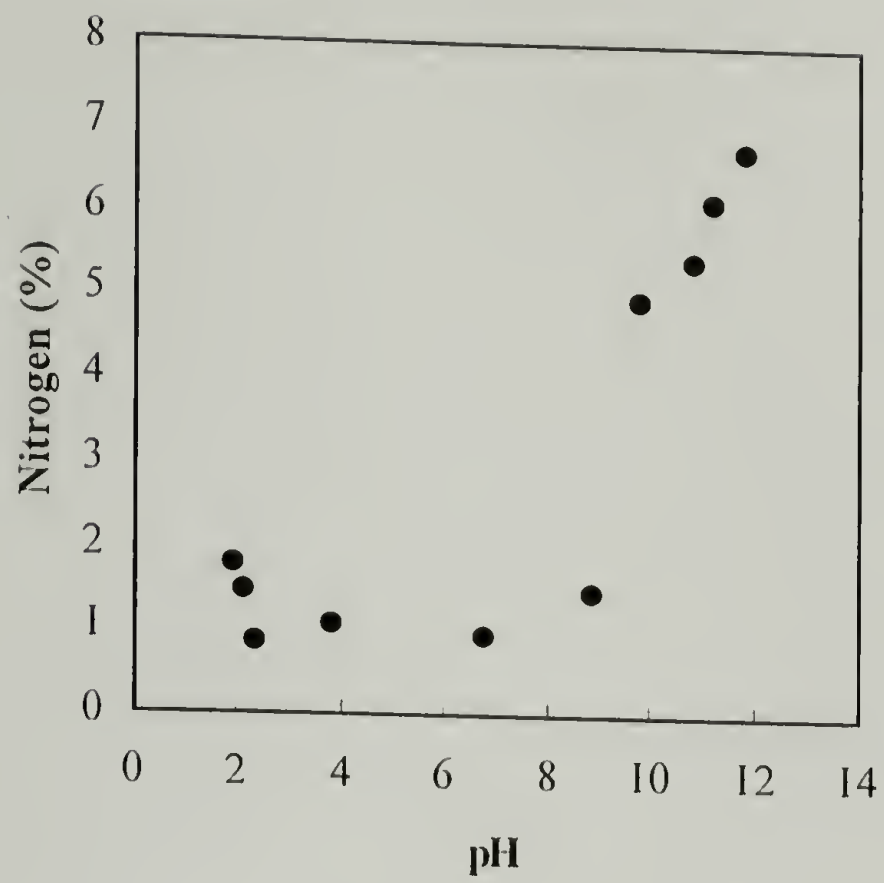

Figure 2.5. XPS atomic concentration (nitrogen) at 15° take-off angle for PET film samples treated with aqueous PAH as a function of pH.

a function of solution pH. A sharp increase in nitrogen content occurs at pH = ~10. The pKa of PAH is ~10.6,[37,38] thus the sharp increase can be attributed to the loss of charge-charge repulsions in deprotonated PAH. XPS analysis indicates that amidation is extensive. Atomic composition of the sample prepared at pH = 11.84 was: C, 82.3%; O, 10.63%; N, 6.7%; amidation is indicated by the low oxygen content (loss of high oxygen content ethylene glycol). A physisorbed layer of PAH (C:N = 3) on PET (C:O = 2.5) with this nitrogen content would have an atomic composition of C, 72.4%; O, 20.9%; N, 6.7%. Amidation is also indicated from the binding energy of the N_{1s} photoelectron line in samples prepared at high pH as shown in Figure 2.6. PAH adsorbed from low pH solutions exhibits a peak with a N_{1s} binding energy of ~403 eV (a). The corresponding photoelectron line for PAH adsorbed at high pH is ~400 eV (b). The 3 eV difference in binding energy is due to the fact that N_{1s} electrons in $-NH_3^+$ are more strongly bound

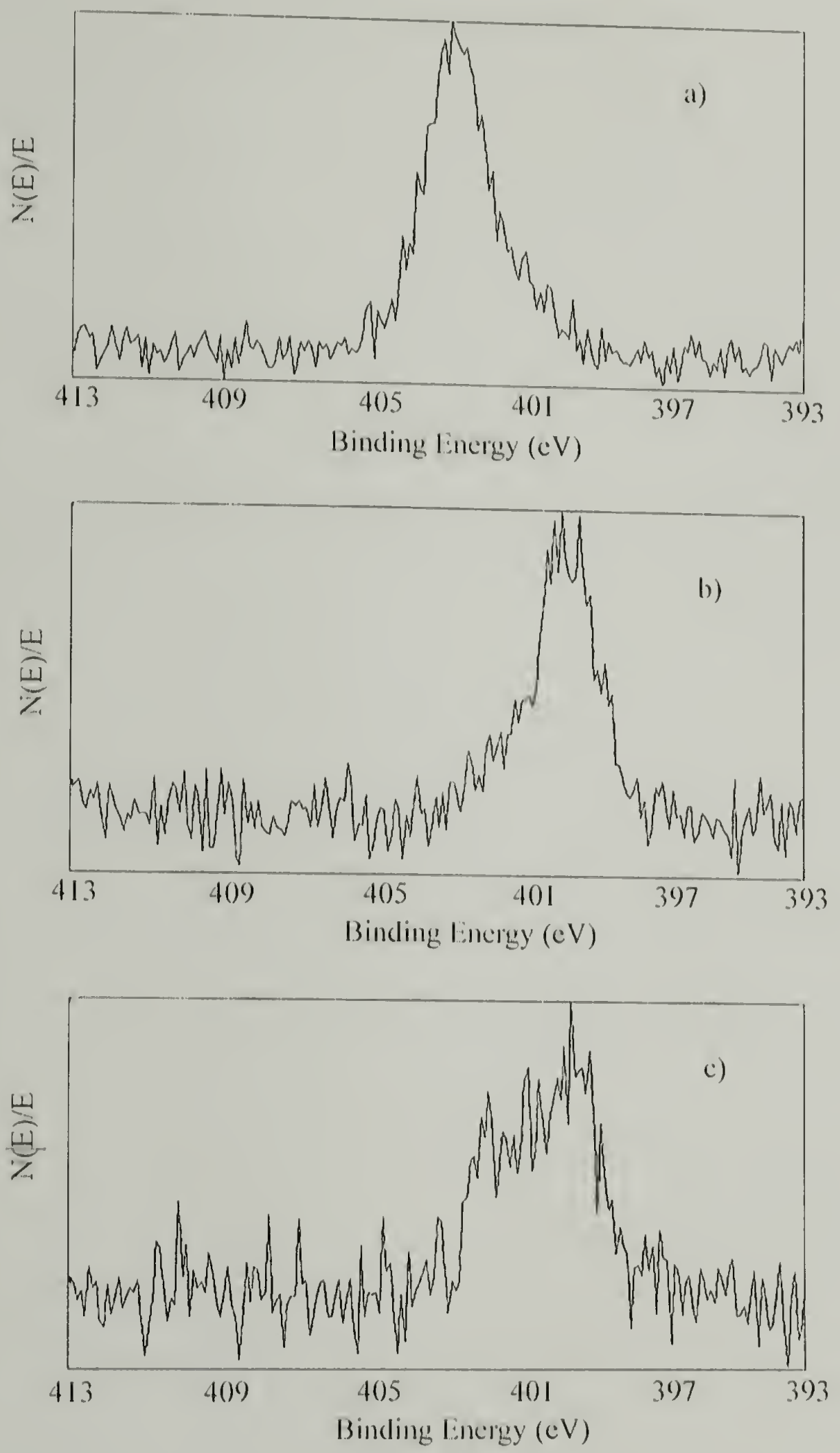

Figure 2.6. XPS spectra of N_{1s} regions: a) 18 layers adsorbed onto PET at pH = 2.2; b) PAH adsorbed onto PET at pH = 11.21; c) PAH adsorbed onto PET at pH = 11.21 followed by protonation at pH = 1.44.

than in -NH_2/-CONH-. Protonation (exposure to pH = 2.2 solution) produced a broad N_{1s} line spanning the 400-403 eV range indicating the presence of both amide and -NH_3^+ (c).

PET-NH_2 samples prepared at high pH contain physisorbed poly(allylamine) as well as chemisorbed (covalently attached through amide linkages) poly(allylamine). As shown in Table 2.1, kinetics of the adsorption/reaction (amidation) at pH = 11.5 were studied to 7 h; the nitrogen content reached a plateau value of ~6.5% (15° take-off angle) after 30 min. Samples prepared at pH = 11.5 for 60 min were soaked in pH = 2.2 solution and desorption kinetics were determined to 100 min. As shown in Table 2.2, the nitrogen content decreased to a minimum value ~5 % after 10 min. PET- NH_3^+ samples used for further experiments were prepared by adsorption of/reaction with poly(allylamine) (0.02 M repeat units) for 60 min at pH = 11.5 followed by desorption for 30 min at pH = 2.2. Scheme 2.1 summaries the routes to the charged substrates used for layer-by-layer adsorption. In an attempt to determine relative charge densities of the PET-NH_3^+ and PET-CO_2^- substrates, we reacted PET-CO_2H with 1,1'-carbonyldiimidazole, a reagent that converts carboxylic acids to acyl imidazolides.

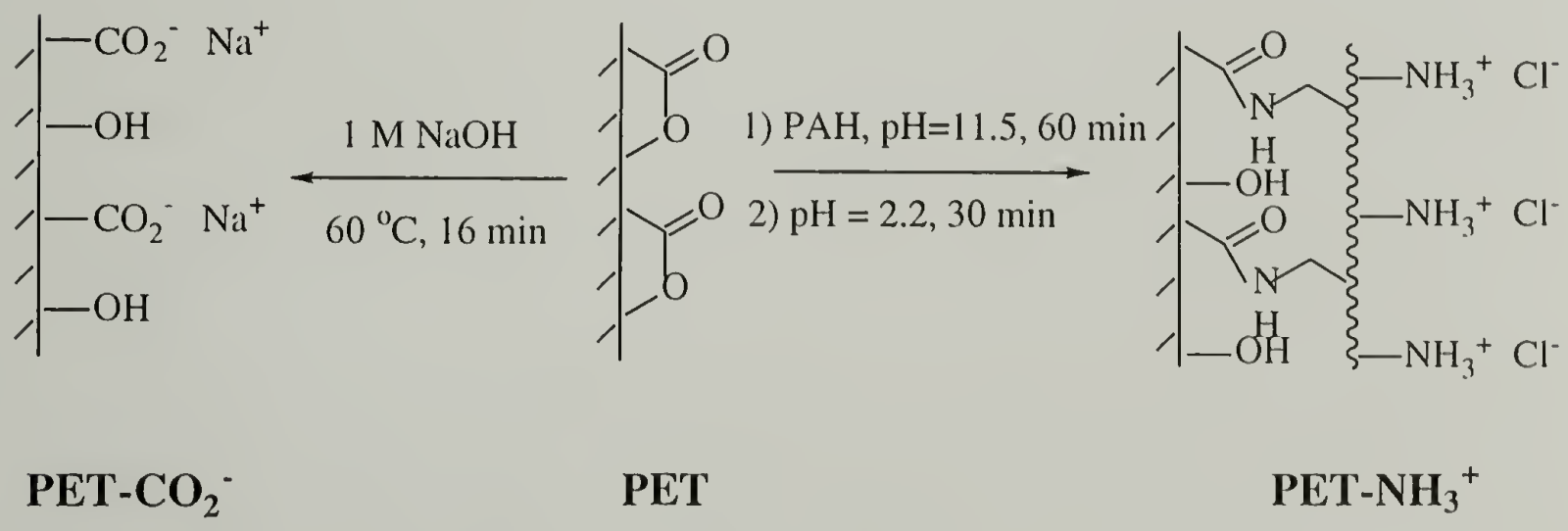

Scheme 2.1. Substrates preparation for layer-by-layer deposition

XPS indicates that there is ~0.7% nitrogen on the reacted surface (there are two nitrogen atoms per carboxylic acid group). This corresponds to about one carboxylic acid functional group per twenty PET repeat units. There is ~5 % nitrogen on the PET-NH_3^+ surface and about half of that is present as PET-NH_3^+ (the nitrogen peak at ~403 eV) and the other half is due to -CONH- (the peak at ~400 eV). The charge density on the PET-NH_3^+ surface is thus significantly greater (~7-fold) than on PET-CO_2^- (assuming that the reaction with 1,1'-carbonyldiimidazole is quantitative).

Table 2.1. Kinetics study of amidation of PET (pH = 11.5); XPS atomic composition data.

	15°			75°		
Time (hr)	%C	%O	%N	%C	%O	%N
0.5	71.48	21.82	6.70	68.89	26.27	4.84
1	70.75	23.13	6.12	68.48	27.06	4.45
2	71.37	21.85	6.77	68.41	27.31	4.28
4	71.15	23.41	5.44	69.14	27.59	3.27
7	71.56	21.82	6.62	68.93	26.60	4.47

Table 2.2. Kinetics study of desorption of PAH from amidated PET (pH = 2.2); XPS atomic composition data.

	15°				75°			
Time (min)	%C	%O	%N	%Cl	%C	%O	%N	%Cl
10	71.70	22.86	4.91	0.53	69.76	26.73	3.15	0.37
30	71.00	23.49	5.35	0.16	68.34	28.17	3.44	0.05
60	71.35	23.02	5.24	0.39	68.84	27.37	3.48	0.31
100	69.97	24.24	5.08	0.71	68.14	27.99	3.37	0.50

Initial Polyelectrolyte Adsorptions

Conditions for layer-by-layer deposition of poly(allylamine hydrochloride) (PAH) and poly(sodium styrenesulfonate) (PSS) were modeled after those reported by Decher[1,2] for inorganic substrates modified by silanation to contain ammonium ions. PAH was used as the polyelectrolyte for the first layer adsorption[39] to PET and PET-CO_2^-; PSS was used as the initial polyelectrolyte for PET-NH_3^+. For consistency, this PSS layer is referred to as the second layer and the covalently attached PAH is regarded as the first layer. Thus all samples described that contain an even number of layers have PSS as the outermost layer and samples with an odd number of layers contain PAH as the outermost layer.

A series of initial experiments were carried out to compare polyelectrolyte adsorption behavior onto the organic substrates with the reported results[1,2] for inorganic substrates. Adsorption kinetics, polyelectrolyte concentration effects and the effect of ionic strength of the solution were studied. XPS atomic composition data for the first layer (PAH) adsorption onto PET and PET-CO_2^- as a function of ionic strength are presented in Tables 2.3 and 2.4. The added salt is effective at screening out charge-charge replusions along the polyelectrolyte backbone to increase the adsorbed amount. The effect of solution ionic strength is discussed again below and is similar to that observed for inorganic substrates. PAH concentration was varied from 0.006 M to 0.024 M (repeat units) and PSS concentration was varied (for the second layer adsorption to PET) from 0.008 M to 0.025 M (repeat units). As shown in Tables 2.5 and 2.6, there was no variation in adsorbed amount as determined by XPS over these concentration ranges. Kinetics, as shown in Table 2.7 and 2.8, indicates that adsorption is rapid when driven by electrostatic interaction (substrate and polyelectrolyte are charged oppositely), reaching a final adsorbed amount (we consciously do not use the term equilibrium[40]) in less than 10 min. The adsorption is noticeably slower when the surfacc is neutral PET. The adsorbed amount of PAH (0.02 M repeat units in 0.01 M HCl - pH = 2.2) on PET increased with

Table 2.3. XPS atomic concentration data for 1st layer (PAH) adsorption on PET as a function of ionic strength.

	15°				75°			
$[MnCl_2]$ (M)	%C	%O	%N	%Cl	%C	%O	%N	%Cl
0	68.30	30.46	1.23		67.33	31.95	0.71	
0.05	68.73	30.06	1.08	0.13	67.41	31.77	0.74	0.08
0.1	68.62	30.21	1.09	0.08	67.55	31.84	0.56	0.05
0.5	66.81	30.67	2.15	0.36	65.22	33.18	1.35	0.25
1	60.67	35.17	2.32	1.83	57.72	39.25	1.86	1.18

Table 2.4. XPS atomic concentration data for 1st layer adsorption (PAH) onto PET-CO_2^- (pH = 8, 1 hr adsorption) as a function of ionic strength.

	15 deg.				75 deg.			
[NaCl] (M)	%C	%O	%N	%Cl	%C	%O	%N	%Cl
0	72.46	25.53	1.9	0.11	70.43	27.74	1.76	0.07
0.1	71.08	26.46	2.05	0.40	70.42	27.35	1.92	0.31
0.2	70.55	26.49	2.32	0.64	69.57	27.43	2.30	0.71
0.5	70.58	26.34	2.48	0.60	69.67	27.58	2.24	0.51
1	70.69	24.28	3.05	1.07	70.21	26.31	2.83	0.35

Table 2.5. XPS atomic concentration data for 1st layer adsorption (PAH) onto PET (with no salt addition) as a function of PAH concentration.

PAH Conc.	15°			
(mg/120mL H_2O)	%C	%O	%N	%Cl
0	69.05	30.95	0	0
50	71.00	27.64	0.84	0.52
100	69.50	29.81	0.62	0.07
150	70.14	28.72	0.72	0.43
167	68.30	30.46	1.23	N/A
200	71.73	26.80	0.87	0.60

Table 2.6. XPS atomic concentration data for 2nd layer adsorption (PSS) onto PET-PAH (with 1 M $MnCl_2$ addition) as a function of PSS concentration.

PSS Conc.	15°				75°			
(mg/120mL H_2O)	%C	%O	%S	%N	%C	%O	%S	%N
150	69.73	27.83	1.36	1.07	66.13	31.76	1.15	0.96
300	62.85	35.33	0.90	0.93	61.18	37.59	0.53	0.71
360	71.74	25.82	1.50	0.93	69.87	28.61	0.75	0.77
450	69.98	28.20	0.99	0.82	68.67	29.92	0.82	0.59

Table 2.7. XPS atomic concentration data from the kinetics study of 1st layer adsorption (PAH) onto PET (with no salt addition).

	15°			75°		
Time (min)	%C	%O	%N	%C	%O	%N
1	68.83	30.60	0.57	68.19	31.50	0.31
10	67.77	31.58	0.64	66.47	33.07	0.46
30	68.30	30.46	1.23	67.33	31.95	0.71
370	70.96	27.76	1.27	68.92	30.38	0.70

Table 2.8. XPS atomic concentration data from the kinetics study of 2nd layer adsorption (PSS) onto PET-PAH (with 1 M $MnCl_2$ addition).

	15°				75°			
Time (min)	%C	%O	%S	%N	%C	%O	%S	%N
1	68.83	29.77	0.70	0.70	66.75	32.78	0	0.48
10	71.74	25.82	1.50	0.93	69.87	28.61	0.75	0.77
30	71.80	27.14	1.06	0	69.12	29.25	0.76	0.87
100	72.91	25.34	1.75	0	71.10	26.65	1.28	0.97

adsorption time up to 30 min as assessed by XPS. The nitrogen content of the PET-PAH surface did not increase further after 370 min total adsorption time. An adsorption time of 60 min for deposition of the first PAH layer on PET was used in all subsequent experiments. The kinetics of adsorption of the second layer (PSS) onto PET-PAH indicates that a rapid adsorption occurs, complete in less than 10 min. Adsorption times of 20 min were used for all experiments described except for adsorption of the first PAH layer onto neutral PET.

The adsorption of PAH onto PET-CO_2^- (PET-CO_2H at low pH) warrants mention because of its dependence on pH. Figure 2.7 shows XPS nitrogen atomic concentration data as a function of the pH of the PAH solution (0.02 M repeat units, 60 min adsorption time).

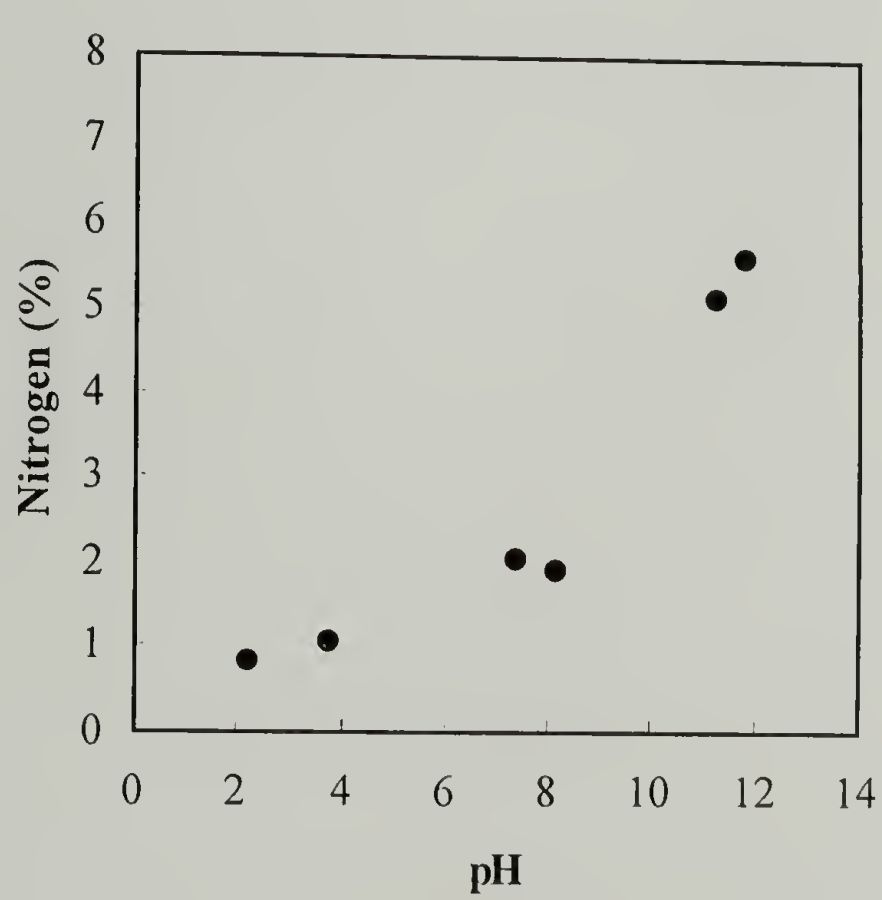

Figure 2.7. XPS atomic concentration (nitrogen) for PET-CO_2^- film samples with one PAH layer adsorbed as a function of pH of the adsorption solution.

Three distinct regions are evident. At low pH the nitrogen content is low; the charged polymer (PAH) adsorbs to the neutral PET-CO_2H surface with low coverage. The interaction between the polyelectrolyte and the surface is weak (likely hydrogen bonding between ammonium protons and acid carbonyl groups[41]) and charge-charge repulsions between ammonium ions force the chain to spread out on the surface leading to a sub-monolayer coverage. At pH = 6-8 the nitrogen content is significantly higher. In this pH range both the polyelcetrolyte and PET-CO_2^- surface (see Fig. 2.4) are charged and the electrostatic attraction leads to more dense coverage. At high pH PAH is neutral and adsorbs to the charged PET-CO_2^- surface as a more collapsed coil than when protonated giving rise to high nitrogen content. Amidation (see above) may occur under these conditions as it does with PET. Adsorptions of polyelectrolytes on PET-CO_2^- in the experiments described below were carried out at pH = 8, conditions under which both the polyelectrolyte and the surface are charged.

Multilayer Assembly

Except for the conditions noted above, PAH/PSS multilayers were built up on PET, PET-CO_2^- and PET-NH_3^+ using conditions essentially identical to those reported for inorganic substrates. The effect of polyelectrolyte solution ionic strength was studied for PET. Substrates were dipped in 0.02 M polyelectrolyte solution (pH = 2.2, except for PET-CO_2^-, in which case pH = 8), removed after 20 minutes, rinsed with three aliquots of water and then dipped in the oppositely charged polyelectrolyte solution. After the desired number of layers were deposited, the polymer film - supported multilayers were rinsed a final three times with water and were dried at room temperature at reduced pressure before XPS and contact angle analyses.

Much of the details that follow concerns variable take-off angle XPS analysis of the multilayer films and the PET substrate immediately beneath the multilayer assembly. Survey and C_{1s} region spectra of a 4-layer film supported on PET-CO_2^- (PET-CO_2^--

PAH-PSS-PAH-PSS) are shown in Figure 2.8. Most of the features of interest are present in these spectra. The intensities of the N_{1s} (403 eV), and S_{2p} (167 eV) photoelectron lines can be used to assess the relative concentrations of PAH and PSS and degree of stratification (layer segregation) in the multilayers. The carbonyl C_{1s} photoelectron line is due entirely to the PET substrate; this peak decreases in intensity and eventually disappears as more layers are deposited. We can estimate (we could calculate if the mean free path were known) the thickness of the multilayer assemblies and individual layers from the decrease in intensity of this substrate peak.

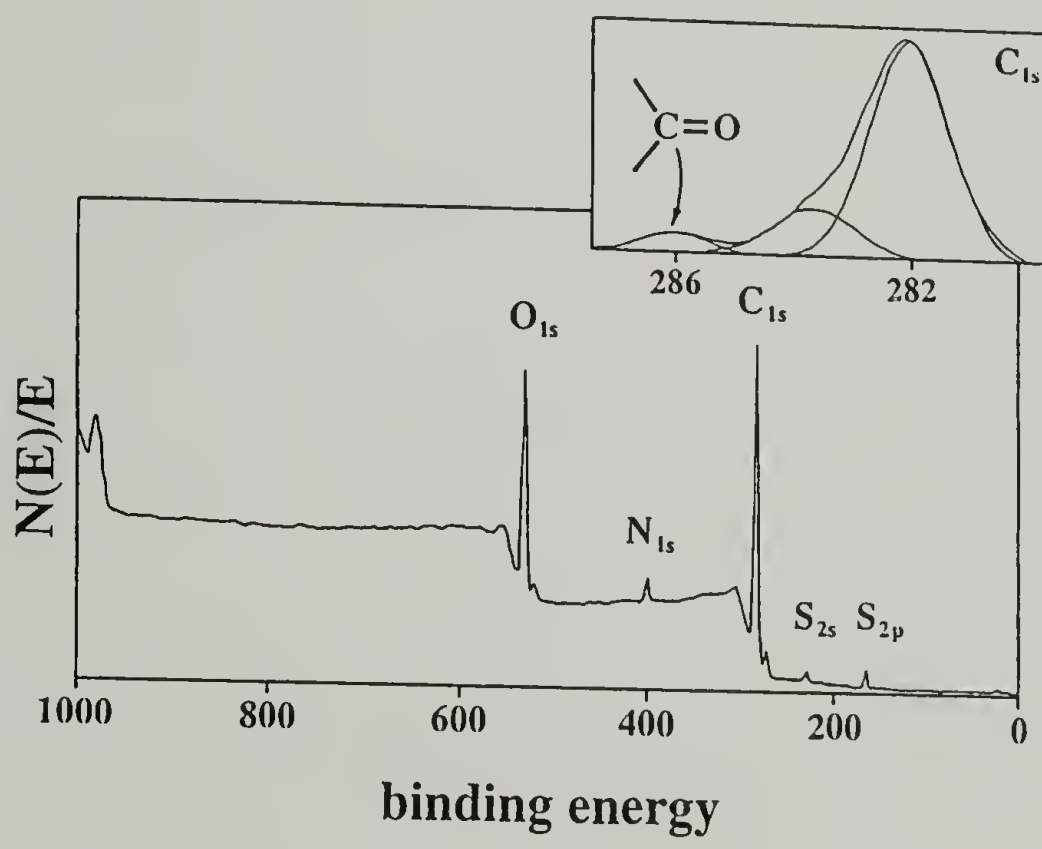

Figure 2.8. Survey and C_{1s} region XPS spectra of a 4-layer polyelectrolyte film supported on PET-CO_2^-.

Multilayer Deposition on PET. Three series of experiments were carried out to surface modify the neutral PET substrate using layer-by-layer deposition. In these experiments manganese chloride (1.0 M $MnCl_2$) was added to either both PAH and PSS solutions, only the PSS solution or neither polyelectrolyte solution. The addition of salt

has been demonstrated[1,2] to increase the thickness of the layers by screening charge-charge repulsions during adsorption. Figure 2.9 shows XPS data indicating that this effect is also observed with the PET substrate. Plotted is the atomic concentration of carbonyl carbons (as percentage of total carbon detected) versus the number of layers in the supported multilayer. The carbonyl C_{1s} photoelectrons (Fig. 2.8) originate only in the substrate and this signal is attenuated as polyelectrolyte layers are applied. The data clearly indicate the effect of $MnCl_2$ on thickness. At 15° take-off angle the carbonyl C_{1s} peak is completely attenuated after application of 4 layers when $MnCl_2$ is present in both solutions, 7 layers when $MnCl_2$ is present in the PSS solution and ~15 layers when no $MnCl_2$ is present. The 75° data exhibit the same trend. The scatter in the data is due in large part to the fact that separate samples were used for analysis of each thickness (number of layers) multilayer. Samples were not used after analysis as substrates for further depositions.

The C_{1s} peak intensity should decrease exponentially with the build-up of the multilayers and the data (Fig. 2.9) qualitatively fit the predicted decay, but the take-off angle dependence is confusing. Equation 2.1[42] expresses the attenuation of photoelectron intensity in solids as a function of sampling depth where N_o is the number of photoelectrons that originate at depth t, N is the number of photoelectrons emitted from

$$N = N_o e^{-t/\lambda \sin\theta} \tag{2.1}$$

the solid that have not been inelastically scattered, λ is the mean free path of the electron and θ is the take-off angle. This expression indicates that 95% of detected photoelectrons originate in the outermost $3\lambda\sin\theta$, thus the carbonyl C_{1s} peak should be attenuated to 5% of its original intensity when the multilayer film thickness is $3\lambda\sin\theta$. Equation 2.1 also indicates that the spectra recorded at a take-off angle of 15° assess the composition of the

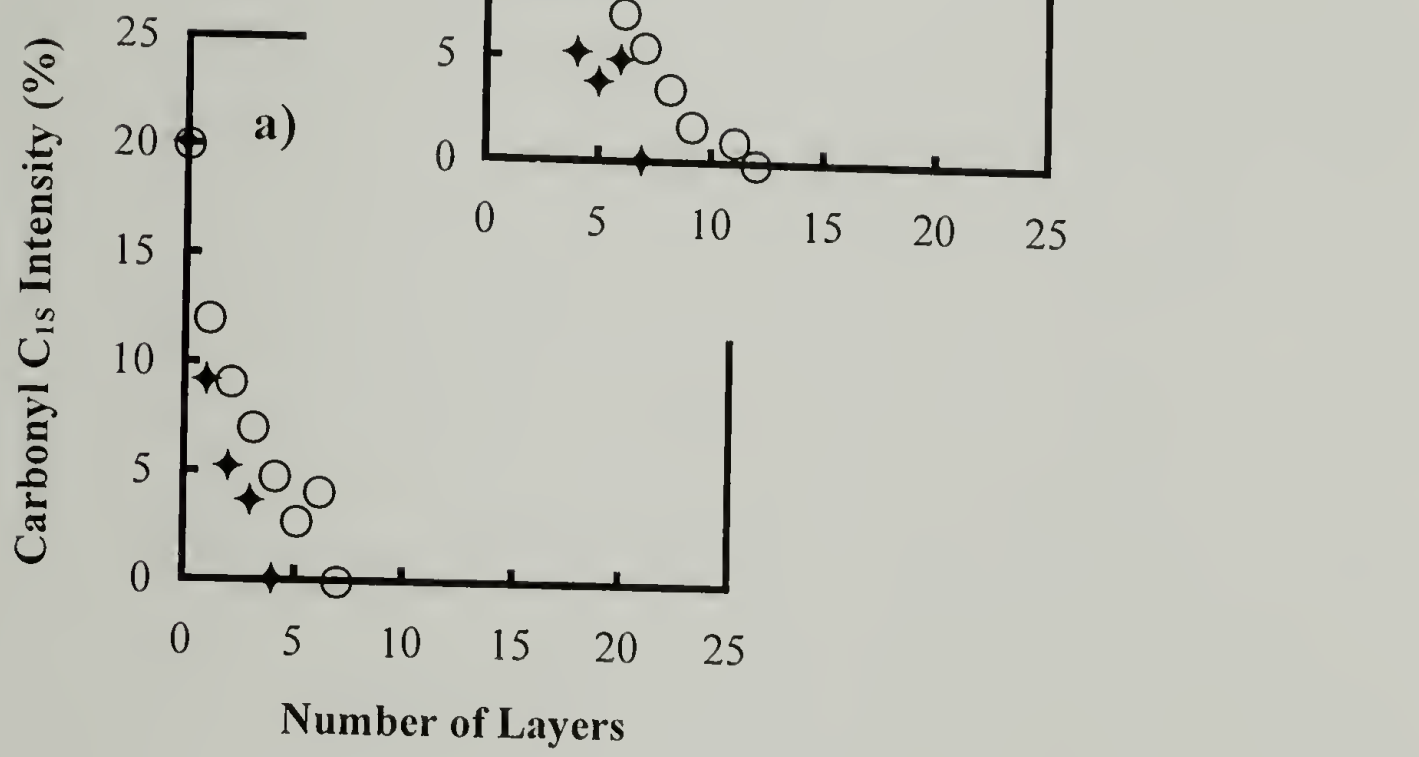

Figure 2.9. Carbonyl C_{1s} intensity (expressed as the percentage of total carbon intensity) versus the number of layers in the multilayer assembly: a) $MnCl_2$ present in both PAH and PSS solutions (layers are thickest), b) $MnCl_2$ present in only the PSS solution, c) no $MnCl_2$ in polyelectrolyte solutions (layers are thinnest). The closed (✦) and open (○) symbols are data recorded at 15° and 75° take-off angles, respectively.

outermost ~27% of the region analyzed at 75° take-off angle. These principles predict that the carbonyl C_{1s} peak intensity should decrease exponentially from 20% (2 of 10 carbons in the PET repeat unit are carbonyls) to 1% when the multilayer thickness reaches $3\lambda\sin\theta$ (0.78λ for 15° and 2.90λ for 75°) and that it should take ~4 times as many layers to attenuate the 75° carbonyl signal to the same extent that the 15° signal is attenuated.

The data in Fig. 2.9 do not support the latter prediction; in all three cases fewer than twice as many layers are required to attenuate the 75° signal to the same extent that the 15° signal is attenuated. Our explanation for this inconsistency is that the mean free paths of electrons in these layered materials have an angular dependence: Rearranging eq. 2.1 and substituting nz for t, where n is the number of layers and z is the average thickness of the individual layers yields the expression in equation 2.2.

$$- \ln(N/N_o)\sin\theta = nz/\lambda \qquad (2.2)$$

In Figure 2.10 are plots of $- \ln(N/N_o)\sin\theta$ versus n where N is the atomic concentration of carbonyl carbons (data from Fig. 2.9) and N_o is the carbonyl carbon concentration for virgin PET. The overall linearity of the data shows that individual layer thicknesses are close to constant and the slopes of the lines indicate the average layer thickness divided by the photoelectron mean free path. In each case, longer mean free paths (approximately twice as long) are indicated by the lower slopes of the 15° take-off angle data. Apparently the structure of these multilayer assemblies allows the "channeling" of electrons at angles close to the plane of layer build-up. The stratification of these structures is discussed below. An alternative explanation for the small take-off angle dependence is surface roughness. We discount this possibility because we have prepared modified PET surfaces using the same film that show pronounced take-off angle-dependent spectra. We have carried out limited scanning electron microscopy studies on

layer-by-layer assemblies on PET-NH_3^+ and PET-CO_2^- surfaces. In each case, the surfaces become smoother after 20 layers have been deposited (Figure 2.11).

We can estimate the thickness of the layers and multilayers using estimates of the electron mean free path. Values for λ in organic polymers are somewhat controversial ranging from the low values reported by Clark[43,44] to higher values reported by others.[45,46] Ashley and coworkers have developed a theoretical approach to the problem[47-50] and calculate mean free paths based on bulk density and molecular structure. The mean free paths of electrons in layer-by-layer assemblies have not been discussed in the literature and as discussed above are certainly a function of the supermolecular structure of the multilayers. We have calculated[31] a mean free path for Si_{2p} electrons in PAH/PSS multilayers using both XPS and X-ray reflectivity analysis of films built up on aminobutyldimethylmethoxysilane - treated silicon wafers. A film consisting of 8 layers (4 PAH/PSS bilayers) attenuates >95% of the Mg K_α - excited Si_{2p} photoelectron intensity at 75° take-off angle (is ~3λ thick) and is 61 Å thick (including the silane coupling agent) as assessed by X-ray reflectivity. A mean free path of ~20 Å for the Si_{2p} electron is indicated. The XPS data reported in this paper were acquired using Al K_α excitation; we calculate[51] a mean free path of ~19 Å for the C_{1s} photoelectron. The slopes of the 75° data in Fig. 2.10 yield average layer thicknesses of 6.1 Å, 4.2 Å and 2.0 Å for multilayers prepared with $MnCl_2$ added to both PAH and PSS solutions, only the PSS solution and neither polyelectrolyte solution, respectively. These values must be regarded only as estimates as we make the assumption that the mean free paths at 75° take-off angle in the PET-supported multilayers are the same as the value determined for the silicon-supported multilayer film. Nevertheless, the data indicate extremely thin individual layers, much thinner in the case of no added $MnCl_2$, than the layers that form on inorganic substrates. We emphasize that these are average thickness values determined from the slopes of the lines in Figure 2.10 (dividing the total multilayer assembly thickness by the number of layers) and that the individual layers, while uniform, are not

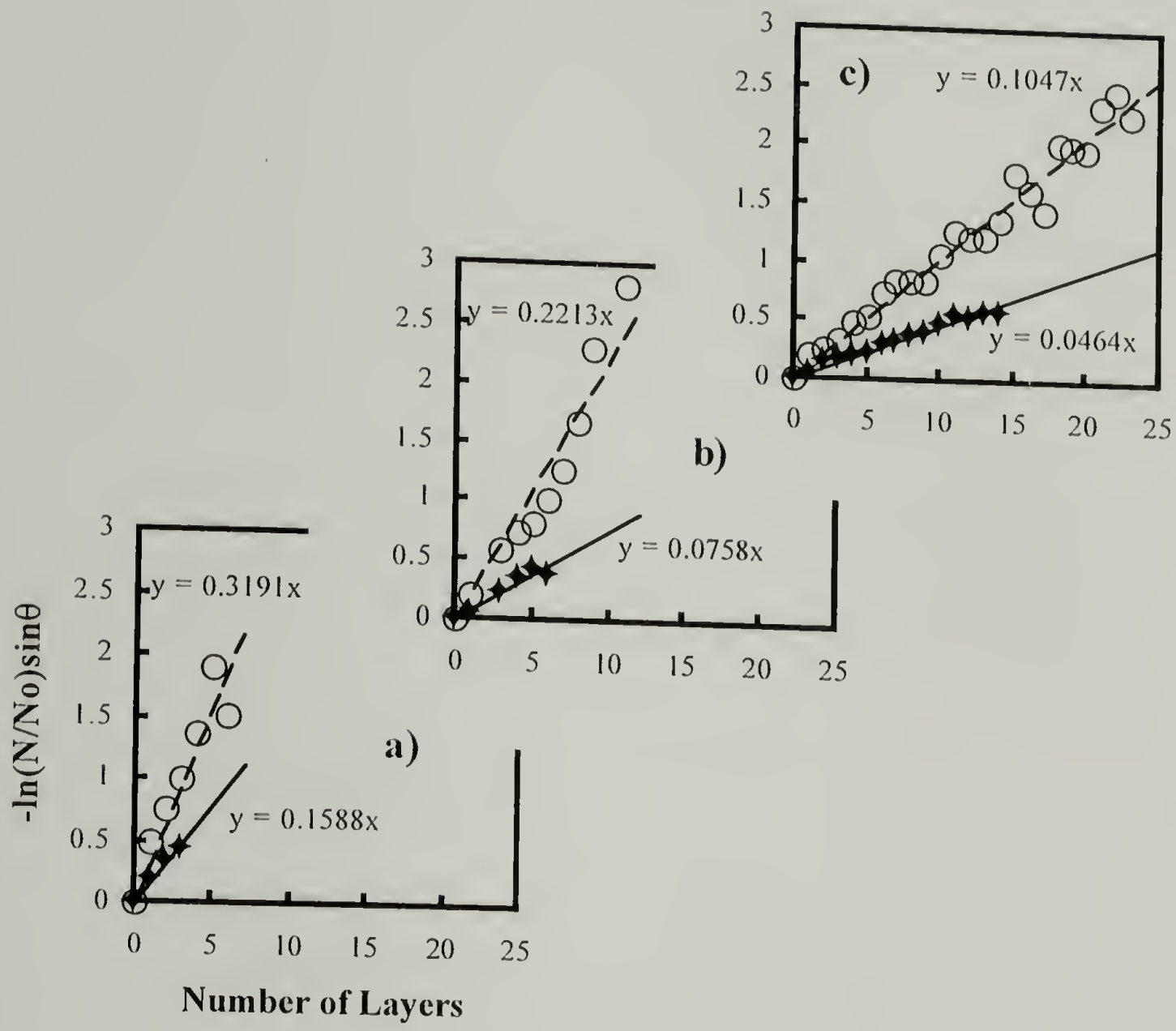

Figure 2.10. Plots of $-\ln(N/N_o)\sin\theta$ vs. number of layers in the multilayer film. The slopes of the lines indieate the ratio of the average layer thickness to the C_{1s} photoelectron mean free path: a) $MnCl_2$ present in both PAH and PSS solutions, b) $MnCl_2$ present in only the PSS solution, c) no $MnCl_2$ in polyelectrolyte solutions. The closed (✦) and open (○) symbols are data recorded at 15° and 75° take-off angles, respectively.

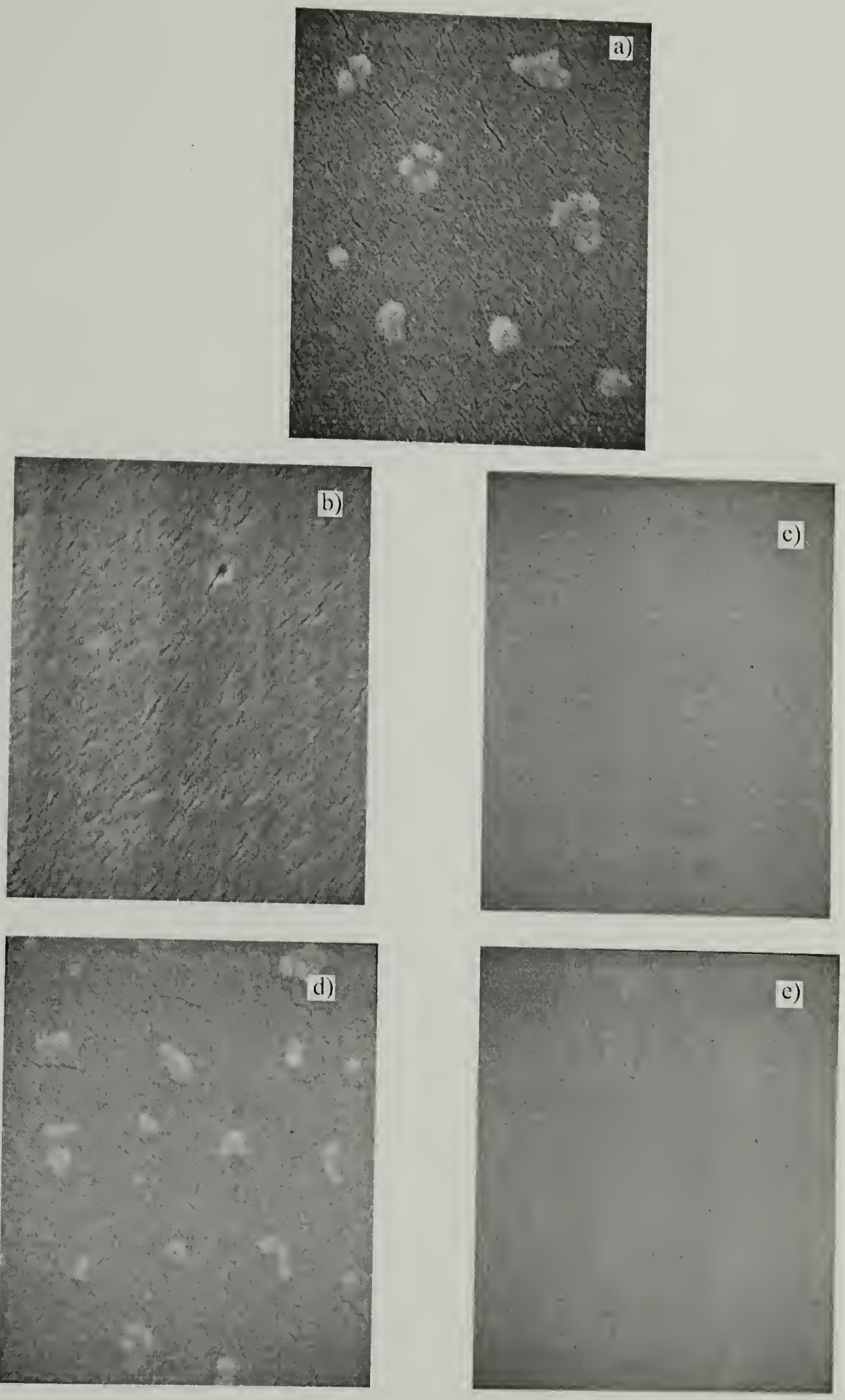

Figure 2.11. SEM photographs (30,000x) of substrates before and after layer deposition: a) clean PET; b) PET-CO_2^-; c) PET-CO_2^- with 20 layers; d) PET-NH_3^+; e) PET-NH_3^+ with 20 layers.

dense, close-packed monolayers, but are interdigitated at functional group dimensions. That the layers are quite rigorously stratified is discussed below. We believe that the multilayer assemblies are quite dense; gas permeability measurements[10, 31] on a very similar system (PAH/PSS multilayers supported on surface-oxidized poly(4-methyl-1-pentene) indicate that the multilayers exhibit good gas barrier properties.

XPS atomic composition data for nitrogen and sulfur are uniformly consistent with the carbonyl intensity data discussed above. Figure 2.12 shows plots of sulfur and nitrogen atomic concentration as a function of the number of layers in the multilayer film for the series of samples prepared with no added $MnCl_2$. The atomic composition levels after a sufficient number of layers (~15 at 15° and ~18 at 75° take-off angle) has been deposited to completely attenuate the C_{1s} and O_{1s} photoelectrons of PET. The unexpectedly small dependence on take-off angle is apparent, again indicating an angular dependent electron mean free path. The sulfur and nitrogen atomic composition for the series of samples prepared with $MnCl_2$ in both solutions level after ~5 layers (15°) and 7 layers (75°) have been adsorbed. Corresponding data for the samples prepared with $MnCl_2$ in only the PSS solution level at ~8 (15°) and 12 (75°) layers.

Sulfur:nitrogen atomic ratio data for the three series of polyelectrolyte multilayers are shown in Figure 2.13. The ratios shown were obtained using 75° take-off angle data; 15° data yield nearly identical ratios due to the near absent take-off angle dependence and the fact that the substrate contains no nitrogen or sulfur. These ratioed data are shown to make three points concerning the structures of the multilayers. First, there is a pronounced odd-even trend in all three sets of data that persists to high layer number, where the addition of one more PSS or PAH layer does not greatly affect the composition of the multilayer assembly. The S:N ratio is relatively high when the outermost layer is PSS and relatively low when the top layer is PAH. This suggests that the layers, even though they are not close-packed monolayers, are stratified. Second, the amplitude of the odd-even trend increases with increasing layer thickness; the exponential decay of

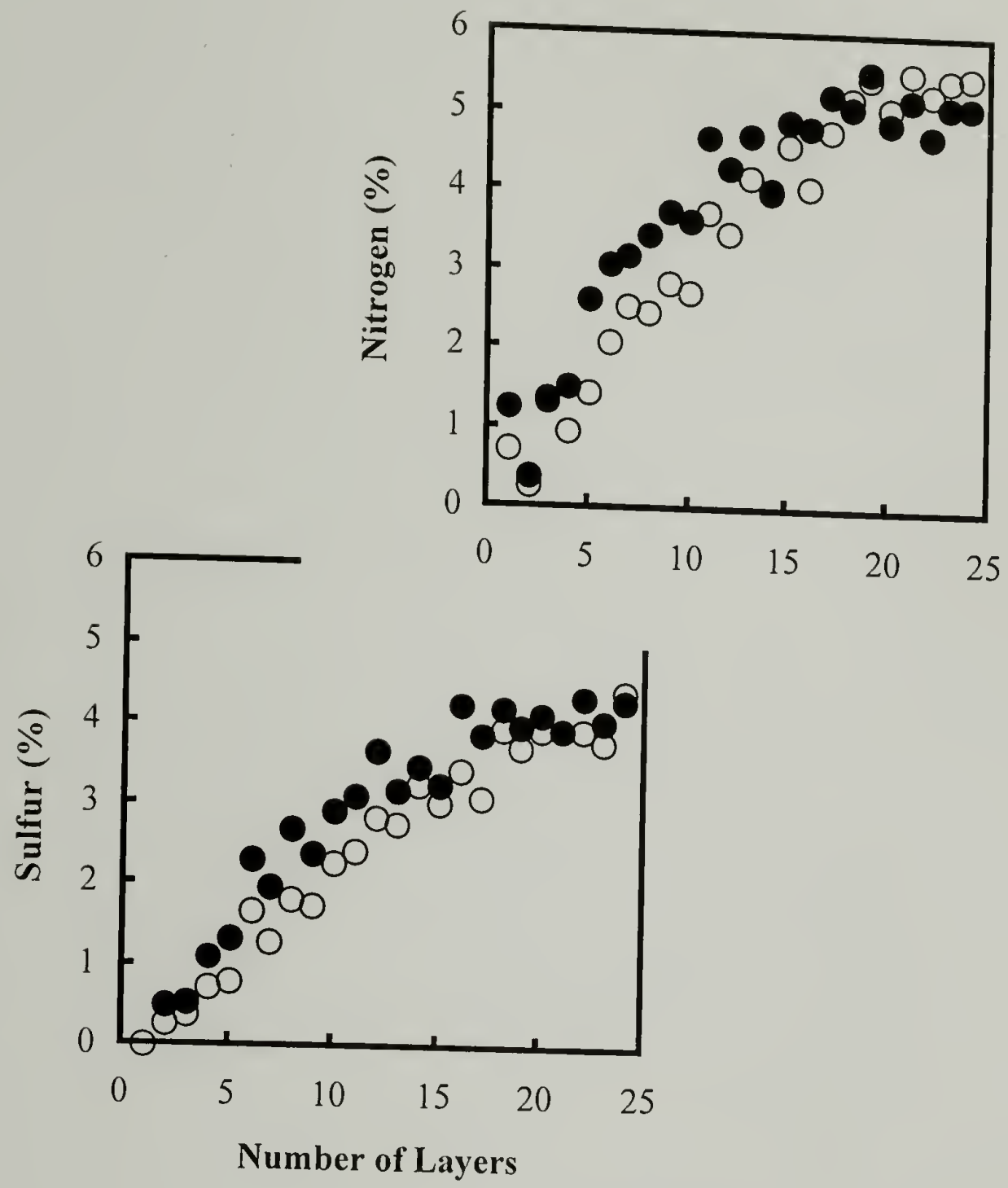

Figure 2.12. Sulfur and nitrogen atomic concentrations determined at 15° (●) and 75° (○) take-off angles as a function of the number of layers in the multilayer film. The multilayers were built up on PET using polyelectrolyte solutions containing no added salt.

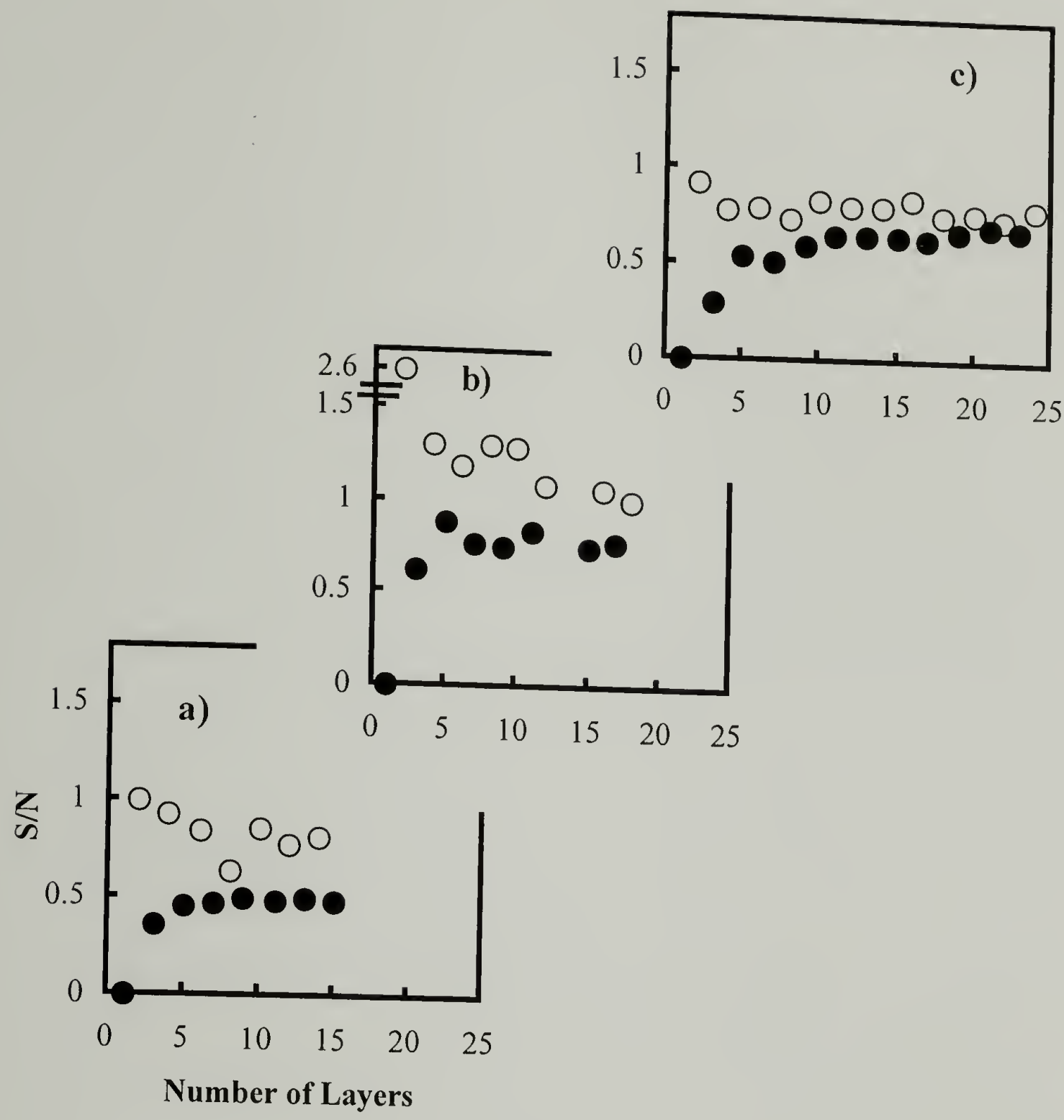

Figure 2.13. Sulfur:nitrogen atomic ratio data (75° take-off angle data) for the three series of polyelectrolyte multilayers: a) $MnCl_2$ present in both PAH and PSS solutions, b) $MnCl_2$ present in only the PSS solution, c) no $MnCl_2$ in polyelectrolyte solutions: odd number of layers (●), even number of layers (○).

photoelectron intensity with depth (eq. 2.1) results in an effective enhancement of the signal from the outermost layer and this enhancement is greater with increasing layer thickness. Third, the stoichiometry of the assembly process (ammonium ion:sulfonate ion ratios) is evident from this data and we note that it is different for each of the series studied. With no $MnCl_2$ in the polyelectrolyte solutions the S:N ratio is ~0.75 indicating that there are approximately 4 ammonium ions per 3 sulfonate ions in the multilayer assembly. With $MnCl_2$ present only in the PSS solution, the ratio is close to unity. With $MnCl_2$ present in both solutions the S:N ratio is ~0.65 which indicates a ~3:2 ratio of ammonium to sulfonate ions. These data emphasize two interesting features of layer-by-layer deposition: the self-assembly process exerts its own stoichiometric control and a particular stoichiometry is not required.

Water contact angle data also indicate the stratified structure of the multilayer assemblies with odd-even trends.[52] Figure 2.14 shows advancing contact angle data for each of the three series of samples. Contact angle is in general a more surface-selective technique than XPS and the contact angle data level after fewer layers are applied (compare with figures 2.9 and 2.10). The contact angles for samples with an odd number of layers (PAH as the outermost layer) are different for each of the series of samples: when $MnCl_2$ was used in both polyelectrolyte solutions, $\theta_A = 70° \pm 1°$ (for 3, 5, 7, 9 and 11-layer films), for samples prepared with $MnCl_2$ in only the PSS solution $\theta_A = 60° \pm 1°$ (for 5, 7, 15 and 17-layer films) and for samples prepared without $MnCl_2$, $\theta_A = 46° \pm 1°$ (for 9, 11, 13, 15 and 19-layer films). The increase in wettability with decreasing layer thickness is due to an increasing contribution to the contact angle from the underlying PSS layer, which is more wettable than PAH. There is less of a layer thickness effect for the samples containing an even number of layers (PSS as the outermost layer). For both series using $MnCl_2$ in the PSS solution, the contact angle levels at $\theta_A = 45° \pm 2°$ and for the series without $MnCl_2$, at $\theta_A = 53° \pm 1°$. The outermost PSS layer more effectively (than PAH) screens the underlying layer from the contact angle analysis. The receding

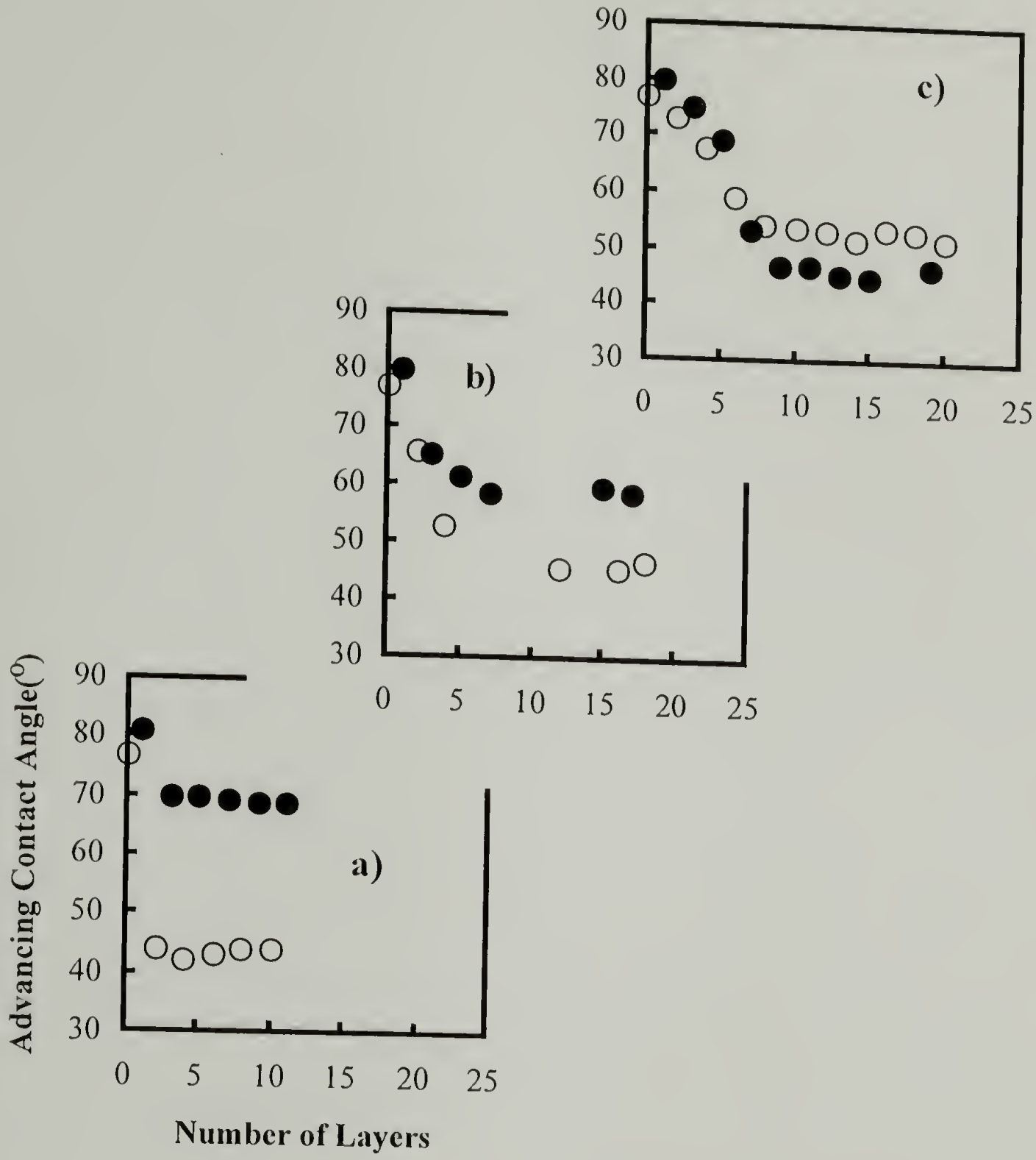

Figure 2.14. Advancing contact angle data for each of the three series of samples: a) $MnCl_2$ present in both PAH and PSS solutions, b) $MnCl_2$ present in only the PSS solution, c) no $MnCl_2$ in polyelectrolyte solutions: odd number of layers (●), even number of layers (○).

contact angle data are less lucid as the values for both odd and even number-of-layer samples are very similar. The series prepared with $MnCl_2$ in both polyelectrolyte solutions did exhibit a statistically significant odd-even trend (the other two series did not) with θ_R oscillating between $22° \pm 2°$ and $16° \pm 1°$.

Contact angles of buffered aqueous solutions on samples prepared with $MnCl_2$ only present in the PSS have also been studied. Advancing contact angles, θ_A, are plotted versus pH for samples with a PAH layer on the top (1, 3, 5, and 7 layers) and for samples with PSS as the outermost layer (2 and 4 layers) in Figures 2.15 and 2.16, respectively. When the strong polyelectrolyte, PSS is the top layer, θ_A has no dependence on the pH of the buffered solution. When the weak polyelectrolyte, PAH is the outermost layer, however, the advancing contact angles decrease at pH > 10 (near the pKa of PAH) for the 3, 5, 7 layer samples. This result is consistent with the earlier discussion that the outermost PSS layer more effectively (than PAH) screens the underlying layer from the contact angle analysis. The lack of pH dependence for the 1 layer sample is difficult to explain. The receding contact angles have very little pH dependence with all the samples studied.

We made attempts to follow the layer-by-layer assembly stoichiometry using XPS data for the counterion (manganese, sodium and chloride) concentrations. For the cases in which no $MnCl_2$ was added to the polyelectrolyte solutions and in which $MnCl_2$ was added to only the PSS solution, the atomic concentrations of sodium, chlorine and manganese were on the order of instrument noise and meaningful data was not obtained. For the case with $MnCl_2$ in both solutions, the manganese and chlorine concentrations were high enough to measure (no sodium was observed), but we caution the use of this data for quantitative analysis for two reasons: the values are at the sensitivity limits of XPS and because the counterions are most certainly not distributed homogeneously throughout the multilayer assembly, a quantitative analysis would be biased. Figure 2.17

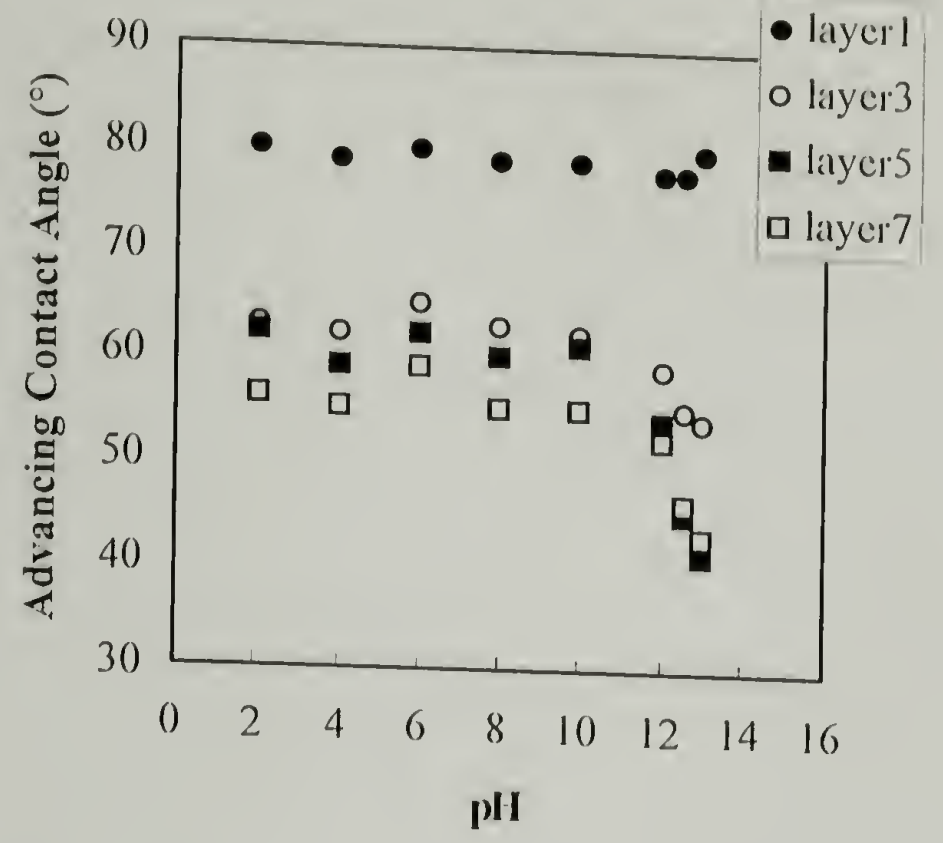

Figure 2.15. Advancing contact angles of buffered aqueous solutions on PET-supported multilayer assemblies (1 M $MnCl_2$ present in PSS solution only) with PAH layer as the outermost layer (1, 3, 5, and 7 layers).

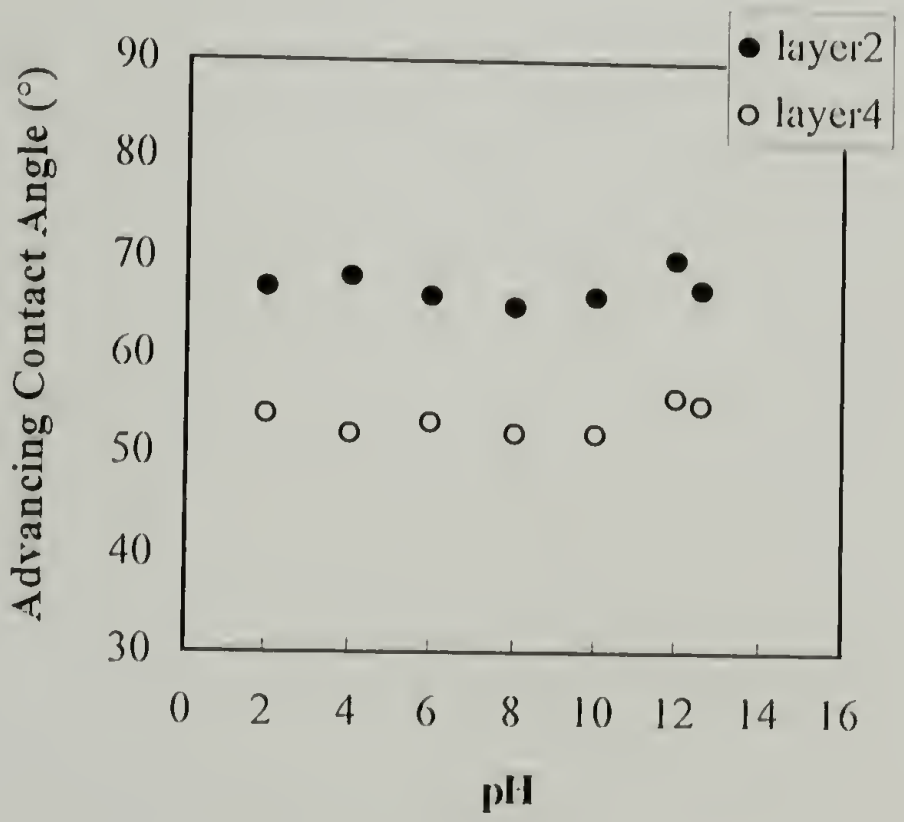

Figure 2.16. Advancing contact angles of buffered aqueous solutions on PET-supported multilayer assemblies (1 M $MnCl_2$ present in PSS solution only) with PSS layer as the outermost layer (2 and 4 layers).

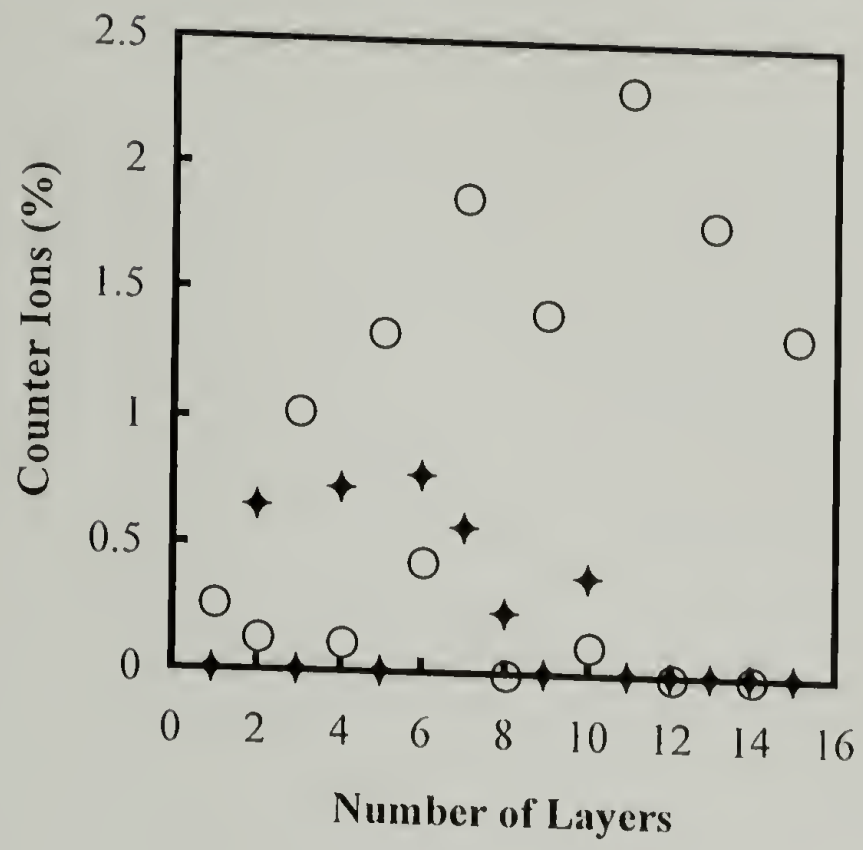

Figure 2.17. Manganese (✦) and chlorine (○) atomic concentrations from 75° take-off angle XPS data as a function of the number of layers in the multilayer film prepared with $MnCl_2$ in both PAH and PSS solutions.

shows manganese and chlorine atomic concentration data as a function of the number of layers deposited. The chlorine concentration oscillates from high in odd number-of-layer samples (PAH as outermost layer) to low in even number-of layer samples (PSS as outermost layer). The manganese concentration oscillates with the reverse trend up to 10 layers: high when PSS is the outermost layer and zero when PAH is the outermost layer.[53] These general trends are expected, but after 10 layers have been deposited, no chlorine is observed in even number-of-layer samples and no manganese is observed at all. As the N:S ratio is greater than 1 for all samples (Figure 2.13), chloride should be present as the counterion for the excess ammonium ion in all samples - we cannot readily explain its absence. The absence of manganese in the 12- and 14-layer samples is readily explained by the excess of ammonium ions present, but these multilayer assemblies

apparently contain no free (from ammonium ion) sulfonate groups (the surfaces must not be negatively charged) to induce the adsorption of the next PAH layer, however the PAH layers clearly adsorb (Figure 2.13). We conclude that these discrepancies must be due to the analytical technique: the counterion contents of the multilayer assemblies observed by XPS (at high vacuum) must not accurately reflect the structure of the assemblies when in contact with aqueous media.

Multilayer Deposition on PET-CO_2^- and PET-NH_3^+. Multilayer assemblies were built up on the charged substrates in the same manner described for PET except that for PET-CO_2^-, the polyelectrolyte solutions were adjusted to pH = 8 and for PET-NH_3^+, PSS was adsorbed first. The effect of adding $MnCl_2$ to the adsorption solutions was not examined. In general, the layer-by-layer assembly processes proceed in the same manner as for PET and the structures of the multilayer films produced are similar; we have characterized these samples to the same extent as those supported on PET. Figure 2.18 shows sulfur:nitrogen atomic ratio data (75° take-off angle) for multilayers built up on these substrates as a function of the number of layers adsorbed. The odd-even trend indicating layer stratification is evident as was the case for neutral PET (Figure 2.13). The stoichiometry of the assembly process (ammonium ion:sulfonate ion ratios) is also affected by the substrate surface chemistry. The S:N ratio levels at ~0.8 for PET-NH_3^+ and at ~0.65 for PET-CO_2^-. It is important to note that the initial substrate surface chemistry controls the structure of not just the first, but all of the layers in the multilayer assembly. The advancing water contact angle data (Figure 2.19) also shows an odd-even trend with θ_A = ~61° (odd, PAH outermost layer) and θ_A = ~53° (even, PSS outermost layer) for PET-CO_2^--supported multilayer films and θ_A = ~60° (odd) and θ_A = ~50° (even) for PET-NH_3^+ substrates.

The presence of surface charge does affect the individual layer thicknesses. Figure 2.20 shows plots of the type discussed above (Figure 2.10) for determining average layer

thickness based on carbonyl C_{1s} photoelectron attenuation. The PET-CO_2^--supported layers are 2.1 times as thick as the PET-supported layers (no added $MnCl_2$). Using the

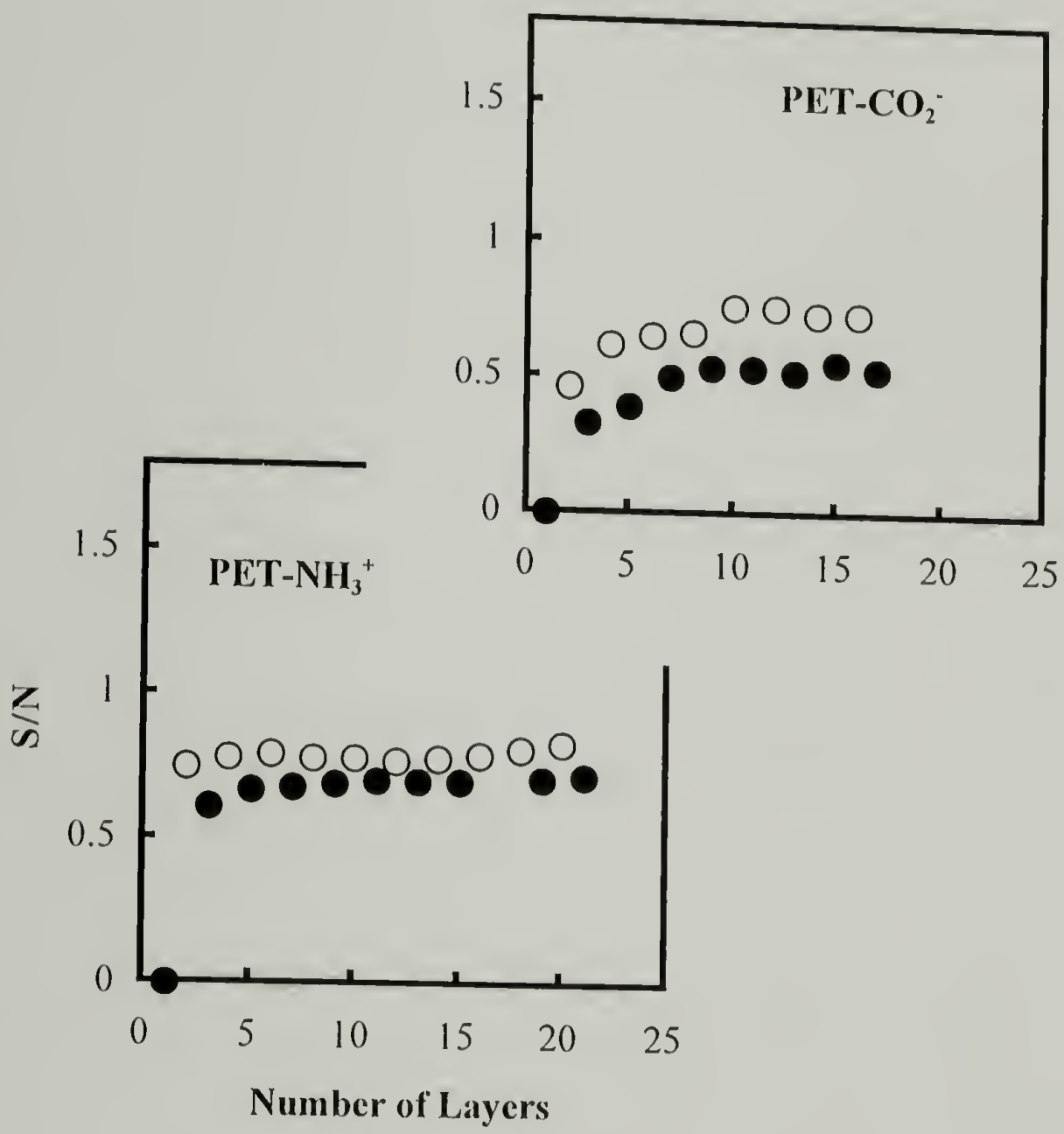

Figure 2.18. Sulfur:nitrogen atomic ratio data (75° take-off angle) for polyelectrolyte multilayers supported on PET-CO_2^- and PET-NH_3^+: odd number of layers (●), even number of layers (○).

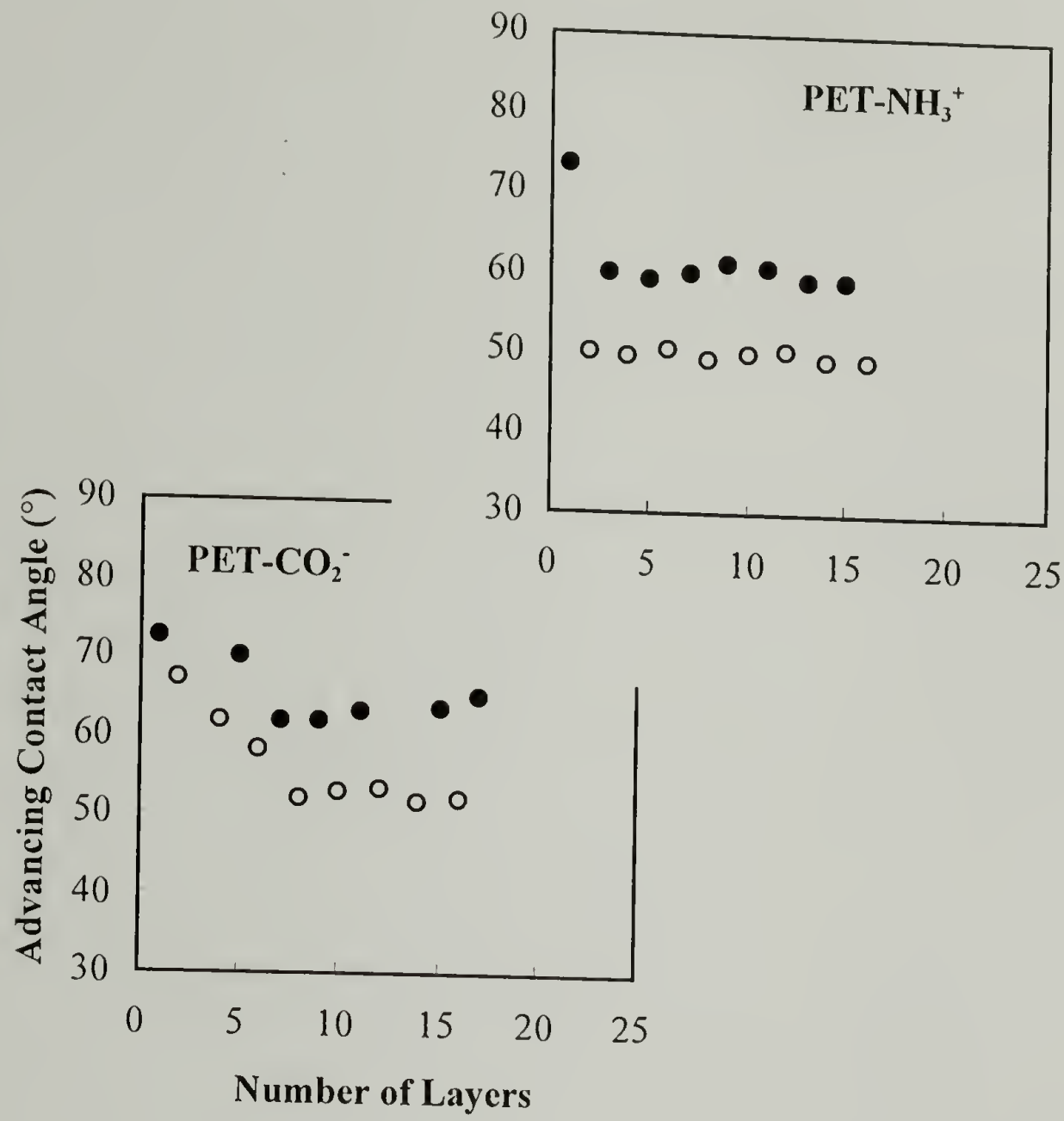

Figure 2.19. Advancing contact angle data for multilayer deposition on charged PET substrates, PET-CO_2^- and PET-NH_3^+: odd number of layers (●), even number of layers (○).

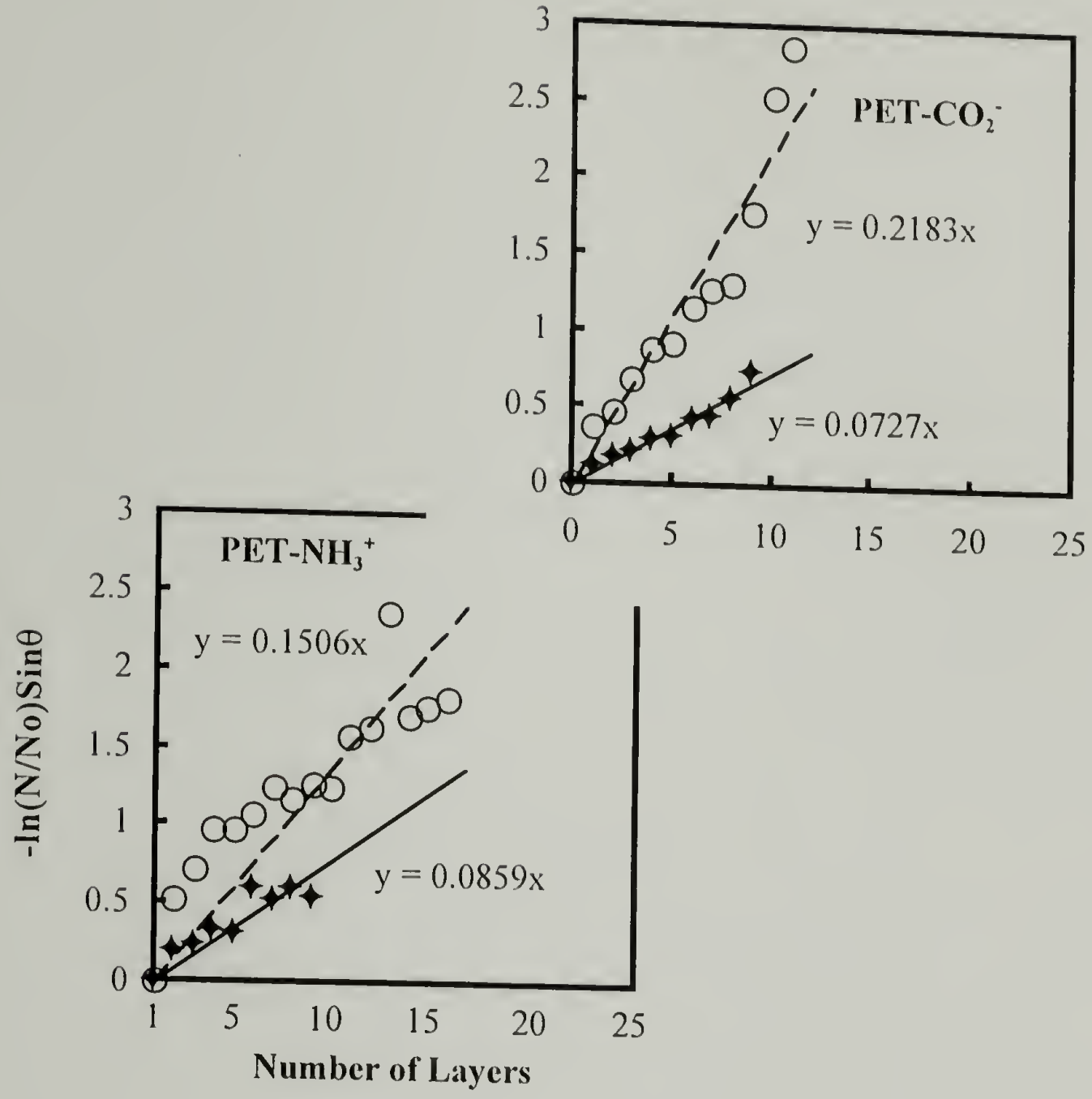

Figure 2.20. Plots of $-\ln(N/N_o)\sin\theta$ vs. number of layers in multilayer films supported on $PET\text{-}CO_2^-$ and $PET\text{-}NH_3^+$. The closed (●) and open (○) symbols are data recorded at 15° and 75° take-off angles, respectively.

75° take-off angle data, a C_{1s} electron mean free path of 19 Å and the assumptions discussed above, the average layer thiekness is ealeulated to be 4.1 Å. The PET-NH_3^+-supported layers are 1.4 times as thick (2.8 Å) as those on PET. The initial surface charge "screens" charge-charge rcpulsions in the adsorbing polyeleetrolyte, allowing a greater adsorbance and thieker resulting layers.

An aging study of samples with 14, 15, 16, and 17 layers adsorbed on PET-CO_2^- was earried out under ambient laboratory eonditions. That XPS atomie composition data did not ehange much over the three week period of time studied (Table 2.9), indicating good stability of the multilayer strueturcs.

Table 2.9. Aging study of multilayer assemblies on PET-CO_2^- at ambient eonditions.

	15deg.				75 deg.			
	%C	%O	%S	%N	%C	%O	%S	%N
Fresh:								
layer14	70.86	19.19	4.39	5.56	68.77	20.11	4.73	6.39
layer15	72.52	16.40	3.76	7.32	70.58	17.72	4.16	7.54
layer16	70.92	19.15	4.36	5.57	68.83	19.92	4.76	6.49
layer17	72.08	16.87	3.81	7.24	69.70	18.67	4.06	7.57
5 day old:								
layer14	71.39	18.57	4.39	5.64	68.52	20.42	4.68	6.38
layer15	73.47	15.83	3.65	7.05	69.57	18.59	4.18	7.66
layer16	70.88	19.29	4.33	5.50	68.53	20.58	4.64	6.26
layer17	72.89	16.52	3.51	7.08	70.43	18.15	3.98	7.44
20 day old:								
layer14	71.10	19.19	4.20	5.51	68.42	20.57	4.70	6.31
layer15	74.70	15.27	3.52	6.51	70.09	18.62	3.99	7.30
layer16	72.25	18.34	4.16	5.25	69.12	20.59	4.52	5.77
layer17	74.22	15.55	3.35	6.88	71.03	17.70	3.99	7.28

Meehanieal Properties of Multilayer Assemblies. As diseussed in the introduetion scetion, our objeetive in this work is to develop layer-by-layer deposition as a method to eontrol surfaee strueture and surfaec properties of solid polymers. For this method to be practieal, the multilayer assemblies must have mechanieal integrity and must adhere to the substrates. We have earried out simple peel tests using pressure-sensitive adhesive tape to determine the locus of failure in substrate/multilayer assembly/adhesive tape composites (Table 2.10). Peel tests on the three substrates were also performed as control experiments.

The tape was applied and peeled from the samples and XPS spectra of both surfaees were compared with speetra obtained before the adhesive joint was formed. The atomie composition of the tape used (3M #810) at 15° take-off angle is: C, 87.2%; O, 12.8%. The composition of PET (C, 71.5%; O, 28.5%) and PET-CO_2^- (C, 69.9%; O, 30.1%) are significantly different than the tape. The other samples contain nitrogen (PET-NH_3^+) or both nitrogen and sulfur so the XPS analyses of the loeus of failure were straight-forward.

The unmodified PET surfaec eomposition did not change after the peel test, however the earbon eontent of the tape decreased to 84.4% indicating that eohesive failure in PET oecurs. A weak boundary layer, likely eonsisting of PET oligomers[54] transfers from PET to the tape. XPS analysis of an unmodified PET sample supporting 14 layers after the peel test indieated that no nitrogen or sulfur was present. Both nitrogen and sulfur as well as PET oligomers were observed on the tape. This eohesive failure in PET indieates that the multilayer assembly is at least as strong as the weak boundary layer and that there is an adhesive interaction between the first polyelectrolyte layer and PET. The peel tests of PET-NH_3^+, PET-CO_2^-, PET-NH_3^+ with 14 layers and PET-CO_2^- with 10 layers all indicated eohesive failure in the tape. The tape eomposition remained unchanged and a thin layer of adhesive was apparent in the film spectra. These results indicate that the mechanical strength of the multilayer assemblies and the adhesive

Table 2.10. Assessment of mechanical properties of multilayer assemblies on various substrates using peel tests with pressure-sensitive adhesive tape.

Substrates and tape	15 deg %C	%O	%S	%N	75 deg %C	%O	%S	%N
Magic tape	87.20	12.80			84.42	15.58		
PET (theoretical)	71.5	28.5			71.5	28.5		
PET (after)	69.92	30.08			68.14	31.86		
Magic tape (after)	84.39	15.61			81.83	18.17		
PET-14 layers	70.55	19.95	4.40	5.10	69.14	20.27	4.77	5.83
PET-14 (after)	71.97	27.33	0.35	0.34	69.99	29.02	0.48	0.50
Magic tape (after)	77.69	17.91	1.86	2.53	75.85	19.01	2.31	2.83
PET-CO_2^-	69.90	30.10						
PET-CO_2^- (after)	71.27	28.73			69.08	30.92		
Magic tape (aftter)	83.11	16.89			82.28	17.72		
PET-CO_2^--10 layers	69.96	20.00	4.43	5.52	69.28	21.19	4.07	5.40
PET-CO_2^--10 (after)	74.55	17.95	3.63	3.87	71.87	20.35	3.65	4.14
Magic tape (after)	84.04	15.89	0.08	0	83.30	16.52	0.08	0.11
PET-CO_2^--9 layers	71.90	17.86	3.42	6.65	71.04	19.67	3.20	5.97
PET-CO_2^--9 (after)	78.69	14.66	3.12	3.53	75.54	17.41	3.15	3.90
Magic tape (after)	83.53	15.99	0.20	0.28	82.59	17.16	0.15	0.09
PET-NH_3^+	71.00	23.49	0	5.35	68.34	28.17	0	3.44
PET-NH_3^+ (after)	72.90	22.67	0	4.43	68.94	27.88	0	3.19
Magic tape (after)	83.02	16.98			82.17	17.83		
PET-NH_3^+-14 layers	71.76	18.97	3.97	5.30	70.51	20.60	3.72	5.17
PET-NH_3^+-14 (after)	75.02	17.21	3.87	3.91	71.84	20.09	3.71	4.36
Magic tape (after)	82.86	17.05	0.08	0	81.83	18.05	0.11	0

strength of the bonds between the multilayers and the charged substrates are stronger than the cohesive strength of the pressure sensitive adhesive tape.

Conclusions

Layer-by-layer deposition of polyelectrolytes (PAH and PSS) has been used to build up multilayer films on three organic polymer substrates: PET, PET-CO_2^- and PET-NH_3^+. XPS and contact angle data indicate that the layers are stratified and the wettability of the multilayer assemblies is largely controlled by the identity of the outermost polyelectrolyte layer. The individual layers are extremely thin (2-6 Å) and this thickness is affected by the substrate surface chemistry and can be controlled by adjusting the ionic strength of the polyelectrolyte solutions. The stoichiometry of the deposition process (ammonium ion:sulfonate ion ratio) is also affected by the substrate chemistry and solution ionic strength; it varies significantly in the series of experiments studied indicating that the layer-by-layer deposition process is quite forgiving and proceeds under a variety of conditions. Peel tests indicate that the multilayer assemblies show good mechanical integrity; no failures were observed in the multilayers. These experiments indicate that layer-by-layer deposition is a viable tool for polymer surface modification.

Notes and References

1. Decher, G.; Hong, J. D.; Schmitt, J. *Thin Solid Films* **1992**, *210/211*, 831.
2. Lvov, Y.; Decher, G.; Mohwald, H. *Langmuir* **1993**, *9*, 481.
3. Keller, S. W.; Kim, H. N.; Mallouk, T. E. *J. Am. Chem. Soc.* **1994**, *116*, 8817.
4. Mallouk, T. E et. al. *J. Am. Chem. Soc.* **1993**, *115*, 11855.
5. Ferreira, M; Cheung, J. H.; Rubner, M. F. *Thin Solid Film* **1994**, *244*, 806.

6. Stockton, W. B.; Rubner, M. F. *Polym. Prepr. (Am. Chem. Soc.: Div. Polym. Chem.)* **1994**, *35*, 319.

7. Kleinfeld, E. R.; Ferguson, G. S. *Science* **1994**, *265*, 370.

8. Mao, G.; Tsao, Y.; Tirrell, M.; Davis, H. T. *Langmuir* **1993**, 3461.

9. Hammond, P. T.; Whitesides, G. M. *Macromolecules* **1995**, *28*, 7569.

10. Leväsalmi, J.-M.; McCarthy, T. J. *Polym. Prepr. (Am. Chem. Soc. Div. Polym. Chem.)* **1996**, *37(1)*, 457.

11. Ferreira, M.; Rubner, M. F. *Macromolecules* **1995**, *28*, 7107.

12. Fou, A. C.; Rubner, M. F. *Macromolecules* **1995**, *28*, 7115.

13. Swalen, J. D.; Allara, D. L.; Andrade, J. D.; Chandross, E. A.; Garoff, A.; Israelachvili, J.; McCarthy, T. J.; Murray, R.; Pease, R. F.; Rabolt, J. F.; Wynne, K. J.; Yu, H. *Langmuir* **1987**, *3*, 932.

14. Dias, A. J.; McCarthy, T. J., *Macromolecules* **1987**, *20*, 2068.

15. Lee, K.-W.; McCarthy, T. J. *Macromolecules* **1988**, *21*, 2318.

16. Bee, T. G.; McCarthy, T. J. *Macromolecules* **1992**, *25*, 2093.

17. Costello, C. A.; McCarthy, T. J. *Macromolecules* **1987**, *20*, 2819.

18. Bening, R. C.; McCarthy, T. J. *Macromolecules* **1990**, *23*, 2648.

19. Dias, A. J.; McCarthy, T. J. *Macromolecules* **1984**, *17*, 2529.

20. Iyengar, D. R.; Brennan, J. V.; McCarthy, T. J. *Macromolecules* **1991**, *24*, 5886.

21. Franchina, N. L.; McCarthy, T. J. *Macromolecules* **1991**, *24*, 3045.

22. Ward, W.; McCarthy, T. J. In *Encyclopedia of Polymer Science and Engineering*, 2nd ed; Mark, H. F., Bikales, N. M., Overberger, C. G., Menges, G., Kroschwitz, J. I., Eds.; John Wiley and Sons: New York, 1989; suppl. vol., p 674.

23. Fleer, G. J.; Lyklema, J. In *Adsorption from Solution at the Solid/Liquid Interface*; Parfitt, G. D., Rochester, C. H., Eds.; Academic Press: New York/London, 1983; p 153.

24. Blaakmeer, J.; Böhmer, M. R.; Cohen Stuart, M. A.; Fleer, G. J. *Macromolecules* **1990**, *23*, 2301.

25. Marra, J.; van der Schee, H. A.; Fleer, G. J.; Lyklema, J. In *Adsorption from Solution*; Ottewill, R. H., Rochester, C. H., Eds.; Academic Press: New York, 1983;

26. van der Schee, H. A.; Lyklema, J. *J. Phys. Chem.* **1984**, *88*, 6661.

27. Papenhuijzen, J.; van der Schee, H. A.; Fleer, G. J. *J. Colloid Interface Sci.* **1985**, *104*, 540.

28. Papenhuijzen, J.; Fleer, G. J.; Bijsterbosch, B. H. *J. Colloid Interface Sci.* **1985**, *104*, 530.

29. Cosgrove, T.; Obey, T. M.; Vincent, B. *J. Colloid Interface Sci.* **1986**, *111(2)*, 409.

30. Lvov, Y.; Haas, H.; Decher, G.; Möhwald, H. *J. Phys. Chem.* **1993**, *97*, 12835.

31. Leväsalmi, J.-M.; McCarthy, T. J. *Macromolecules*, **1997**, *30*, 1752.

32. Phuvanartrukus, V.; McCarthy, T. J. Manuscript in Preparation.

33. Cooper, T. M.; Campbell, A. L.; Crane, R. L. *Langmuir*, **1995**, *11*, 2713.

34. Lvov, Y.; Decher, G.; Sukhorukov, G. *Macromolecules*, **1993**, *26*, 5396.

35. Lvov, Y.; Haas, H.; Decher, G.; Möhwald, H. *Langmuir,*. **1994**, *10,* 4232.

36. Robinson, R.A. In *CRC Handbook of Chemistry and Physics*, 67th ed.; Weast, R.C., Astle, M.L., Beyer, W.H. Eds; CRC Press, Inc: Boca Raton, Florida, 1986; D144-D145.

37. Arnett, E.M. *Prog. Phys. Org. Chem.* **1963**, *1*, 223.

38. Brown, H.C.; McDaniel, D.H.; Hflinger, O. In *Determination of Organic Structures by Physical Methods*; Braude, E.A., Nachod, F.C., Eds; Academic Press: New York, 1955; p 567.

39. The adsorption of PSS to PET was studied as well, but multilayers were not prepared using PSS as a first layer. XPS analysis of a PET sample treated with a PSS solution containing $MnCl_2$ indicated the composition: C, 65.86%; O, 33.34%; S, 0.47%; Mn, 0.12%; Na, 0.21%.

40. The adsorptions described here are most certainly irreversible.

41. A specific enthalpic interaction between PET and the substrate polymer is not necessary for adsorption. The adsorption could be driven by a decrease in interfacial free energy and/or by entropy (release of water molecules from the interface). These factors are discussed in: Shoichet, M.S.; McCarthy, T.J. *Macromolecules* **1991**, *24*, 1441.

42. Andrade, J. D. *Surface and Interfacial Aspects of Biomedical Polymers, Surface Chemistry and Physics;* Plenum Press: New York, 1985; Vol. 1, p 176.

43. Clark, D.T.; Thomas, H.R.; Shuttleworth, D. *J. Polym. Sci., Polym. Lett. Ed.* **1978**, *16*, 465.

44. Clark, D.T.; Thomas, H.R. J. *Polym. Sci., Polym. Chem. Ed.* **1977**, *15*, 2843.

45. Hall, S.M.; Andrade, J.D.; Ma, S.M.; King, R.N. *J. Electron Spectroscopy* **1979**, *17*, 181.

46. Clark, D.T.; Adams, D.B.; Dilks, A.; Peeling, J.; Thomas, H.R. *J. Electron Spectroscopy* **1976**, *8*, 51.

47. Ashley, J.C. *IEEE Trans. Nucl. Sci.* **1980**, *NS-27*, 1454.

48. Ashley, J.C.; Williams, M.W. *Rad. Res.* **1980**, *81*, 364.

49. Ashley, J.C. *J. Electron Spectroscopy* **1982**, *28*, 177.

50. Ashley, J.C.; Tung, C.J. *Surf. Interfac. Anal.* **1982**, *4*, 52.

51. Reference 42, p 180.

52. Odd-even trends in water contact angle data for polyelectrolyte multilayer assemblies have been reported: Yoo, D.; Rubner, M.F. *Antec '95 (Proc. Soc. Plast. Eng.)* **1995**, 2568; Chen, W.; Leväsalmi, J.-M.; Watkins, J.J.; McCarthy, T.J. *Antec '95 (Proc. Soc. Plast. Eng.)* **1995**, 2506.

53. The relatively high manganese concentration for the 7-layer sample is anomolous. We have not repeated this experiment.

54. Bensnoin, J.-M.; Choi, K.Y. *J. Macromol. Sci. Rev., Macromol. Chem. and Phys.* **1989**, *C29*, 55.

CHAPTER 3

ADSORPTION OF A SURFACE-ACTIVE AGENT FROM THE BULK TO THE POLYMER/AIR INTERFACE

Introduction

The interfacial properties of a material depend primarily on the surface structure and chemical composition of the outermost surface layer. Research in McCarthy's group has concentrated on the preparation of specifically-functionalized and well-characterized polymer surfaces with the objective of controlling macroscopic properties by manipulating microscopic surface structures. Among the approaches to surface modification are polymer adsorption from solution,[1] chemical modification,[2] (Chapter 1), layer-by-layer deposition[3] (Chapter 2), and surface reconstruction.[4]

Surface reconstruction has been reported in the literature extensively from both theoretical[5-11] and experimental[12-31] point of views. Polymers differ from other materials in the sense that polymer chains are mobile under the appropriate conditions. The mobility of the polymer chains enables materials to reconstruct in response to environmental changes and to minimize surface free energy.[32] Systems with surface-modified polymers,[33-34] surface-active small molecules,[12-13] block copolymers,[14-26] and polymer blends[27-31] all demonstrate that polymer surfaces are dynamic and reconstruct to lower surface free energy.

The objective of this research is to find a general approach to enhance the efficiency of flame retardant additives in polymer materials by using surface free energy minimization. We suspect that ignition is controlled primarily by interfacial properties. The flame retardants of interest are fullerenes, that should starve the flame of a source of hydrogen and form an insulating char layer on the surface. Furthermore, their electron-deficiency should enable them to function as radical traps to stop the propagation of a

fire. We have prepared a perfluoroalkylated-C_{60} sample and studied its mobility and surface activity in a polymer matrix (polystyrene). Surface activity of the perfluoroalkylated-C_{60} was studied as a function of bulk concentration, molecular weight of the polymer matrix, annealing temperature, and annealing time.

Reconstruction of Polymers

Solid polymers are nonequilibrium entities. The mobility of polymer chains gives polymer materials the ability to reconstruct in response to environmental changes. Reconstructed surface structure and composition depend on bulk concentration,[23,26,27,31] polymer molecular weight,[29,30] incompatibility of the components,[24-27,31] casting solvent,[18,23,27,31] annealing time,[33] annealing temperature,[18,33] temperature of measurement,[29] and the nature of the surface-migrating species.[35]

Dynamic Polymer Surfaces

In general, polymer structures are temperature and time dependent. Because polymer molecules have relatively large size, they are unlikely to ever be in their "true equilibrium state". Solid polymers have nonequilibrium structures with chains rotating and repatating, and exhibit a range of relaxations and transitions in response to time, temperature, and other environmental changes.[32] Mobility of chains in a sample can result in a preferred bond orientation which can affect the properties of a surface. In general, reconstruction tends to concentrate to the surface the component that is the most similar to the phase above it.

Segregation to Interfaces

In systems employing block copolymers, polymer blends or homopolymers, the lower energy moiety partitions preferentially near the surface to minimize the surface free

energy. The Gibbs adsorption equation has been used to describe the change in surface tension, γ, with surface migration,[36] where $\Gamma_i = N_i / A_S$, represents the number of species

$$-d\gamma = \sum_i \Gamma_i d\mu_i \tag{3.1}$$

i per area A, and the chemical potential, μ, describes the free energy change with each species adsorbed to the surface, and in this sense, can describe surface energy differences between two molecular species in a given material. We define the dimensionless difference in adsorption energies between segments A and B as:[6]

$$\chi_S = \chi_S^A - \chi_S^B = -\frac{\mu_S^A - \mu_S^B}{kT} \tag{3.2}$$

The quantity χ_S is a measure of the differential affinity of A and B for adsorption on the surface. When components have similar affinities for the surface, the material has a small value of χ_S. At higher values of χ_S, the component with higher surface affinity will be preferentially partitioned to the surface.

For block copolymers and homopolymer blends, surface-segregation of one component depends on surface energy, compatibility differences between the components, bulk composition, casting solvent, molecular weight of the components, and temperature of measurement.

For the PS/PMMA block copolymer system,[25] polystyrene is the lower surface energy component. XPS indicates that polystyrene locates preferentially at the surface. The surface excess of polystyrene decreases with increasing temperature because the chemical potential difference favoring polystyrene decreases with increasing temperature. When triblock copolymer is compared to the corresponding diblock copolymer,

remarkably similar surface compositions and topographies are found,[26] e.g. PEO/PS/PEO triblock copolymer vs. PEO/PS.

The degree of surface segregation in a homopolymer blend has been compared with a block copolymer with the same bulk composition. Gardella et al.[27] studied the surface segregation of bisphenol A polycarbonate (BPAC) and poly(dimethylsiloxane) (PDMS) blends and copolymers. BPAC and PDMS have surface tensions of 32 and 24 dyn/cm, respectively. The lower surface energy component, PDMS, segregates to a much greater extent in the blends than it does in the block copolymers according to XPS and ISS results. In this case, the greater mobility of the blend samples was an important factor. In another study of PEO/PS (44/36 dyn/cm) using angle-resolved XPS, Thomas and O'Malley[31] found that the concentration of polystyrene on the surfaces of the blends is significantly less than on the surfaces of the copolymers for identical bulk composition. For both of the systems, the surface free energy difference between the two components is the same, ~ 8 dyn/cm. The studies demonstrate that while surface energy values are useful for predicting which species should show a surface preference, they alone are not useful for predicting the degree of surface enrichment expected. The amount of surface segregation appears to be dependent on the degree of "compatibility" present in the system and the final morphology of the sample.

Casting solvent can have a significant effect on the surface composition as well as on the bulk compatibility. PMMA and PVC have solid surface tensions of 41.2 and 42.0 dyn/cm, respectively. PMMA is thus expected to slightly enrich the surface of the PMMA/PVC blend. This was observed when THF was used as the casting solvent. However, when MEK was used, a homogeneous mixture with little detectable surface segregation was produced.[28]

The surface/interfacial tension of polymer samples depends on their molecular weight, as well as the temperature of measurement. In general, it decreases in a linear fashion with temperature and increases with molecular weight, $C_1 + C_2Mn^{-Z}$, where C_1

and C_2 are some contants and z varies from 2/3 to 1 in the homopolymer and blend systems studied. For a polydisperse sample, the conformational loss by longer chains at a surface exceeds that loss by the shorter ones because of chain connectivity. The relationship between molecular weight and surface tension implies that for a polydisperse sample, shorter chains preferentially partition at the surface to minimize surface free energy.[29]

Theoretical Model for Surface-Active Molecules

Microscopic structure (local composition, bond orientation, chain shape) and thermodynamic properties (interfacial tension) of homopolymers, copolymers, and surface-active polymers at interfaces are predicted by Theodorou using a lattice model approach.[5,6,37,38] This model is inspired by the Scheutjens and Fleer polymer adsorption model, in which properties vary along a principal direction perpendicular to the interface.

In particular, the interfacial behavior of surface-active polymers of the type AB_{r-1} with surface-active segment A, was described quantitatively by the model.[38] Since type A segments have greater affinity for the surface than type B, the surface interaction parameter $\chi_S > 0$. Some of the assumptions made are: segment density in the system is uniform, all lattice sites are occupied, Flory interaction parameter $\chi = 0$. Structural and thermodynamic parameters were explored as a function of chain length (r) and relative tendency for adsorption at the surface (χ_S).

The volume fraction ϕ_{Ai} at large distance from the interface is equal to:

$$\lim_{i \to \infty} \phi_{Ai} = \phi_{A\infty} = r_A / r \qquad (3.3)$$

In the case of AB_{r-1} type polymers studied here, $r_A = 1$. The reduced profile $(r/r_A)\ \phi_{Ai}$ for chain length r = 50 and for different χ_S values is shown in Figure 3.1. In the pure

homopolymer case ($\chi_S = 0$), there is a very weak tendency for the chain ends (segment A) to concentration on the surface. As χ_S increases, segment A preferentially adsorbs at the surface ($(r/r_A)\phi_{Ai} >> 1$). The tendency for surface enrichment of segment A, as measured by $(r/r_A)\ \phi_{Ai}$, also increases when chain length increases, even though the average volume fraction of segment A in the polymer decreases. Surface adsorption is accompanied by a depletion of lower lying layers of segment A, as shown by an immediate drop of $(r/r_A)\phi_{Ai}$. This is because the lower lying layers have to accommodate the B segments. As the distance from the surface increases, the reduced profile $(r/r_A)\phi_{Ai}$ should approach the bulk value, 1. The characteristic distance is an increasing function of both χ_S and r.

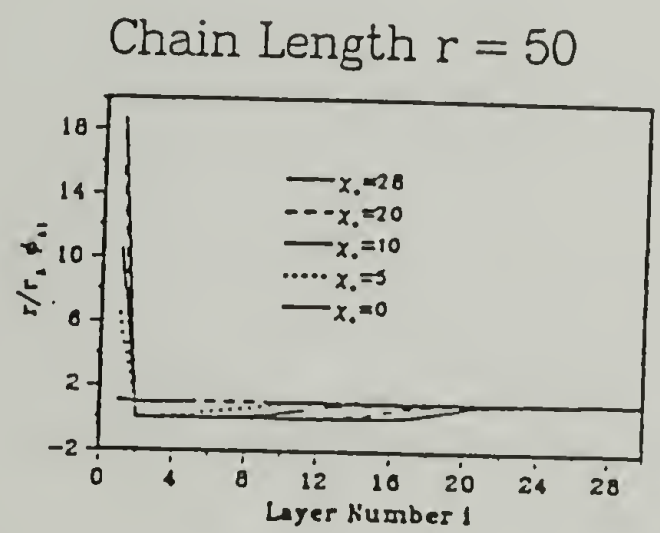

Figure 3.1. Spatial distribution of surface-active segment A for various values of χ_S in bulk AB_{r-1} system (r = 50).[38]

The presence of an interface causes bond orientation to deviate from isotropy. Since in the AB_{r-1} system, all chains strive to expose their surface-active segment A to the surface, chain conformations elongate in a direction perpendicular to the surface.

The interfacial free energy of the system is expected to change with the preferential adsorption of segment A to the interface. The difference between the

nondimensional interfacial free energy of a surface-active polymer, $\varepsilon(\chi_S, r)$, and that of the corresponding homopolymer, $\varepsilon(0, r)$, is a function of both χ_S and r:[38]

$$\varepsilon(0, r) - \varepsilon(\chi_S, r) = 0.31565\ \chi_S^{1.5258}\ r^{-0.5243} \qquad (3.4)$$

The interfacial free energy decreases as χ_S increases and as r decreases.

Surface Activity of Fluorine-Containing Molecules

In a study[13] involving the surface modification of poly(methyl methacrylate) and a UV-curable acrylic lacquer, small amounts of polymerizable, monomeric surfactants, and polymer both containing a perfluorooctyl end group were added to the polymer matrix. The incompatibility of the perfluoroalkyl groups with the matrix is an essential feature which facilitates surface reconstruction. Both XPS and contact angle measurements indicate that surface modification of polymers is effectively achieved by surface-active compounds. The extent of the surface enrichment of the fluorinated group is a function of the nature of the additive (size, molecular structure, fluorine content), bulk concentration of the additive, viscosity of the polymer matrix, and the compatibility between the additive and the host medium. Of the different additives studied, it is more favorable to use a low molecular weight, monomeric surfactant. Such surfactants diffuse rapidly through the bulk material due to their small size, and can be made to react and become chemically bound to the material at the surface.[13]

A more systematic surface reconstruction study involving functionalized poly(styrene) and poly(styrene-b-4-hydroxystyrene) with perfluoroalkyl groups was carried out in McCarthy's group.[39,40] The variables chosen for manipulation are time and temperature of heating to allow reconstruction, molecular weight of the surface-active polymers (SAP), concentration of SAP, size of the surface-active group, number of surface-active groups on a chain, and chain architecture of the SAP. Experiments were

designed with the objective of elucidating how certain molecular and environmental parameters influence the rate and extent of surface reconstruction. These polymers were prepared by anionic polymerization and have four different chain architectures: (1) with mono-fluorinated end group (SAP-E1), (2) with two perfluoroalkyl end groups (SAP-E2), (3) with one functional group in the middle (SAP-M1), (4) a block copolymer with one block containing a fluorinated group (SAP-AyBx). Reconstructed film samples were analyzed by XPS and contact angle measurements to assess changes in surface atomic composition and wettability. Heat treatment of samples ($>T_g$) was required to reach "the final state" of surface reconstruction; For the same chain architecture, the plateau F/C value decreases as the molecular weight of SAPs increases; The maximum surface excess for 10K SAP-E1, SAP-E2, and SAP-$A_{10}B_{104}$ samples at the plateau are 10, 25, and 80 times the bulk F/C ratio, respectively. Only limited reconstruction occurs in 10K SAP-M1 samples due to entropic constraints and lower mobility of chain middles than chain ends; As predicted by Theodorou's model, chains appeared to be more stretched compared to the "unperturbed state" as calculated from XPS data, especially for the high molecular weight SAP-E1 samples.

Fullerenes

Discovery

Fullerenes were discovered upon laser vaporization of graphite by Kroto and Smalley in 1985.[41] The generation of fullerenes by resistive heating of graphite was the first technique to produce macroscopic quantities.[42] The cagelike molecules constitute the third allotropic form of carbon along with diamond and graphite. Fullerenes include a class of molecules which have the form of a closed cage and are composed of 12 pentagons and n hexagons. C_{60} is the lowest member, followed by C_{70}, C_{76}...

Properties

Solid C_{60} forms a face-centered-cubic (FCC) crystal at room temperature.[43] The density in the solid state is 1.68 g/cm^3.[42] C_{60} is not very soluble in polar solvents and alkanes. In aromatic solvents and carbon disulfide, appreciable solubilities are observed. A significant increase of solubility is observed from benzene to naphthalenes.[44-46]

Reactivity

Fullerenes consist entirely of sp^2-hybridized carbon, however, it is not so much an aromatic molecule as a giant closed alkene. The delocalization of electrons is poor, so C_{60} is much more reactive than originally expected. The molecules appear to undergo all the reactions associated with poorly-conjugated and electron-deficient alkenes. (Scheme 3.1).[47]

Reduction. A property that governs many of the chemical reactions of C_{60} is its electron-deficiency and up to six electrons can be added, reversibly.[48-50] Anions prepared by reacting C_{60} with alkali metal, such as lithium, can then react with methyl iodide and form a mixture of polymethylated derivatives.[51] Up to 24 methyl groups can be added with six- and eight-methyl derivatives dominant.

Radical Addition. The electron-deficiency of C_{60} also enables the addition of a large variety of radicals. Perfluoroalkylated-C_{60}s have been prepared by reaction with perfluoroalkyl radicals, which are generated by thermal or photochemical decomposition of perfluoroalkyl iodide or perfluorodiacyl peroxide (scheme 3.2).[52] The reaction products consist of a mixture of polydisperse perfluoroalkylated-C_{60} with up to 16 radicals added. These molecules are thermally quite stable, soluble in fluoroorganic solvents, chemically resistant to corrosive solutions, and more volatile than the parent fullerenes.

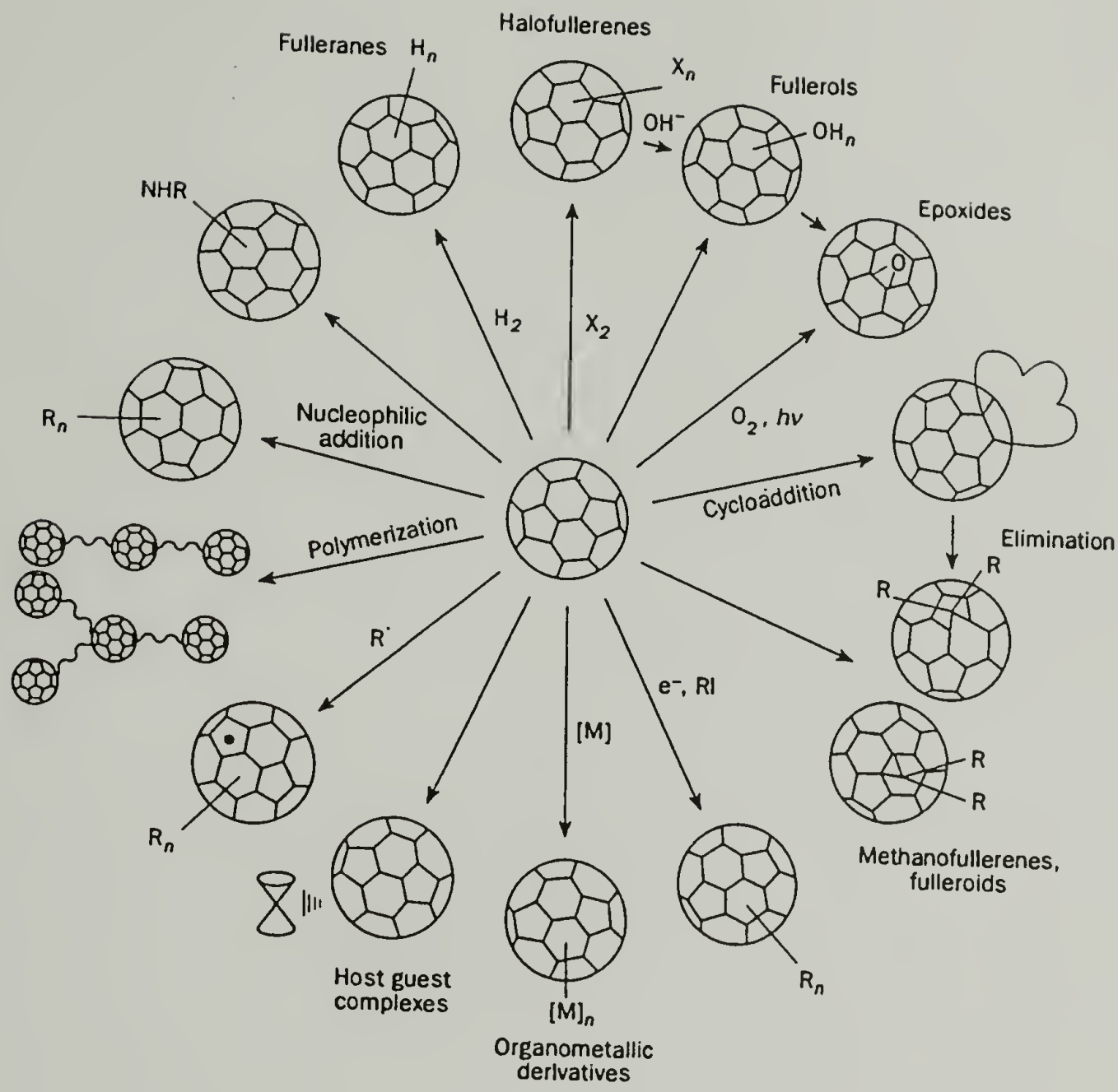

Scheme 3.1. Reactivities of C_{60}.[47]

TGA of the perfluorohexylated-C_{60} mixture showed a weight loss at 270 °C with complete weight loss occurring at ~ 400 °C. Under high vacuum, the mixture is sublimed quantitatively to deposit a thin film on a glass slide. Advancing and receding contact angle (θ_A/θ_R) of the surface was determined with water (124°/64°) and hexadecane (65°/24°).[52]

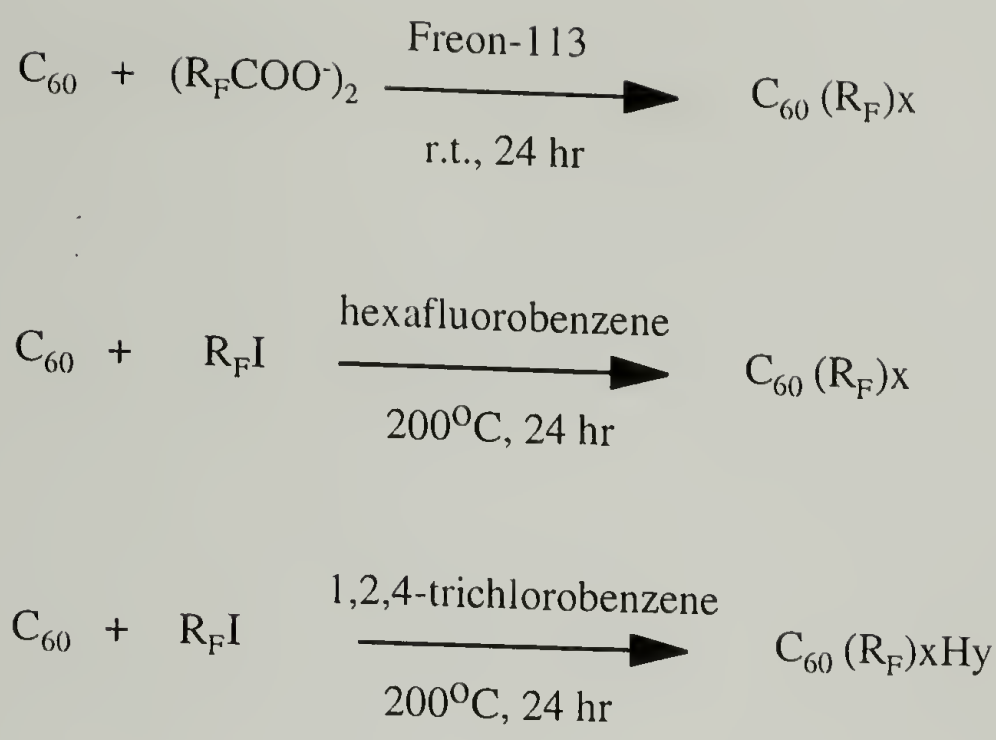

Scheme 3.2. Synthesis of perfluoroalkylated-C_{60}.

Halogenation. Halogenations of C_{60} have been reported and up to 24 groups can be added by both chlorination[53-54] and bromination.[55,56] The addition of up to sixty fluorines has been reported.[57] The halogeno compounds decomposed to C_{60} upon heating, with the stability in the order of fluoro > chloro > bromo. Even though the fluoro compounds are the most stable, they decompose rapidly on heating above 80 °C with the more highly fluorinated species being less stable.[47]

Oxidation. C_{60} can be oxidized by reacting with fuming sulfuric acid. Subsequent hydrolysis of the intermediates results in the formation of fullerols, $C_{60}(OH)_X$. The water soluble fullerols were found to contain an average of 12 hydroxyl groups. Fullerols can be used as reactive intermediates to a whole range of C_{60} derivatives through the reaction of -OH functionality, however, esterification with trifluoroacetic anhydride was not quantitative: only 3 out of the 12 hydroxyl groups were converted to ester upon reaction with trifluoroacetic anhydride.[58]

The chemistry of fullerenes has been explored to a great extent. It is now possible to covalently bind almost any class of compounds to the fullerene core. A large number of reactive double bonds are accessible on C_{60}, thus reaction products are most often polydisperse and lack defined regio- and stereo-specific characteristics. A lot of current work concentrates on the formation of monoaddition products of C_{60}.

Flame Retardants

Fire occurs when an ignition source contacts a flammable material. When the heat from the source produces a high enough temperature to cause bond scission in the material, chemical fragments are created that vaporize and react with oxygen in the air to release more heat. Some of the heat convects back to the material, causing more bond scissions. Fire thus spreads.

Flame retardant polymers have either inherently more stable polymeric structures or fire-retardant additives. The former usually have strong chemical bonds in the backbone so that they are stable at elevated temperature, however, these polymers are usually high-priced. Polyimides, polybenzimidazoles, polyetherketones, polyphosphazenes, and polysiloxanes, are examples of polymers in this class.[59]

Fire-retardant additives are often used to improve the fire performance of low-to-moderate cost commodity polymers. Retardants such as hydrated alumina increase the heat capacity, increasing the enthalpy needed to cause fracture of the chemical bonds of the product. The endothermic vaporization of the bound water is a significant contributor to the effectiveness of this type of flame retardants. Organophosphates can also be used as fire-retardant additives by changing decomposition mechanism. They can either cause cross-linking reactions that form a more stable solid or lead to surface char formation. This layer insulates the product from more thermal degradation. Flame retardants can also function in the vapor phase, which is the case for halogenated additives. The

halogens are effeetive at reducing the eonecntration of free radicals that propagate flamcs, and thus reduce the flame intensity.

Usually high loading (> 10%) of fire-retardant additivcs is nccessary to be cffeetivc. The high coneentration can have a negative impaet on thc properties of thc materials. This projcet is designcd to enhanee the efficaey of flamc-rctardant additives.

Expcrimental

Materials and Handling

Fullerenes were purehased from Materials & Eleetrochemieal Researeh (MER) Corporation. All materials were obtained from Aldrieh unless otherwisc spccificd. Styrene was distilled from ealcium hydride (b.p. = 52 °C/20 mm) and refrigeratcd in darkness. Immediately prior to use, it was stirred over dibutylmagnesium until yellow and then degassed with a freeze-pump-thaw eyele and trap-to-trap distilled. Bcnzcne was distilled from calcium hydride and stored in refrigerator. Immediately prior to use, it was stirred over polystyryllithium until orange and then distilled. Toluene was distilled from ealeium hydride; tetrahydrofuran was distilled from sodium benzophcnone dianion; hcxadeeane was distilled from ealeium hydride at reduced prcssure. Distillcd water was further purified by reversed osmosis (Milli-RO 6 plus, Millipore). Polystyrcnc (498 K, PDI < 1.2, Pressure Chemieal Co.), alumina trihydrate (KC-350 series with medium partiele size of 3.5 μm, Georgia Marble), caleium hydride, dibutylmagnesium, scc-butyllithium (1.3 M in eyclohexane), heptadeeafluoro-1,1,2,2-tetrahydrodccyl-dimethylehlorosilane (Gelest), heptadeeafluoro-1,1,2,2-tetrahydrodeeyl-trichlorosilanc (Gelest), 30 % hydrogen peroxide, eoneentrated sulfurie aeid (Fisher, HPLC grade), perfluorohexyl iodide, 1,2,4-triehlorobenzcne, Freon-113 (1,1,2-trichlorotrifluoroethanc), and methylene ehloride (Fisher, HPLC grade) were all used as reeeived. All solvents and

reagents were either used immediately or stored under nitrogen in Schlenk flasks; reagents and solvents were transferred via either cannula or syringes; all distillations and reactions were performed under nitrogen.

Methods

Spin casting was performed with a Headway Research spin coater. X-ray photoelectron spectra (XPS) were obtained with a Perkin-Elmer-Physical Electronics 5100; advancing and receding contact angle measurements were made with a Ramè-Hart telescopic goniometer; elemental analysis was performed by Galbraith Laboratories; molecular weights and polydispersities of polymer samples were determined by gel permeation chromatography (GPC) relative to calibration with polystyrene using a system equipped with Polymer Laboratories PL gel columns (10^4, 10^3, 10^2 Å), a Rainin Rabbit solvent pump with THF as the mobile phase, and an IBM LC9563 Variable UV detector; thermogravimetric analysis was performed with a DuPont TGA 2950.

Polymer Matrix

Polystyrene (PS) samples were prepared in benzene using *sec*-butyllithium as initiator at room temp. overnight.[39] Four different molecular weight samples were used: M_n = 6,560 (PDI = 1.037), M_n = 62,107 (PDI = 1.033), and Mn = 147,533 (PDI = 1.034), and Mn = 498,000 (PDI < 1.2).

Surface-Active Fullerenes ($C_{60}[CF_2(CF_2)_4CF_3]_{5.2}$)[52]

A mixture of C_{60} (350 mg), perfluorohexyl iodide (6 mL), and 1,2,4-trichlorobenzene (15 mL) were added to a thick wall ampule (2.5 cm x 15 cm). The

ampule was freeze-pumped before it was sealed with CH_4/O_2 flame and heated in a sand bath for 24 h at 200 °C. The dark brown solution was vacuum dried yielding a brown solid. The solid was purified by two precipitations from Freon-113 solutions into methylene chloride and vacuum dried overnight (0.8 g). Elemental analysis: C, 44.37%; F, 52.01%; Cl, 0.13%; H, < 0.5%.

Film Sample Preparation

Supported film samples of composites of fullerenes/surface-active fullerenes and polystyrene were prepared on Si wafers (1.5 cm x 1.5 cm). The wafers were cleaned by immersion in 30% H_2O_2 and conc. H_2SO_4 (1:9, v/v) for 30 min, rinsing with distilled water (6 times), and then drying in an oven (100 °C, 2 h). Polystyrene (100 mg) and 10 mg C_{60} were dissolved in 10 mL toluene. Polystyrene (10 mg) and 10 mg surface-active fullerenes were dissolved in 1 mL toluene (distilled from CaH_2) and 10 mL Freon-113, respectively. A prescribed amount of Freon solution (for the desired concentration) was added to the toluene solution via a syringe. The toluene solution containing polystyrene and C_{60} or the toluene/Freon solution containing polystyrene and perfluorohexylated-C_{60} was added dropwise to a clean Si wafer surface until the sample had rounded edges (~8 drops). The film samples were air dried (1 h) and then vacuum dried (0.02 mm, room temp., 24 h) before annealing studies were carried out (either at room temp. under reduced pressure or at 110 °C under N_2).

Surface Reconstruction

1 % w/w $C_{60}[CF_2(CF_2)_4CF_3]_{5.2}$ and 6.5 K polystyrene film samples were prepared on Si wafers as described above. The film samples were then vacuum dried (0.02 mm, room temp., 24 h) before annealing (110 °C under N_2, 24 h). A thin polystyrene film was constructed over the composite material via either spin-casting or

transferring a free-standing film. The film samples were air dried (1 h) and then vacuum dried (0.02 mm, room temp., 24 h) before annealing (110 °C under N_2).

Spin-Casting. A 2.5 % w/v polystyrene toluene solution was prepared. A composite film sample was overflowed with the toluene solution, and immediately spun at 2000 rpm for 10 - 15 sec on a spin coater. The spin-casting process was repeated three times. The film samples were air dried (1 h) and then vacuum dried (0.02 mm, room temp., 24 h) before annealing (110 °C under N_2).

Transfer of a Free-Standing Film. A 2.5 % w/v 498 K polystyrene toluene solution was prepared. A pre-cleaned microscope slide was overflowed with the toluene solution, and spun at 2000 rpm for 10 - 15 sec. The slide was marked ~ 3 mm from the edges with a razor blade, and immersed slowly at ~ 45° in a bucket of water to detach the polystyrene film. A Si wafer covered with the composite film was placed underneath the floating polystyrene film, and lifted up gently. The film samples were air dried (2 h) and then vacuum dried (0.02 mm, room temp., 24 h) before annealing (110 °C under N_2).

Attempted Preparation of Surface-Active Alumina Trihydrate

1 g of alumina trihydrate was dried either by heating in a 16 x 150 mm KIMAX heat resistant test tube equipped with a septum and a small stirrer at 110 °C under N_2 for 24 h or under vacuum (0.02 mm, room temp., 16 h) after addition of ~1 mL of benzene. 10 mL of dry THF / dry toluene and heptadecafluoro-1,1,2,2-tetrahydrodecyl-trichlorosilane (0.3 mL) / heptadecafluoro-1,1,2,2-tetrahydrodecyl-dimethylchlorosilane (0.5 mL) were added to the test tube either via cannula or syringes. The reaction mixture was stirred under N_2 for 24 hr. The test tube was centrifuged and the top clear solution was decanted. 10 mL of dry toluene / dry THF was added to the test tube and the mixture was stirred under N_2 for ~ 1 min. In the case of THF, the wash cycle was

repeated six times. In the case of toluene, the wash cycle was repeated twice with toluene and then six times with THF.

Results and Discussion

XPS and contact angle measurements were used to monitor surface reconstruction in film samples containing specific concentrations of surface-active agent in a polystyrene matrix. The surface-active agent studied here is perfluorohexylated-C_{60}. For this system, several variables were chosen for manipulation, namely, time and temperature of heating to allow reconstruction, molecular weight of polystyrene, and concentration of the surface-active agent in the film samples. Experiments utilizing these variables were designed to elucidate how certain molecular and environmental parameters influence the rate and extent of surface reconstruction in films of this type.

Surface reconstruction of the film samples containing perfluorohexylated-C_{60} in polystyrene was studied at both room temperature and 110 °C. The purpose of heat-treatment of these samples was to maximize surface reconstruction while minimizing surface oxidation. Previous studies in our group showed that polystyrene samples heated at 110 °C exhibited significant fluorine surface-enrichment with minimal oxidation.[60]

Due to different solubility characteristics of perfluoroalkylated-C_{60} and polystyrene, film samples were prepared from a mixed solvent system, toluene/1,1,2-trichlorotrifluoroethane. The films were supported on Si wafers cut to an appropriate size for XPS analyses. Scheme 3.3 is a depiction of a reconstructed film sample. A control system containing C_{60} in polystyrene was also studied.

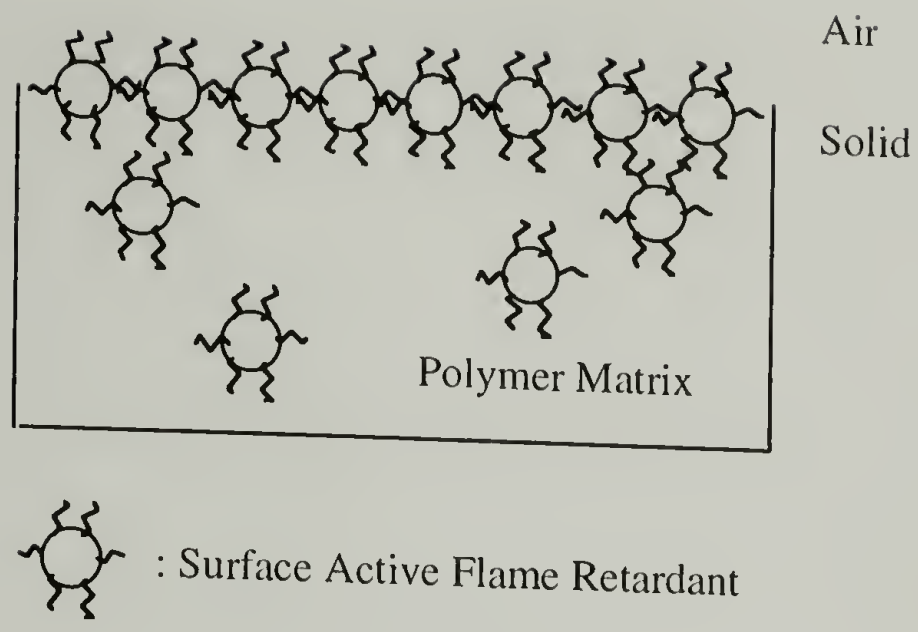

Scheme 3.3. Reconstructed film sample containing surface-active perfluoroalkylated-C_{60} in polystyrene matrix.

Surface Activity of Perfluoroalkylated-C_{60} in Polystyrene Matrix

Surface activity of neat C_{60} in a polystyrene matrix was examined as a control. A composite containing 10 % w/w of C_{60} in 6.5 K polystyrene was prepared by solution casting onto a Si wafer from toluene solution. Water and hexadecane contact angle measurements were performed on the composite film samples annealed at both room temperature and 110 °C. Figure 3.2 indicates that contact angles of the composite materials did not change over time under the annealing conditions studied. The plateau values of the contact angles agree very well with those of neat polystyrene as shown in Table 3.1. This indicates that in the C_{60} and polystyrene system, polystyrene is the component that has relatively lower surface energy.

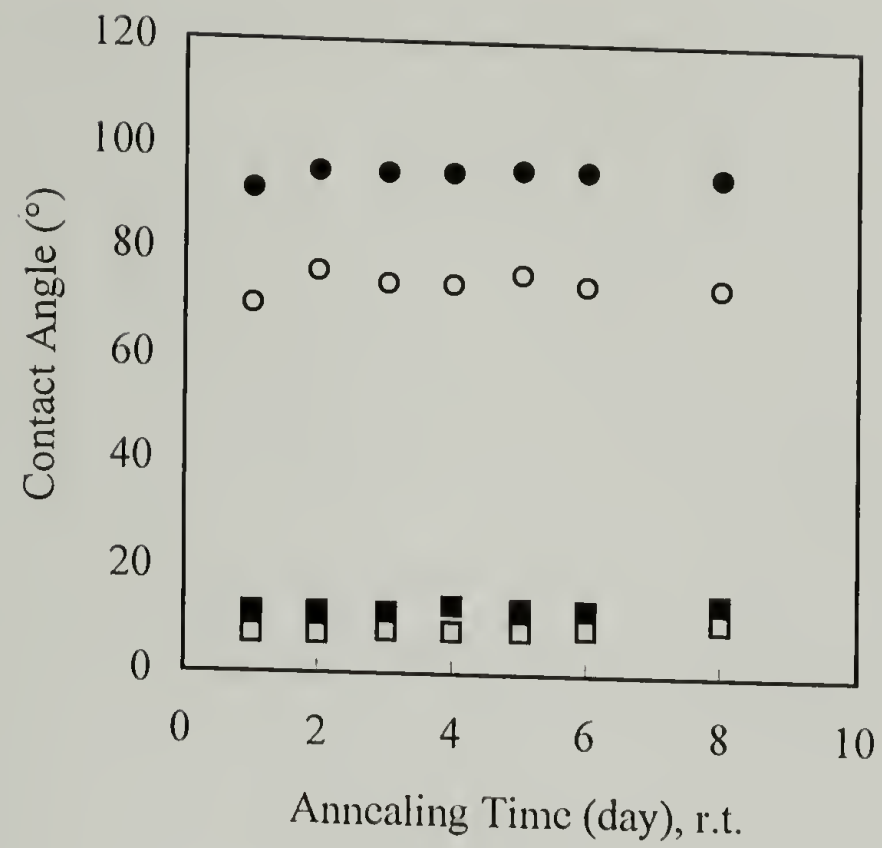

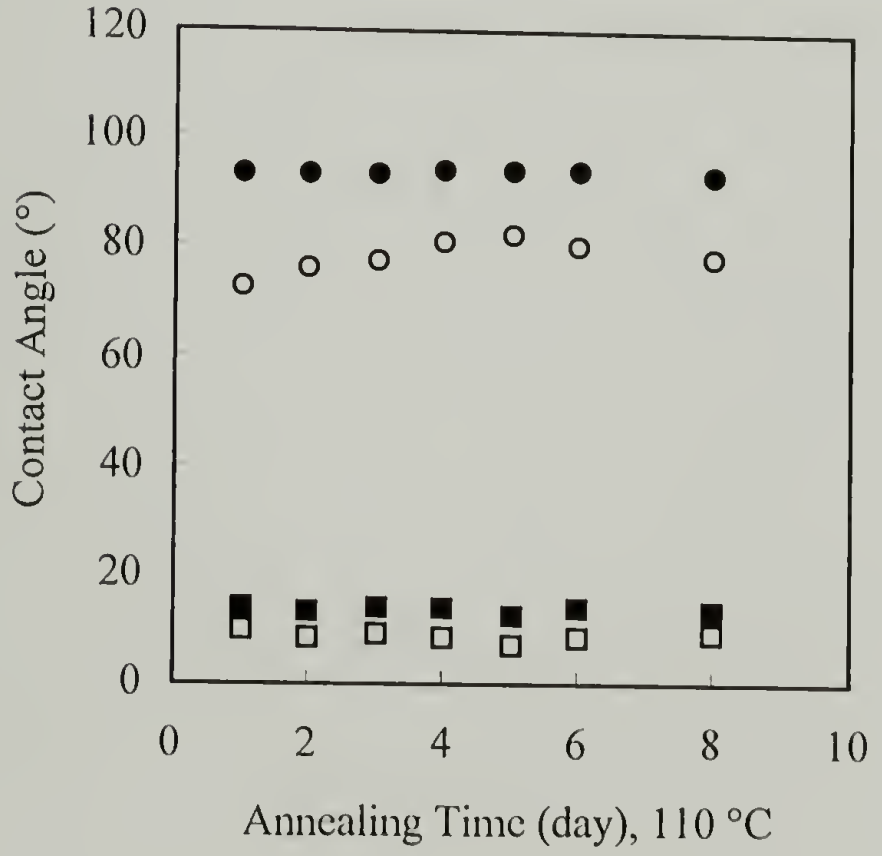

Figure 3.2. Contact angles of composite film samples of C_{60} in a 6.5 K polystyrene matrix (10 % w/w) after annealing at r.t. and 110 °C (advancing water contact angles (●); receding water contact angles (○); advancing hexadecane contact angles (■); receding hexadecane contact angles (□)).

Synthesis and Characterization of Perfluoroalkylated-C_{60}. Since neat C_{60} does not have the desired surface activity in polystyrene, we would like to make it surface active by attaching low surface energy moieties, such as perfluoroalkyl groups. We have prepared perfluorohexylated-C_{60} and studied its surface activity in a polystyrene matrix. Three protocols were used for its synthesis as shown earlier in Scheme 3.2 (page 102). The reactions taking place in fluoro-solvent gave such low yields that the products were not characterized. The reaction between perfluorohexyl iodide and C_{60} in 1, 2, 4-trichlorobenzene gave ~ 70 % yield. Elemental analysis indicated that the average chemical composition of the products is $C_{60}(CF_2CF_2CF_2CF_2CF_2CF_3)_{5.2}$. TGA indicates

Table 3.1. Water and hexadecane contact angles of polystyrene (6.5 K) solution cast on a Si wafer, C_{60} solution cast on a Si wafer, and a Si wafer.

	Water (θ_A/θ_R)	Hexadecane (θ_A/θ_R)
Polystyrene	94° / 79°	13° / 10°
C_{60}	69° / 15°	12° / 9°
Si wafer	47 ° / 26°	14 ° / 10°

that sharp weight losses (almost 100 %) occur at 700 - 800 °C for C_{60} and at ~ 400 °C for $C_{60}(C_6F_{13})_{5.2}$ which is due to sublimation.[52] The low sublimation temperature of $C_{60}(C_6F_{13})_{5.2}$ is an advantage for our objectives. That it vaporizes readily, may make it a more effective flame retardant, since fire takes place in the gas phase. We should be cautious, however, when choosing heat treatment conditions since severe conditions (high

temperature, high vacuum, and long time) will result in loss of $C_{60}(C_6F_{13})_{5.2}$. Surface reconstruction of the film samples containing perfluorohexylated-C_{60} in polystyrene was studied either at room temperature under reduced pressure or at 110 °C under nitrogen.

Figure 3.3 shows XPS survey and C_{1s} region spectra (75° take-off angle) of a composite film sample containing 1% w/w perfluorohexylated-C_{60} in a polystyrene matrix (Mn = 6.5 K). The assignment of the five peaks in the C_{1s} region is also shown in the figure. Table 3.2 gives XPS atomic composition of the outer 10 - 40 Å of the film sample. Fluorine atomic composition could be biased high due to its high surface affinity. Comparing the atomic composition obtained from XPS to the chemical composition of perfluorohexylated-C_{60} (C, 44.37%; F, 52.01%), indicates that there is ~ 5% and ~ 15% polystyrene in the outer 10 Å and 40 Å, assuming perfluorohexylated-C_{60} molecules near the surface have 5.2 perfluorohexyl groups per C_{60} on average and the groups are distributed evenly around C_{60}.

Table 3.2. XPS atomic composition data of a film sample containing 1 % w/w $C_{60}(C_6F_{13})_{5.2}$ in 6.5 K polystyrene solution-cast onto a Si wafer and subsequently dried at r.t. under reduced pressure for 3 days.

XPS take-off angle	%C	%F
15° take-off angle	48.86	51.14
75° take-off angle	54.01	45.99

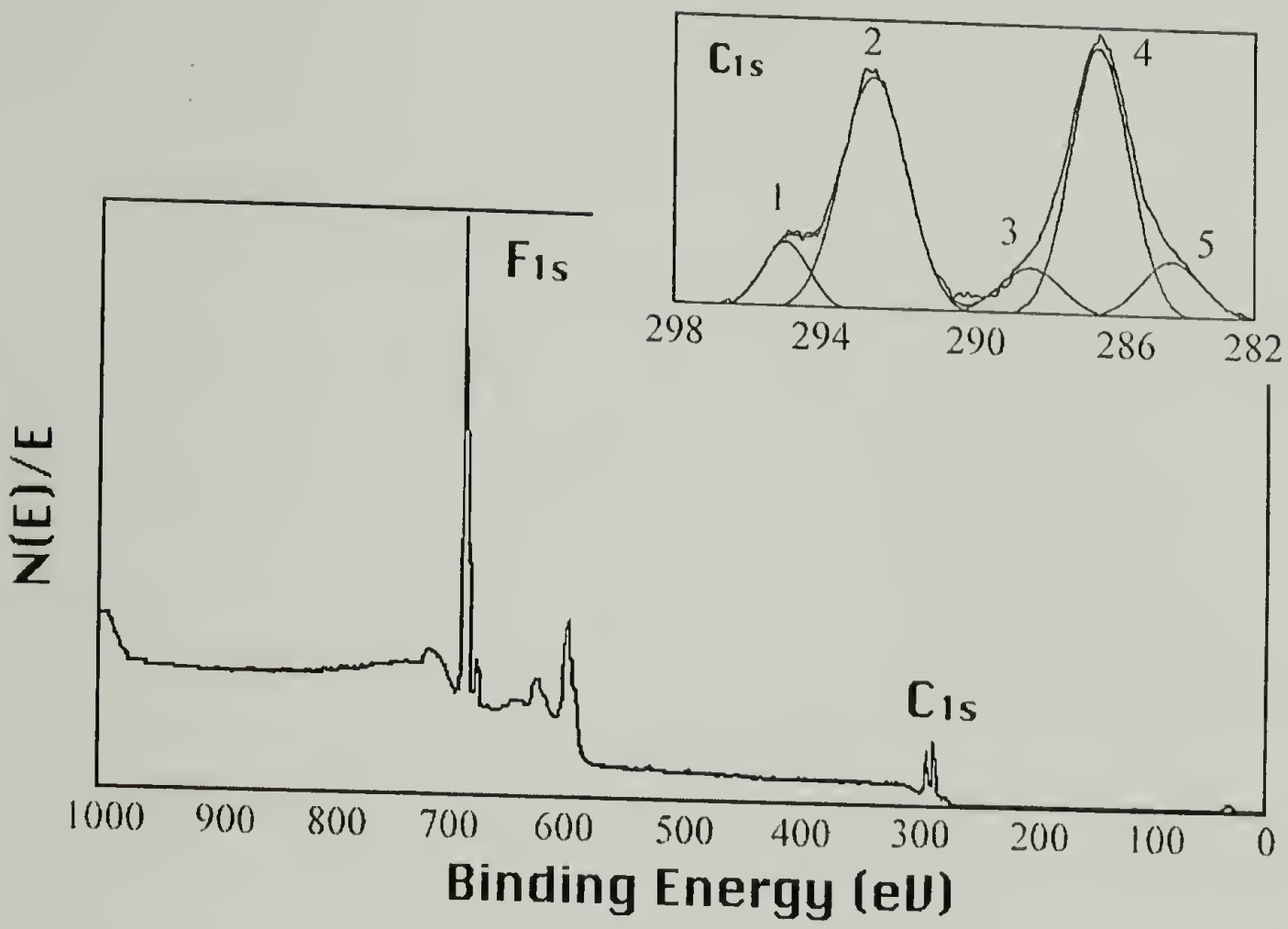

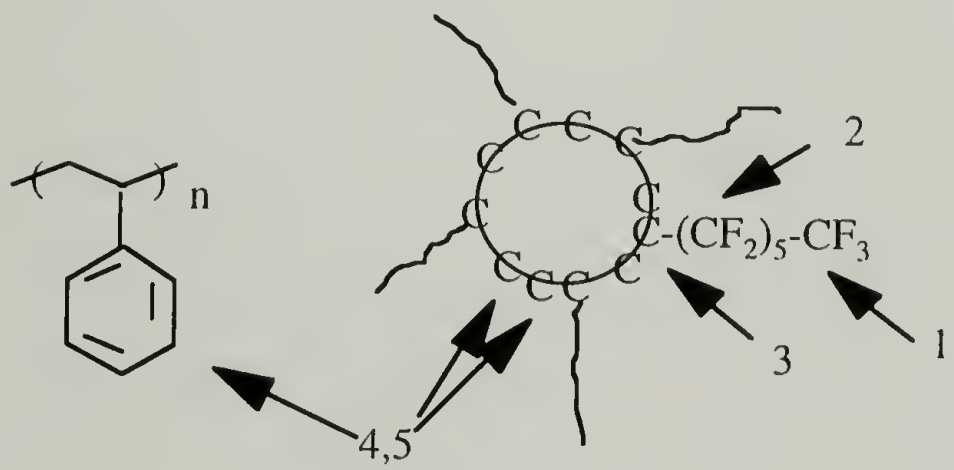

Polystyrene $C_{60}(C_6F_{13})_{5.2}$

Figure 3.3. XPS survey and C_{1s} region spectra (75° take-off angle) of a composite film sample containing 1% w/w perfluorohexylated-C_{60} in polystyrene matrix (Mn = 6.5 K).

Table 3.3 gives the percentages of each type of C_{1s} atom at both 15° and 75° take-off angles. The theoretical intensity ratio of peak #1 : peak #2 : peak #3 should be 1 : 5 : 1, which should be observed only if perfluorohexyl groups lie parallel to the surface. At 15° take-off angle, the observed ratio is 1.4 : 5.3 : 1. The discrepancy is presumably due to the orientation of the perfluorohexyl chain, lying at an angle (> 0°) relative to the surface. The orientation of the perfluorohexyl chain is discussed further below. The 75° take-off angle data deviate less from the theoretical prediction because they are less surface-selective than 15° take-off angle data.

Table 3.3. Deconvoluted XPS C_{1s} region of a film sample containing 1 % w/w $C_{60}(C_6F_{13})_{5.2}$ in 6.5 K polystyrene solution-cast onto a Si wafer and subsequently dried at r.t. under reduced pressure for 3 days.

XPS take-off angle	peak #1 (%)	peak #2 (%)	peak #3 (%)	peak #4 (%)	peak #5 (%)
15° take-off angle	9.96	37.47	7.09	38.74	6.74
75° take-off angle	7.75	31.88	7.22	45.93	7.22

Adsorption Kinetics. Figures 3.4 and 3.5 show how surface composition (F/C ratio determined by XPS) and contact angles (water and hexadecane) change with annealing time for a film sample containing 1% w/w perfluorohexylated-C_{60} in polystyrene (Mn = 6.5 K) at both room temperature and 110 °C. There are several

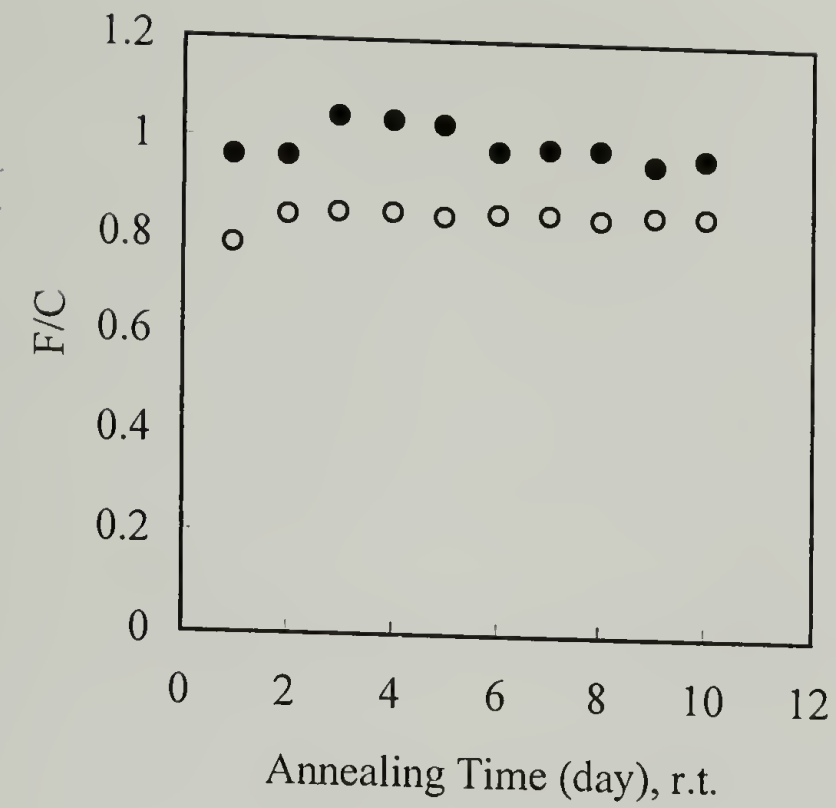

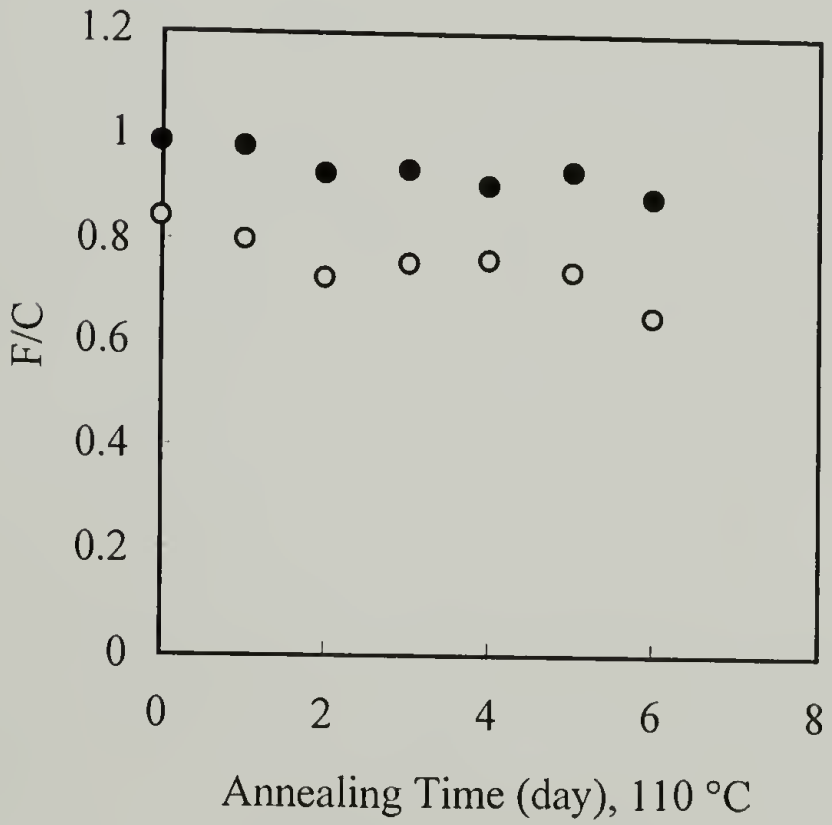

Figure 3.4. Adsorbed amount (F/C) of 1 % w/w perfluorohexylated C_{60} in 6.5 K polystyrene matrix as a function of time at either r.t. or 110 °C, at 15° (●) and 75° (○) take-off angles.

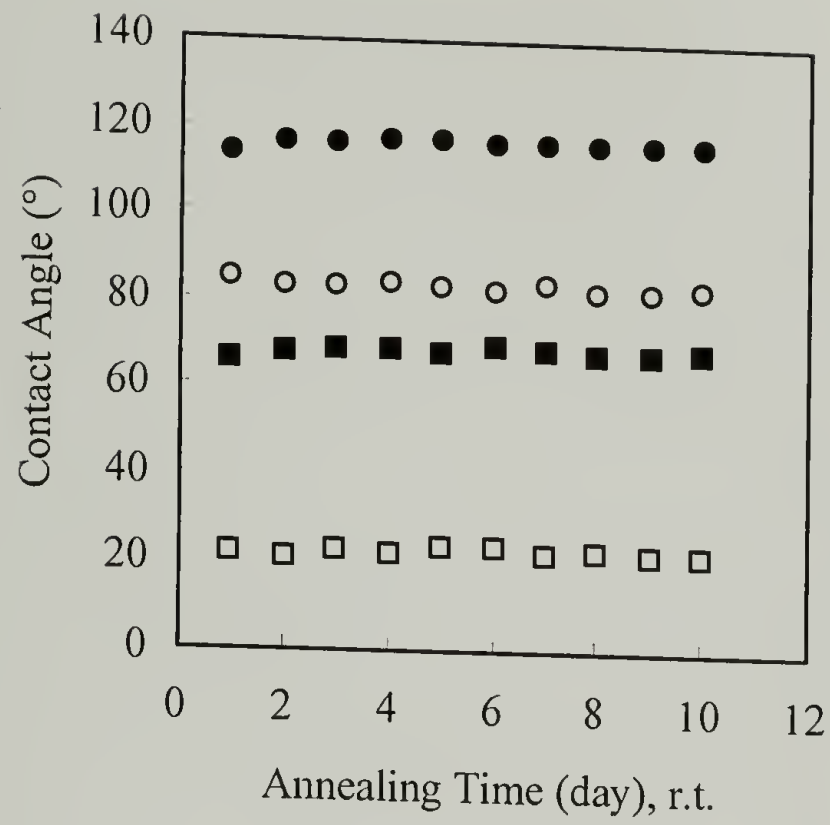

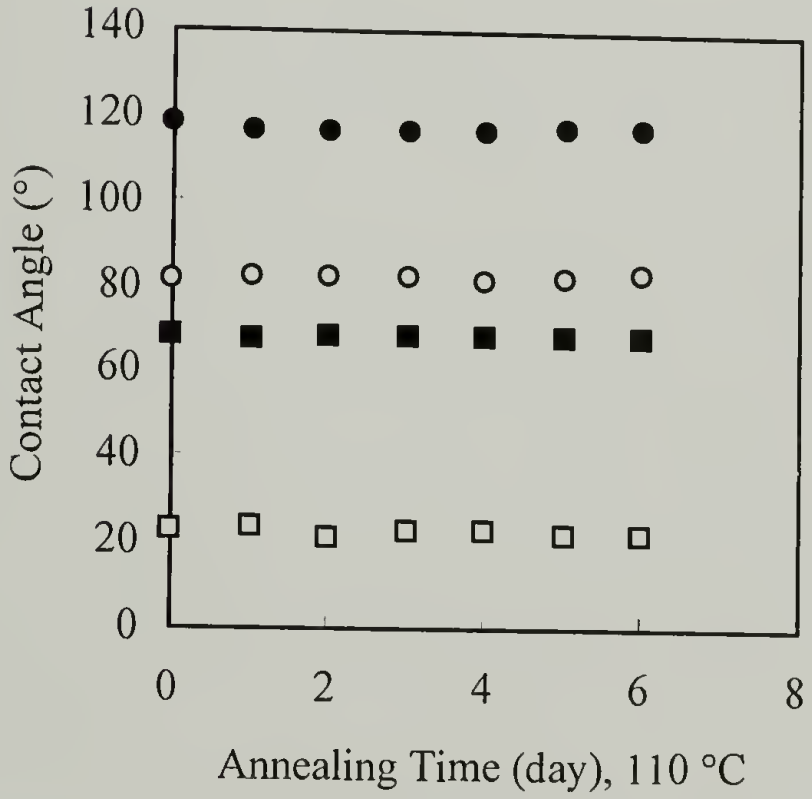

Figure 3.5. Contact angles of 1 % w/w perfluorohexylated C_{60} in 6.5 K polystyrene matrix as a function of time at either r.t. or 110 °C (advancing water contact angles (●); receding water contact angles (○); advancing hexadecane contact angles (■); receding hexadecane contact angles (□)).

issues that to discuss regarding the two figures. One important feature is the discrepancy between the F/C atomic ratios measured at 15° and 75° take-off angles. The 15° take-off angle data represent the composition of the outer ~10 Å of the film sample (95 % of the photoelectrons detected originate from this region). Spectra recorded at a 75° take-off angle are representative of the outer ~40 Å of the sample (95 % of the photoelectrons detected originate from this region) and 54 % of the electrons measured at this angle are ejected from the outermost ~10 Å. Data obtained at 75° take-off angle (F/C = ~ 0.8) are about 80 % of that observed at 15° (F/C = ~1). This indicates that there is a 10 Å - 40 Å thick fluorine-enriched layer at the surface. This thickness is on the same scale as the size of the perfluorohexylated-C_{60} molecules. XPS take-off angle dependence is more pronounced in the cases of surface-active polymers, where fluorine is concentrated in the outer few angstroms and a layer that is depleted of fluorine exists below this region at the film surface.[60] The fluorine-depleted layer is not obvious in this case due to the structural difference between the surface-active polymers and perfluorohexylated-C_{60}.

The water and hexadecane contact angles in the plateau regions are 116° ± 2°/83° ± 2° (θ_A/θ_R) and 68° ± 2°/22° ± 2° (θ_A/θ_R), respectively. The hexadecane contact angles were compared with literature θ_A values[61] of 45° for poly(tetrafluoroethylene) (PTFE) and 72° for a monolayer containing -CF_3 groups at the surface. A sample of PTFE in our laboratory exhibited hexadecane contact angles of 42°/9°. These data indicate that the surface of the composite material is close to that of -CF_3, with perfluorohexyl chains lying at some angle (> 0°) to the surface exposing mostly -CF_3 end groups. The observed hysteresis is presumably due to surface roughness.

Another feature is that plateau values are reached prior to annealing, which implies that surface-active fullerenes migrate to the surface in the liquid phase during solution casting. That elevated temperatures and time were not necessary to reach the "final state" means that reconstruction was complete during solution casting.

Lastly, F/C ratios of the film samples heated at 110 °C seem to decrease over time. One possible explanation is the slow sublimation of $C_{60}(C_6F_{13})_{5.2}$ from the composite materials at high temperature.

A 1% w/w composite film was also prepared by spin-casting from Freon/toluene solution onto Si wafer. The XPS atomic composition data and contact angle results are given in Tables 3.4 and 3.5. Again, plateau regions of fluorine concentration and contact angles are reached right away, however, they are not as high as the solution-cast results. It is presumably because the spin-cast film is so thin (< 1000 Å) that there is not enough surface-active agent in the composite to saturate the surface.

Adsorption Isotherms. The surface activity of $C_{60}(C_6F_{13})_{5.2}$ was also assessed by determining a concentration isotherm. Figures 3.6 and 3.7 show how F/C ratios and contact angles (water and hexadecane) change as a function of the concentration of perfluorohexylated-C_{60} in 6.5 K polystyrene. Both F/C ratios and contact angles increase as a function of surface-active agent concentration before they reach plateau regions. The F/C ratio reached "steady state" after only 0.2 % w/w of $C_{60}(C_6F_{13})_{5.2}$ was incorporated into the polystyrene matrix. The maximum surface excess is ~500. Since contact angle is a more surface-sensitive technique, both water and hexadecane contact angles reached the plateau values even sooner, at about 0.1 %.

Mechanical Integrity of the Composite Film. As mentioned earlier, XPS data of the composite material containing 1 % w/w $C_{60}(C_6F_{13})_{5.2}$ in 6.5 K polystyrene matrix indicate that the surface consists primarily of $C_{60}(C_6F_{13})_{5.2}$. Peel tests (180°) were

Table 3.4. Adsorption kinetics study (XPS atomic composition data) of film samples spin-cast at 2000 rpm from a solution containing 1 mg of $C_{60}(C_6F_{13})_{5.2}$ in 1 mL of Freon-113 and 100 mg of 6.5 K PS in 10 mL of toluene onto Si wafers after drying at r.t. for 24 h followed by annealing at 110 °C.

Time (day)	15° %C	%O	%F	75° %C	%O	%F
0	83.33	1.58	15.09	93.35	0.38	6.27
1	79.79	1.79	18.41	92.49	0.43	7.07
2	80.92	2.28	16.81	93.11	0.55	6.34
3	80.55	1.40	18.04	92.64	0.72	6.65
4	81.77	1.48	16.75	93.21	0.29	6.51

Table 3.5. Adsorption kinetics study (water and hexadecane contact angles) of film samples spin-cast at 2000 rpm from a solution containing 1 mg of $C_{60}(C_6F_{13})_{5.2}$ in 1 mL of Freon-113 and 100 mg of 6.5 K PS in 10 mL of toluene onto Si wafers after drying at r.t. for 24 h followed by annealing at 110 °C.

Time. (day)	$\theta_A(H_2O)$ (deg)	θ_R (H_2O) (deg)	θ_A ($C_{16}H_{34}$) (deg)	θ_R ($C_{16}H_{34}$) (deg)
0	97	82	33	11
1	98	82	32	12
2	98	84	31	12
3	97	82	31	12
4	97	82	30	12

performed using pressure-sensitive adhesive tape (3M # 810) to determine how strongly the perfluorohexylated-C_{60} is incorporated into the polystyrene matrix. Very little fluorine-containing species were detached from the surface of the film sample onto the tape surface after peeling (Table 3.6). The peel test data indicate good mechanical integrity of the composite material.

Table 3.6. Assessment of the mechanical integrity of 1 % w/w $C_{60}(C_6F_{13})_{5.2}$ in 6.5 K polystyrene matrix dried at room temperature for 7 days using peel tests with pressure-sensitive adhesive tape.

		$C_{60}(C_6F_{13})_{5.2}$ and PS Film		Pressure-sensitive Tape	
		15° take-off	75° take-off	15° take-off	75° take-off
Before	%C	50.36	54.04	87.20	84.42
	%O	~0	~0	12.80	15.58
	%F	49.64	45.96	0	0
After	%C	51.92	53.96	82.96	83.39
	%O	~0	~0	15.67	16.16
	%F	48.08	46.04	1.36	0.46

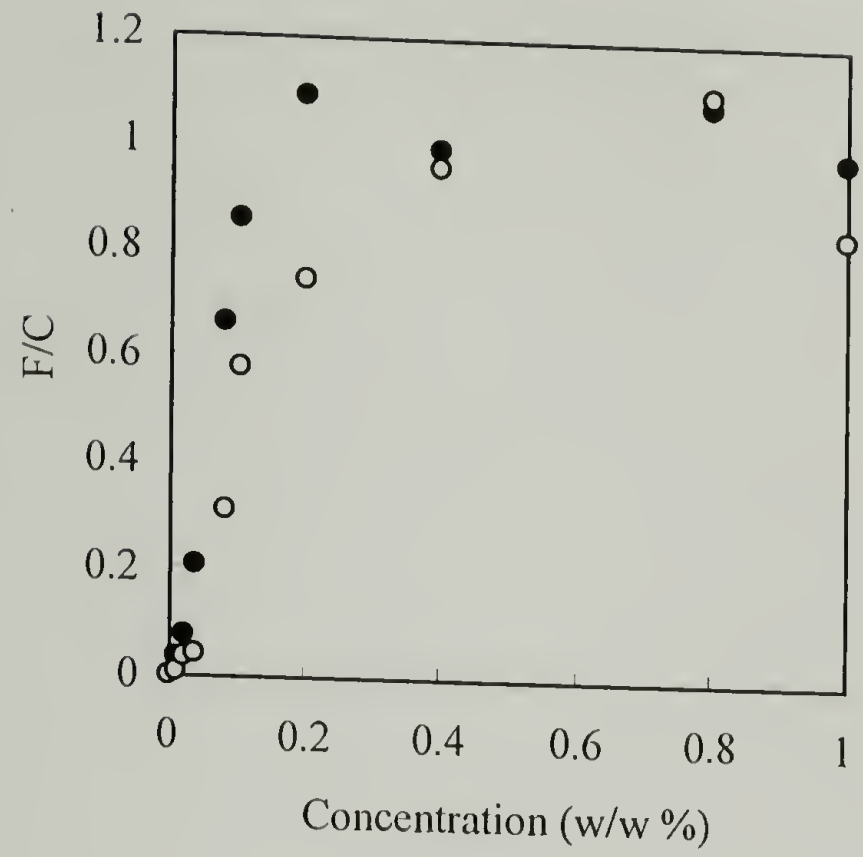

Figure 3.6. Adsorption isotherm (F/C) of perfluorohexylated C_{60} in 6.5 K polystyrene matrix, at 15° (●) and 75° (○) take-off angles.

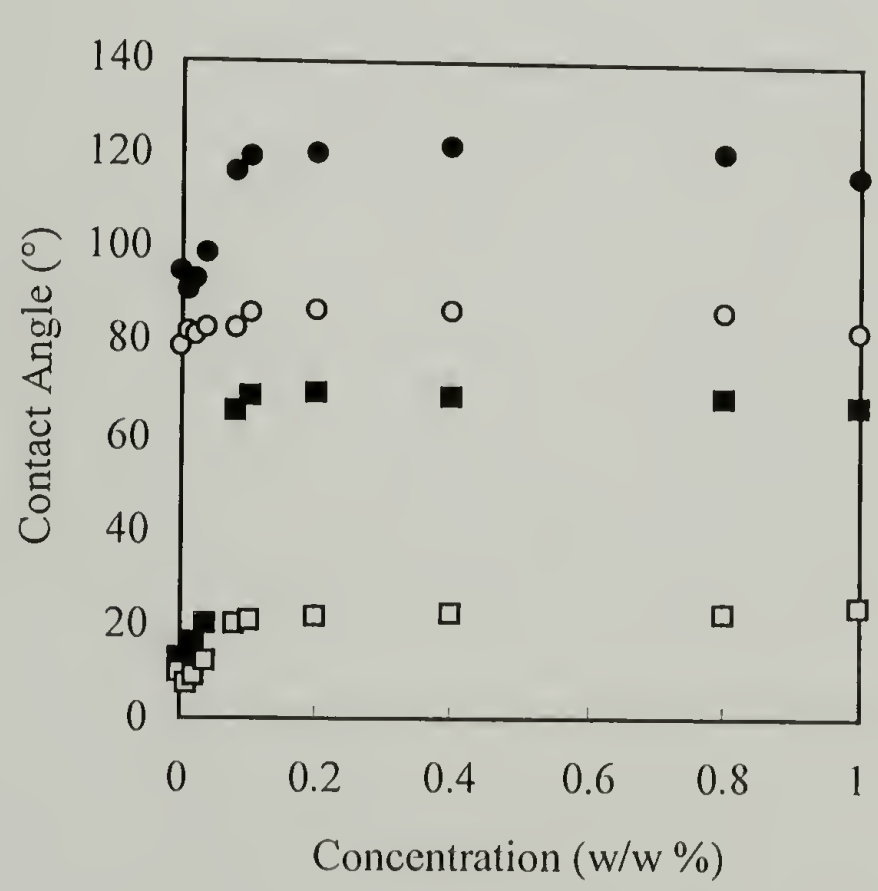

Figure 3.7. Adsorption isotherm (contact angles) of perfluorohexylated C_{60} in 6.5 K polystyrene matrix (advancing water contact angles (●); receding water contact angles (○); advancing hexadecane contact angles (■); receding hexadecane contact angles (□)).

Reconstruction Studies

Due to the high surface affinity of perfluorohexylated-C_{60} in the liquid phase during solution casting, the process of its migration from the bulk to the polymer/air interface is too fast to demonstrate in the adsorption kinetics studies at both room temperature and 110 °C. In order to study the surface reconstruction of the composite film samples, a thin polystyrene film was constructed over the composite material containing 1% w/w perfluorohexylated-C_{60} in 6.5 K polystyrene via either spin-casting or transferring a free-standing film. The migration of surface-active C_{60} through the spun-cast and transferred polystyrene films to the new surfaces was monitored by XPS and contact angle measurements.

Spin-Casting. In initial experiments, either 6.5 K or 62 K polystyrene was spin-cast once onto the composite film containing 1 % w/w perfluorohexylated-C_{60} in 6.5 K polystyrene. In Figure 3.8, F/C ratios calculated from XPS atomic composition data are plotted as a function of annealing time at 110 °C (no surface reconstruction was observed at room temperature). There are some interesting features in this figure. First of all, the F/C plateau values, 0.8/0.4 (15°/75°) for 6.5 K and 0.7/0.3 (15°/75°) for 62 K, are lower than those for the composite film, 1.0/0.8 (15°/75°). The polystyrene film cast on top of the composite acts as a barrier for the migration of the surface-active agent from the bulk to the surface. The thickness of the polystyrene film obtained under the experimental condition (2.5 % polystyrene toluene solution and 2000 rpm spin rate) is expected to be ~ 1000 Å.[62] The actual thickness, however, may vary since the dissolution of the surface-active agent in the polystyrene/toluene solution and mixing with the polystyrene cast on the top are evident from the nonzero starting point of the curve. The thickness was not estimated by difference because of the surface roughness of the solution-cast composite film. The migration seems to become slower when the molecular weight of polystyrene

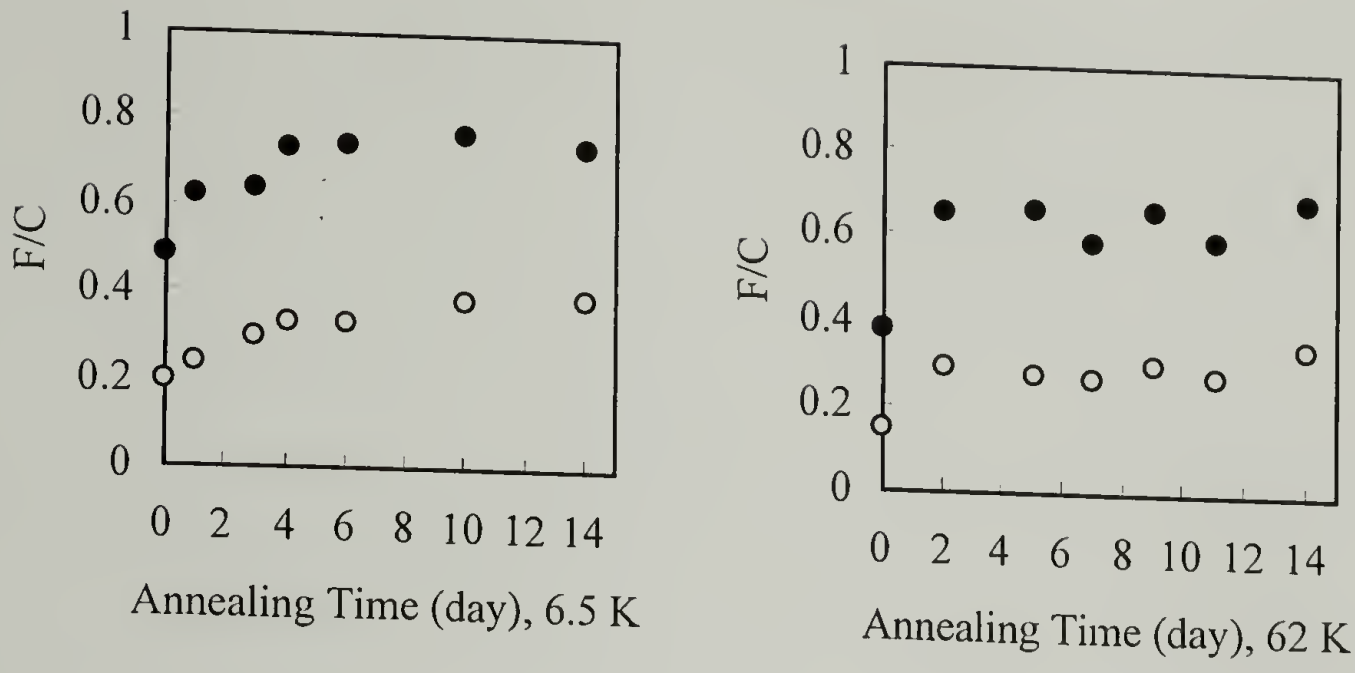

Figure 3.8. Surface reconstruction (F/C) monitored as a function of annealing time at 110 °C after 6.5 K/62 K polystyrene (toluene solution) was spin-cast once onto the composite film samples, at 15° (●) and 75° (○) take-off angles.

is increased from 6.5 K to 62 K. Furthermore, both of the plots start from some nonzero values and increase as a function of annealing time until plateau values are reached. The shape of the curves implies that migration of perfluorohexylated-C_{60} occurs during spin-casting and the rate of migration is slower than the speed of drying. This information should enable us cover the surface-active agent completely, i.e. to move the starting point of the curve to zero, by spin-casting more than once.

Figures 3.9 and 3.10 show the results of spin-casting various molecular weight samples of polystyrene three times onto the composite film. By spin-casting three times, the initial F/C ratios become very close to zero. The plateau F/C ratios, however, are lower than those of samples spin-cast only once (6.5 K and 62 K), and lower than those of the composite samples. Spin-casting three times compared to only once created a thicker barrier layer for the migration of the surface-active agent from the bulk to the surface. Both water and hexadecane contact angles are also lower than those of the composite samples. Another important feature is that the plateau values of F/C ratios

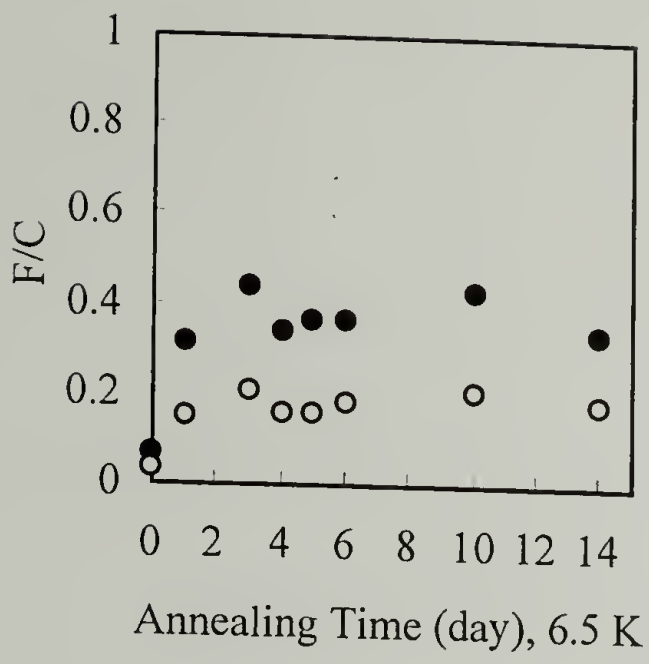

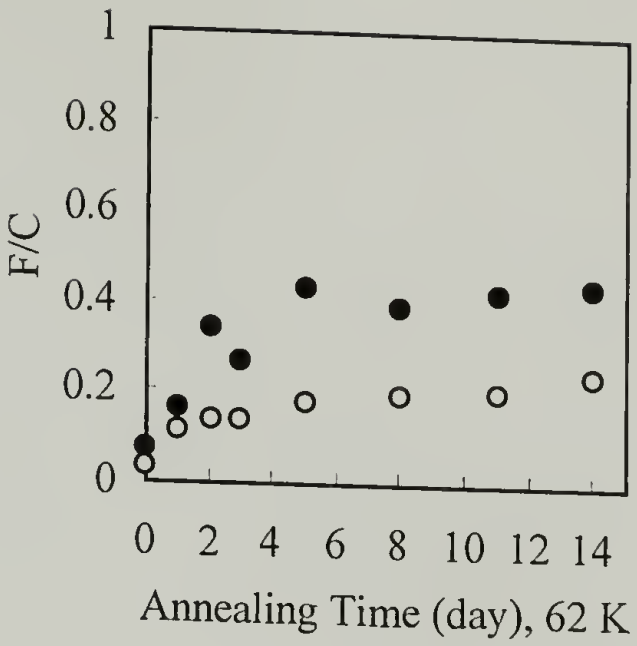

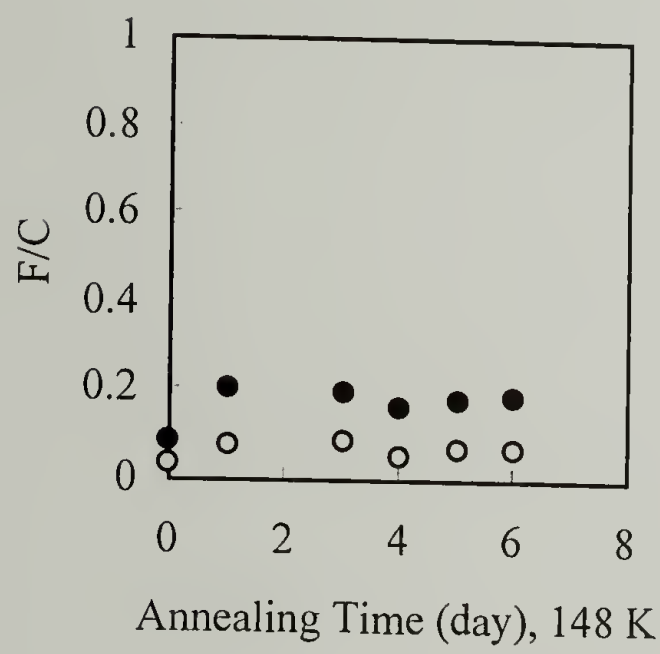

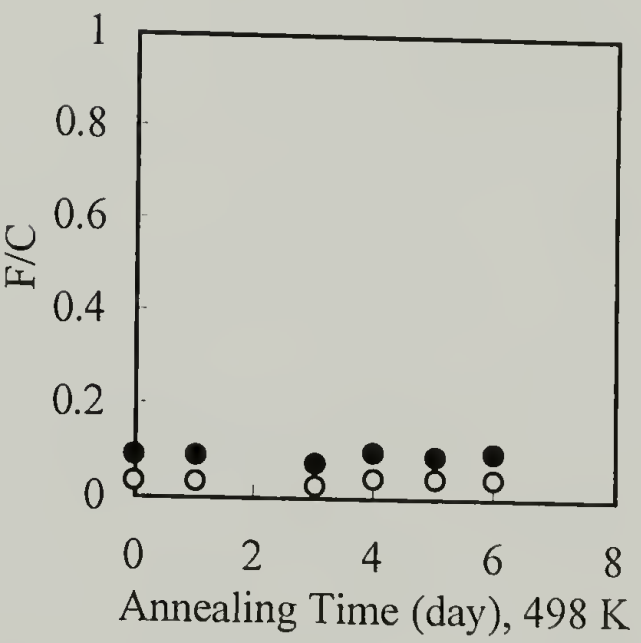

Figure 3.9. Surface reconstruction (F/C) is monitored as a function of annealing time at 110 °C after various molecular weight polystyrene solutions were spin-cast three times onto the composite film samples, at 15° (●) and 75° (○) take-off angles.

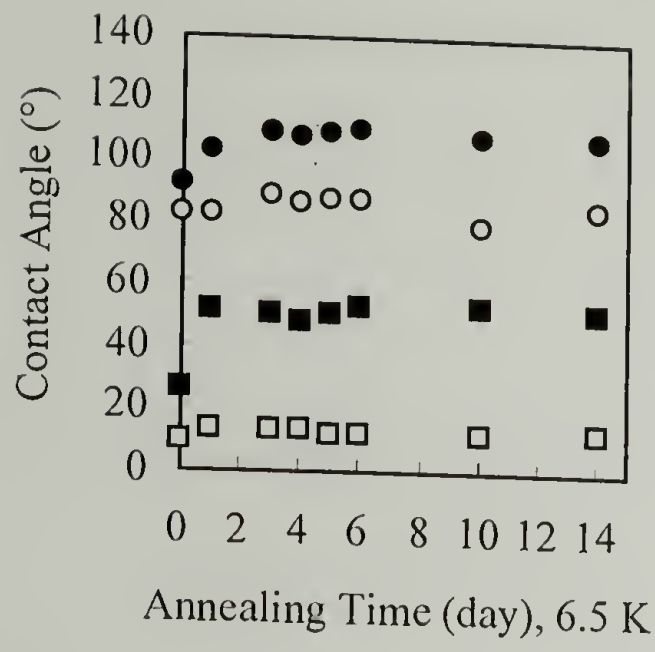

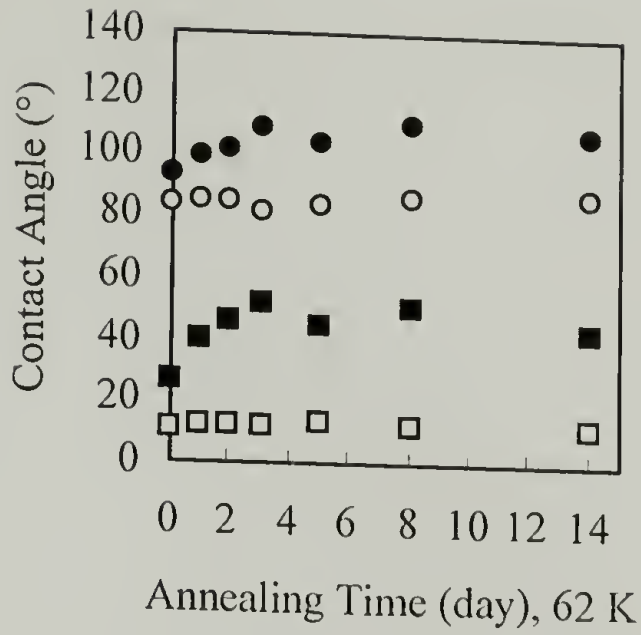

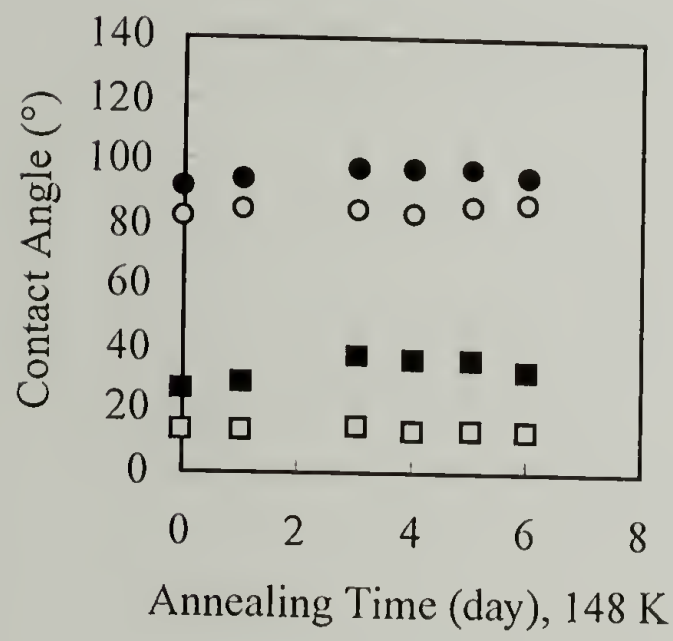

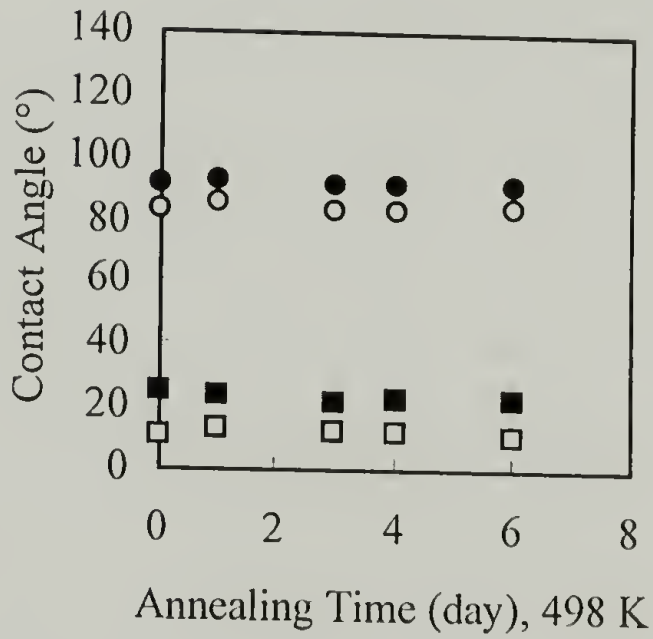

Figure 3.10. Surface reconstruction (contact angle) monitored as a function of annealing time at 110 °C after various molecular weight polystyrene solutions were spin-cast three times onto the composite film samples (advancing water contact angles (●); receding water contact angles (○); advancing hexadecane contact angles (■); receding hexadecane contact angles (□)).

and contact angles decrease as a function of molecular weight of polystyrene. In Figure 3.11, plateau F/C ratios are plotted as a function of molecular weight. There is not much change from 6.5 K to 62 K, followed by a sharp decrease to 148 K, and further decease to 498 K. Presumably increased entanglement density in the polystyrene matrix at higher molecular weight slows the migration of the surface-active agent.

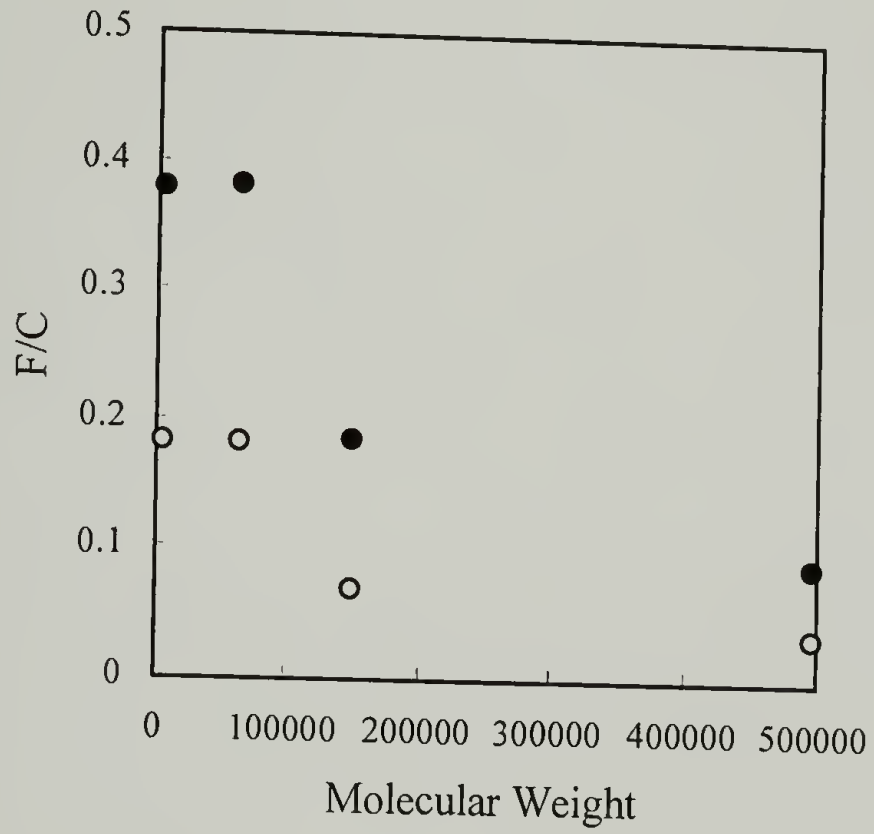

Figure 3.11. The extent of surface reconstruction (plateau values of F/C in Figure 3.9) as a function of the molecular weight of polystyrene spin-cast on the composite, at 15° (●) and 75° (○) take-off angles.

Transfer of a Free-Standing Film. To avoid mixing of the polystyrene cast on the top with the surface-active agent in the composite sample underneath, a free-standing polystyrene film was pre-cast on a glass slide and transferred over the composite sample. The limitation of this approach is that only high molecular weight polystyrene films are mechanically strong enough to be transferred. Of the four different molecular weight

samples, the highest molecular weight polystyrene, 498 K, was chosen. The thickness of the polystyrene film obtained under the experimental condition (2.5 % polystyrene toluene solution and 2000 rpm spin rate) is ~ 1000 Å.[62] Both F/C ratios and contact angles were monitored as a function of annealing time at 110 °C (Figures 3.12 and 3.13). Figure 3.12 is almost identical to Figures 3.9 except that the starting point of the spin-cast samples was higher due to the migration of the surface-active agent during casting. That the plateau value is almost the same as that of 498 K polystyrene spin-cast three times onto the composite samples suggests that no loss of perfluorohexylated-C_{60} occurred during spin-casting even though its dissolution in the polystyrene/toluene solution and mixing with the polystyrene cast on the top is evident from earlier results (Figure 3.8).

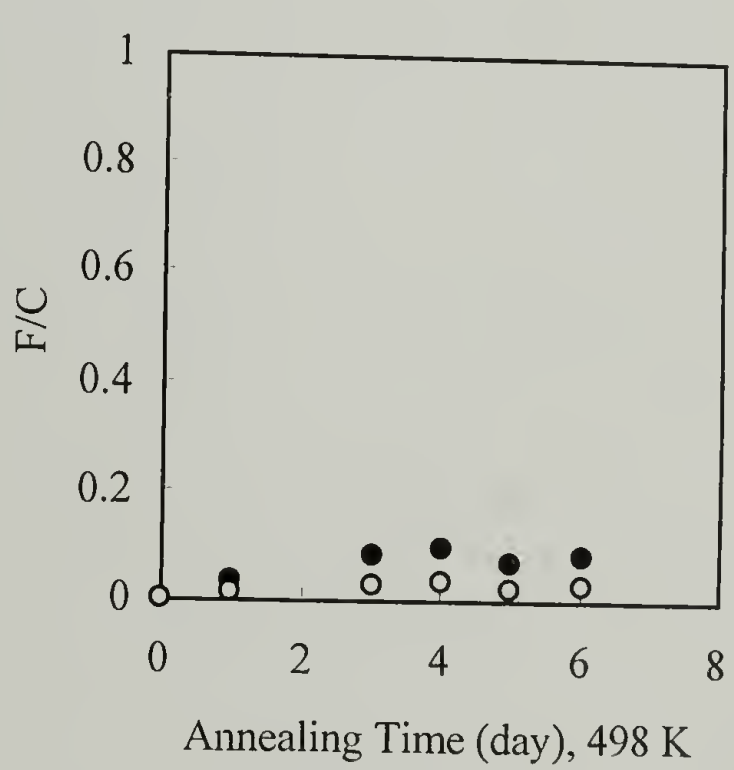

Figure 3.12. Surface reconstruction (F/C) monitored as a function of annealing time at 110 °C after a ~ 1000 Å thick 498 K polystyrene film was transferred onto the composite film samples, at 15° (●) and 75° (○) take-off angles.

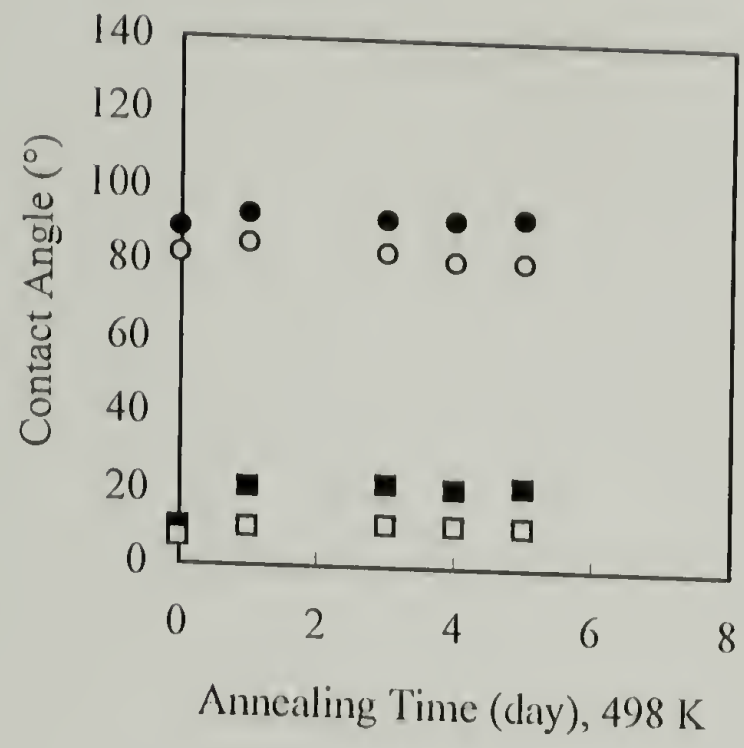

Figure 3.13. Surface reconstruction (represented by contact angle) monitored as a function of annealing time at 110 °C after a ~ 1000 Å thick 498 K polystyrene film was transferred onto the composite film samples (advancing water contact angles (●); receding water contact angles (○); advancing hexadecane contact angles (■); receding hexadecane contact angles (□)).

Failed Preparation of Surface-Active Alumina Trihydrate

The preparation of surface-active alumina trihydrate was not successful. In several attempts of silane coupling reactions, very little fluorine was observed by XPS on the modified alumina trihydrate. It is suspected that the alumina trihydrate used was not very clean and the surface -OH sites were blocked and not available for coupling reactions. We were not able to clean alumina trihydrate without losing its crystallized water which is essential for it to function as a flame retardant.

Conclusion

We have prepared a perfluorohexylated-C_{60} and studied its surface activity and mobility in a polymer matrix (polystyrene). Adsorption/migration of the

perfluorohexylated-C_{60} from the bulk to the polymer/air interface was studied as a function of bulk concentration, annealing temperature, and annealing time. Perfluorohexylated-C_{60} is extremely surface-active in the polystyrene matrix and occupies 95% - 85% of the outermost 10 Å - 40 Å (XPS results), and renders a surface that is similar to a monolayer containing -CF_3 groups (hexadecane contact angle data). Surface reconstruction studies were carried out via either spin-casting or transferring a free standing polystyrene film over the composite materials (the surface-active agent and polystyrene). Both approaches show similar results: migration of perfluorohexylated-C_{60} from the bulk to the surface is driven by surface free energy minimization and is a function of annealing temperature, annealing time, and molecular weight of the polymer matrix. Peel tests indicate that the composite materials have good mechanical integrity. Flammability of the polymer matrix with and without the addition of perfluoroalkylated-C_{60} is yet to be evaluated.

References

1. Shoichet, M. S.; McCarthy, T. J. *Macromolecules* **1991**, *24*, 1441.

2. Bee, T. G.; McCarthy, T. J. *Macromolecules* **1992**, *25*, 2093 and references cited therein.

3. Leväsalmi, J.-M.; McCarthy, T. J. *Polym. Prepr. (Am. Chem. Soc. Div. Polym. Chem.)* **1996**, *37(1)*, 457.

4. Cross, E. M.; McCarthy, T. J. *Macromolecules* **1990**, *23*, 3916.

5. Theodorou, D. N. *Macromolecules* **1988**, *21*, 1391.

6. Theodorou, D. N. *Macromolecules* **1988**, *21*, 1411.

7. Hariharan, A.; Kumar, S. K.; Russell, T. P. *Macromolecules* **1990**, *23*, 3584.

8. Hariharan, A.; Kumar, S. K.; Russell, T. P. *Macromolecules* **1991**, *24*, 4909.

9. Broseta, D.; Fredrickson, G. H.; Helfand, E.; Leibler, L. *Macromolecules* **1990**, *23*, 132.

10. Kumar, S. K.; Vacatello, M.; Yoon, D. Y. *Macromolecules* **1990**, *23*, 2189.

11. Kumar, S. K.; Russell, T. P. *Macromolecules* **1991**, *24*, 3816.

12. Jarvis, N. L.; Fox, R. B.; Zisman, W. A. *Adv. Chem. Ser.* **1964**, *43*, 317.

13. Torstensson, M.; Ranby, B.; Hult, A. *Macromolecules* **1990**, *23*, 126.

14. Shull, K. R.; Kramer, E. J.; Bates, F. S.; Rosedale, J. H. *Macromolecules* **1991**, *24*, 1383.

15. Shull, K. R.; Winey, K. I.; Thomas, E. L.; Kramer, E. J. *Macromolecules* **1991**, *24*, 2748.

16. Gaines, G. L., Jr. *Macromolecules* **1979**, *12*, 1011.

17. Gaines, G. L., Jr.; Bender, G. W. *Macromolecules* **1972**, *5*, 82.

18. Green, P. F.; Christensen, T. M.; Russell, T. P. *Macromolecules* **1991**, *24*, 252.

19. Schmitt, R. L.; Gardella, J. A., Jr.; Magill, J. H.; Salvati, L., Jr.; Chin, R.L. *Macromolecules* **1985**, *18*, 2675.

20. Shull, K. R.; Kramer, E. J.; Hadziioanou, G.; Tang, W. *Macromolecules* **1990**, *23*, 4780.

21. Green, P. F.; Russell, T. P. *Macromolecules* **1991**, *24*, 2931.

22. LeGrand, D. G.; Gaines, G. L., Jr. *Polym. Prepr. (Am. Chem. Soc., Div. Polym. Chem.)* **1970**, *11*, 442.

23. Thomas, H. R.; O'Malley, J. J. *Macromolecules* **1979**, *12*, 323.

24. Clark, D. T.; Peeling, J.; O'Malley, J. J. *J. Polym. Sci., Polym. Chem.* **1976**, *14*, 543.

25. Green, P. F.; Christensen, T. M.; Russell, T. P.; Jérôme, R. *Macromolecules* **1989**, *22*, 2189.

26. O'Malley, J. J.; Thomas, H. R.; Lee, G. M. *Macromolecules* **1979**, *12*, 996.

27. Schmitt, R. L.; Gardella, J. A., Jr.; Salvati, L., Jr. *Macromolecules* **1986**, *19*, 648.

28. Schmitt, R. L.; Gardella, J. A., Jr.; Salvati, L., Jr. *Macromolecules* **1989**, *22*, 4489.

29. Anastasiadis, S. H.; Gancarz, I.; Koberstein, J. T. *Macromolecules* **1988**, *21*, 2980.

30. Creton, C.; Kramer, E. J.; Hadziioannou, G. *Macromolecules* **1991**, *24*, 1846.

31. Thomas, H. R.; O'Malley, J. J. *Macromolecules* **1981**, *14*, 1316.

32. Andrade, J. D. In *Surface and Interfacial Aspects of Biomedical Polymers, Surface Chemistry and Physics*; Plenum Press: New York, 1985; Vol. 1, p 15.

33. Cross, E. M.; McCarthy, T. J. *Macromolecules* **1990**, *23*, 3916.

34. Gagnon, D. R.; McCarthy, T. J. *J. Appl. Polym. Sci.* **1984**, *29*, 4335.

35. Bates, F. S. *Science* **1991**, *251*, 898.

36. Koberstein, J. T. In *Encyclopedia of Polymer Science and Engineering*, 2nd ed.; Mark, H. F.; Bikales, N. M.; Overberger, C. G.; Menges, G.; Kroschwitz, J. I., eds.; John Wiley & Sons: New York, 1989; Vol. 8, p237.

37. Theodorou, D. N. *Macromolecules* **1988**, *21*, 1400.

38. Theodorou, D. N. *Macromolecules* **1988**, *21*, 1422.

39. Franchina, N. L. *Ph.D. Dissertation*, University of Massachuestts at Amherst, 1993.

40. Viviano, K. *Ph.D. Dissertation*, University of Massachusetts at Amherst, 1994.

41. Kroto, H. W.; Heath, J. R.; O'Brien, S. C; Curl, R. F.; Smalley, R. E. *Nature* **1985**, *318*, 162.

42. Krätschmer, W.; Lamb, L. D.; Fostiropoulos, K.; Huffman, D. R. *Nature* **1990**, *347*, 354.

43. Fleming, R. M.; Hessen, B.; Siegrist, T.; Kortan, A. R.; March, P.; Rycko, R.; Dabbagh, G.; Haddon, R. C. In *Fullerenes: Synthesis, Properties, and Chemistry of Large Carbon Clusters*; Hammond, G. S.; Kuck, V. J., eds.; Am. Chem. Soc. Sym. Ser. 481, 1992; p 25.

44. Sivaraman, N.; Dhamodaran, R.; Kaliappan, I.; Srinivasan, T. G.; Rao, P. R. V.; Mathews, C. K. *J. Org. Chem.* **1992**, *57*, 6077.

45. Ruoff, R. S.; Tse, D. S.; Malhorta, R.; Lorents, D. C. *J. Phys. Chem.* **1993**, *97*, 3379.

46. Srivens, W. A.; Tour, J. M. *J. Chem. Soc., Chem. Commun.* **1993**, 1207.

47. Taylor, R.; Walton, D. R. M. *Nature* **1993**, *363*, 685.

48. Ohsawa, Y.; Saji, T. *J. Chem. Soc., Chem. Commun.* **1992**, 781.

49. Xie, Q.; Perez-Cordero, E.; Echegoyen, L. *J. Am. Chem. Soc.* **1992**, *114*, 3978.

50. Zhou, F.; Jehoulet, C.; Bard, A. J. *J. Am. Chem. Soc.* **1992**, *114*, 11004.

51. Bausch, J. W. et al. *J. Am. Chem. Soc.* **1991**, *113*, 3205.

52. Fagan, P. J.; Krusic, P. J.; McEwen, C. N.; Lazar, J.; Parker, D. H.; Herron, N.; Wasserman, E. *Science* **1993**, *262*, 404.

53. Tebbe, F. N. et al. *J. Am. Chem. Soc.* **1991**, *113*, 9900.

54. Olah, G. A. et al. *J. Am. Chem. Soc.* **1991**, *113*, 9385.

55. Birkett, P. R.; Hitchcock, P. W.; Kroto, H. W.; Taylor, R.; Walton, D. R. M. *Nature* **1992**, *357*, 479.

56. Tebbe et al. *Science* **1992**, *256*, 822.

57. Holloway, J. H. et al. *J. Chem. Soc., Chem. Commun.* **1991**, 966.

58. Chiang, L. Y.; Wang, L.-Y.; Swirczewski, J. W.; Soled S.; Cameron, S. *J. Org. Chem.* **1994**, *59*, 3960.

59. Gann, R. G. In *Kirk-Othmer Encyclopedia of Chemical Technology*, 4th ed.;John Wiley and Sons: New York, 1993; Vol. 10; p 930.

60. Chen, W.; Franchina, N. L.; Viviano, K.; McCarthy, T. J. *Polym. Mat. Sci. Eng.* **1996**, *75*, 44.

61. Zisman, W. A. *Adv. Chem. Ser.* **1964**, *43*, 1.

62. Russell, T. P. Personal communication.

APPENDIX A

ADDITIONAL DATA TABLES FOR CHAPTER 1

Table A.1. Effect of reagent concentration, [LAH], after solvent annealing in THF for 4.5 hr at room temperature prior to reduction of PET.

	Reduction			Labeling with HFBC after reduction			
Conc. (M)	Wt. gain (%)	θ_A (deg)	θ_R (deg)	F (15°) (%)	F (75°) (%)	θ_A (deg)	θ_R (deg)
0	0.16	78	46	1.66	1.08	80	50
0.002		79.2	45.8	1.65	1	80.5	47.8
0.004		75.8	34	6.68	4.23	85.2	51
0.008		72.4	33.4	6.3	4.46	84	52.8
0.012		72.6	32	6.57	4.41	83.4	53.8
0.016		72.4	32.4	6.46	4.26	84.2	53
0.02	0.04	70.2	34.6	6.97	5.16	86.6	53.6
0.027		76.2	37.8	6.25	4.02	83	49.8
0.038		78	37.4	5.77	3.61	81.6	49.4
0.057		78.2	39.4	5.28	3.68	81.2	49.2
0.074	0.04	75.8	38.2	5.77	3.95	82	49.4
0.2		77.5	34.5	4.93	3.77	81.6	42.2

Table A.2. Effect of time ([*tert*-BuOK] = 0.60 M, reaction temperature = room temp.) of glycolysis reaction.

Time (hr)	Glycolysis Wt. gain (%)	θ_A (deg)	θ_R (deg)	Labeling with HFBC after glycolysis F (15°) (%)	F (75°) (%)	θ_A (deg)	θ_R (deg)
0.5	-0.03	64	30.2	8.62	6.74	93.7	53.8
1	-0.01	63.5	29.5	8.99	7.81	100	49.6
2	-0.02	63.4	26.4	9.38	8.16	102.8	48.4
4	0	63	25	10.88	9.63	104.4	45
6	0.02	64.2	25	10.94	9.53	104.2	50.5

APPENDIX B

ADDITIONAL DATA TABLES FOR CHAPTER 2

Table B.1. Contact angle of buffered aqueous solutions on PET and PET-COOH/PET-CO_2^- films.

	PET		PET-COOH/PET-CO_2^-	
pH	θ_A(deg)	θ_R(deg)	θ_A(deg)	θ_R(deg)
2	80	59	65	19
4	76	50	57	17
5			56	15
6	77	54	53	15
7			54	15
8	73	42	53	14
10	71	44	52	16
12	69	22	54	18
13	70	26		

Table B.2. XPS atomic concentration data for 1st layer (PAH) adsorption on PET (no salt addition) as a function of pH.

	15deg.				75deg.			
pH	%C	%O	%N	%Cl	%C	%O	%N	%Cl
1.87	69.4	28.8	1.76		66.6	32.4	0.98	
2.13	67.6	31.0	1.43		65.6	33.7	0.69	
2.31	67.6	31.6	0.82		65.6	34.0	0.40	
3.83	67.9	31.0	1.07		65.0	34.5	0.50	
6.72	77.81	21.1	0.94	0.15				
8.84	80.50	17.86	1.47	0.16				
9.76	82.84	12.02	4.93	0.21	79.89	16.26	3.72	0.13
10.86	80.27	14.03	5.39	0.30	75.40	19.89	4.42	0.29
11.21	82.06	11.59	6.10	0.24	77.30	17.89	4.52	0.29
11.84	82.29	10.63	6.71	0.36	77.09	16.72	5.81	0.39

Table B.3. XPS atomic concentration data for 1st layer (PAH) adsorption onto PET-COOH/PET-CO_2^- (with no salt addition) as a function of pH.

	15 deg.				75 deg.			
pH	%C	%O	%N	%Cl	%C	%O	%N	%Cl
2.2	69.59	29.57	0.84	0	69.03	30.19	0.78	0
3.76	70.24	28.67	1.05	0.03	69.33	29.90	0.77	0
7.34	69.76	28.12	2.02	0.10	70.10	28.42	1.42	0.07
8.14	72.46	25.53	1.9	0.11	70.43	27.74	1.76	0.07
11.21	73.07	21.73	5.13	0.06	70.45	25.03	4.52	0
11.84	74.33	19.96	5.61	0.10	72.29	22.47	5.17	0.07

Table B.4. XPS atomic concentration data for 2nd layer (PSS) adsorption onto PET-CO_2^--PAH as a function of pH.

	15 deg						75 deg					
pH	%C	%O	%N	%S	%Na	%Cl	%C	%O	%N	%S	%Na	%Cl
2.25	69.60	26.14	2.40	1.73	0.08	0.05	68.92	27.80	1.77	1.29	0.14	0.07
5.56	71.03	25.38	2.11	1.33	0.05	0.10	69.21	27.78	1.83	1.06	0.06	0.06
6.8	71.72	24.64	2.14	1.33	0.11	0.06	69.80	27.36	1.73	1.02	0.01	0.08
8.28	70.92	25.79	2.12	1.13	0	0.05	69.86	27.28	1.95	0.90	0	0

Table B.5. XPS atomic concentration data for multilayer deposition onto PET (with 1 M $MnCl_2$ added to both PAH and PSS).

	15deg.						75deg					
Layer#	%C	%O	%S	%N	%Mn	%Cl	%C	%O	%S	%N	%Mn	%Cl
1(PAH)	67.58	29.24	0	2.74	0	0.44	64.99	32.58	0	2.16	0	0.27
2(PSS)	64.88	29.88	2.20	2.12	0.67	0.26	64.04	31.81	1.70	1.69	0.64	0.13
3(PAH)	68.70	22.81	1.88	5.28	0	1.33	66.63	26.84	1.48	4.03	0	1.03
4(PSS)	67.70	24.48	3.45	3.49	0.69	0.19	66.64	26.36	2.98	3.21	0.71	0.11
5(PAH)	72.01	16.93	3.09	6.64	0	1.34	69.68	19.28	3.06	6.65	0	1.35
6(PSS)	67.79	22.68	4.24	4.49	0.57	0.24	66.05	25.21	3.47	4.06	0.78	0.44
7(PAH)	71.75	17.87	2.86	5.85	0.32	1.35	68.13	18.56	3.47	7.39	0.57	1.88
8(PSS)	66.27	22.51	3.48	7.57	0.12	0.06	65.85	22.91	4.30	6.72	0.23	0
9(PAH)	72.21	16.14	3.09	7.07	0	1.48	69.07	18.54	3.69	7.26	0	1.44
10(PSS)	70.18	20.77	3.85	4.29	0.53	0.39	68.20	21.76	4.44	5.11	0.38	0.12
11(PAH)	71.29	16.45	2.99	6.90	0	2.37	68.34	18.23	3.61	7.48	0	2.33
12(PSS)	71.56	19.06	4.34	5.04	0	0	68.99	21.58	4.15	5.29	0	0
13(PAH)	72.42	15.08	3.33	7.54	0	1.64	70.58	15.67	3.99	7.95	0	1.8
14(PSS)	70.55	19.95	4.40	5.10	0	0	69.14	20.27	4.77	5.83	0	0
15(PAH)	71.92	15.58	3.47	7.71	0	1.32	70.42	16.92	3.67	7.62	0	1.36

Table B.6. XPS atomic concentration data for multilayer deposition onto PET (with 1 M $MnCl_2$ added to PSS only).

	15deg.						75deg					
Layer#	%C	%O	%S	%N	%Mn	%Cl	%C	%O	%S	%N	%Mn	%Cl
1(PAH)	68.30	30.46	0	1.23			67.33	31.95	0	0.71		
2(PSS)	69.69	27.24	1.38	0.85	0.74	~0	68.05	29.99	0.94	0.36	0.56	~0
3(PAH)	70.56	25.54	1.36	2.29	0	0.25	69.46	27.84	0.87	1.42	0.26	0.10
4(PSS)	69.60	24.50	2.77	1.99	1.13	~0	67.71	27.91	1.94	1.49	0.93	~0
5(PAH)	72.90	20.49	2.54	3.47	0.19	0.32	70.25	24.82	2.12	2.43	0.06	0.18
6(PSS)	70.12	23.04	3.25	2.23	1.08	0.29	67.79	25.02	3.05	2.59	1.10	0.38
7(PAH)	77.56	14.96	3.27	3.83	~0	0.39	77.77	14.14	3.34	4.38	~0	0.36
8(PSS)	68.94	21.48	5.06	3.27	1.18	~0	67.85	23.40	4.21	3.26	1.27	~0
9(PAH)	71.15	21.34	4.11	3.17	~0	0.22	76.09	15.08	3.61	4.80	~0	0.42
10(PSS)	68.99	21.46	4.63	3.66	0.90	0.31	67.41	22.40	4.76	3.70	1.25	0.43
11(PAH)	76.74	14.38	4.04	4.68	~0	0.16	75.86	15.13	3.99	4.80	~0	0.23
12(PSS)	68.75	20.74	4.60	4.03	1.15	0.68	66.89	22.03	4.93	4.57	1.31	0.27
15(PAH)	69.71	22.88	3.14	4.14	0.12	0.12	68.37	22.45	3.90	5.18	0.10	0.09
16(PSS)	68.58	23.71	4.10	3.58	0.60	0	67.43	23.80	4.51	4.22	0.51	0.01
17(PAH)	72.03	19.06	3.84	5.01	0.10	0.06	70.13	22.67	3.14	4.03	0.08	0.03
18(PSS)	70.06	22.07	4.15	3.71	0.44	0	67.95	22.66	4.69	4.64	0.52	0.07

Table B.7. XPS atomic concentration data for multilayer deposition onto PET (with no salt addition).

	15deg						75deg					
Layer#	%C	%O	%S	%N	%Na	%Cl	%C	%O	%S	%N	%Na	%Cl
1(PAH)	68.30	30.46	0	1.23			67.33	31.95	0	0.71		
2(PSS)	71.91	26.79	0.49	0.38	0.32	0.10	69.96	29.32	0.25	0.27	0.16	0.04
3(PAH)	73.10	25.03	0.54	1.31	0	0.02	69.50	28.70	0.39	1.36	0.03	0.03
4(PSS)	72.92	24.24	1.09	1.5	0.19	0.06	69.80	28.29	0.73	0.93	0.24	0.02
5(PAH)	73.56	22.47	1.31	2.62	0	0.04	69.70	28.01	0.78	1.43	0	0.08
6(PSS)	72.10	22.20	2.31	3.05	0.24	0.10	70.47	25.53	1.67	2.09	0.19	0.05
7(PAH)	73.94	20.86	1.95	3.17	0	0.08	71.29	24.80	1.30	2.52	0	0.10
8(PSS)	71.87	21.67	2.69	3.42	0.25	0.09	69.84	25.66	1.82	2.44	0.18	0.05
9(PAH)	72.49	21.33	2.38	3.72	0	0.08	71.20	24.21	1.72	2.84	0	0.04
10(PSS)	71.51	21.67	2.89	3.61	0.22	0.09	69.64	25.11	2.26	2.71	0.20	0.09
11(PAH)	71.36	20.83	3.09	4.67	0	0.05	70.77	22.63	2.42	3.72	0.38	0.09
12(PSS)	71.27	20.47	3.66	4.29	0.21	0.10	69.72	23.66	2.82	3.47	0.23	0.10
13(PAH)	71.29	20.76	3.18	4.71	0.01	0.06	70.61	22.44	2.74	4.18	0	0.03
14(PSS)	71.97	20.34	3.47	4.04	0.07	0.11	70.53	22.11	3.23	3.99	0.05	0.08
15(PAH)	72.89	18.82	3.24	4.89	0.10	0.06	71.18	20.56	3.01	4.61	0	0.04
16(PSS)	70.42	20.30	4.25	4.84	0.12	0.08	70.11	22.10	3.45	4.07	0.18	0.08
17(PAH)	70.66	19.17	3.87	5.26	0	1.04	70.07	21.26	3.1	4.78	0.04	0.75
18(PSS)	70.30	19.59	4.23	5.11	0.13	0.65	68.88	21.29	3.97	5.21	0.15	0.51
19(PAH)	70.78	18.60	4.01	5.56	0	1.05	68.93	21.04	3.73	5.46	0	0.85
20(PSS)	69.28	20.93	4.15	4.91	0.20	0.54	69.28	20.95	3.96	5.09	0.14	0.59
21(PAH)	71.98	18.72	3.97	5.20	0.01	0.13	68.83	20.43	3.96	5.56	0.17	0.05
22(PSS)	71.57	19.03	4.36	4.75	0.16	0.14	69.60	21.00	3.97	5.29	0.10	0.04
23(PAH)	72.42	18.27	4.08	5.14	0	0.08	70.73	19.91	3.81	5.47	0	0.09
24(PSS)	71.12	19.20	4.34	5.14	0.11	0.09	69.26	20.61	4.47	5.50	0.05	0.10

Table B.8. XPS atomic concentration data for multilayer deposition onto PET-CO_2^- (with no salt addition).

	15deg.						75deg					
Layer#	%C	%O	%S	%N	%Na	%Cl	%C	%O	%S	%N	%Na	%Cl
1(PAH)	72.46	25.53	0	1.90	N	N	70.43	27.74	0	1.76	N	N
2(PSS)	70.92	25.79	1.13	2.12	E	E	69.86	27.28	0.90	1.95	E	E
3(PAH)	73.90	21.94	1.01	3.09	G	G	71.75	24.83	0.83	2.51	G	G
4(PSS)	72.79	21.67	2.09	3.36	L	L	71.78	23.80	1.66	2.72	L	L
5(PAH)	74.53	19.79	1.58	3.98	I	I	72.61	22.15	1.45	3.70	I	I
6(PSS)	71.85	20.48	3.02	4.53	G	G	70.04	23.36	2.59	3.97	G	G
7(PAH)	71.83	19.36	2.94	5.77	I	I	70.73	21.46	2.58	5.18	I	I
8(PSS)	71.10	20.65	3.42	4.85	B	B	69.79	21.93	3.27	4.89	B	B
9(PAH)	71.90	17.86	3.42	6.65	L	L	71.04	19.67	3.20	5.97	L	L
10(PSS)	69.96	20.00	4.43	5.52	E	E	69.28	21.19	4.07	5.40	E	E
11(PAH)	72.57	16.67	3.65	7.11			70.29	18.60	3.86	7.24		
12(PSS)	71.68	18.53	4.38	5.42			69.18	20.03	4.67	6.12		
13(PAH)	72.62	16.86	3.57	6.95			70.72	18.32	3.73	7.22		
14(PSS)	70.86	19.19	4.39	5.56			68.77	20.11	4.73	6.39		
15(PAH)	72.52	16.40	3.76	7.32			70.58	17.72	4.16	7.54		
16(PSS)	70.92	19.15	4.36	5.57			68.83	19.92	4.76	6.49		
17(PAH)	72.08	16.87	3.81	7.24			69.70	18.67	4.06	7.57		

Table B.9. XPS atomic concentration data for multilayer deposition onto PET-NH_3^+ (with no salt addition).

	15deg				75deg			
Layer#	%C	%O	%S	%N	%C	%O	%S	%N
1(PAH)	71.00	23.49	0	5.35	68.34	28.17	0	3.44
2(PSS)	70.85	22.44	3.00	3.72	68.80	26.01	2.22	2.97
3(PAH)	70.38	22.13	2.95	4.53	67.90	26.08	2.28	3.73
4(PSS)	70.92	21.41	3.45	4.22	68.37	25.04	2.90	3.68
5(PAH)	71.33	21.21	3.08	4.38	68.81	24.82	2.56	3.81
6(PSS)	71.87	19.77	3.86	4.50	69.08	23.84	3.13	3.94
7(PAH)	71.55	19.97	3.57	4.90	70.05	22.67	2.96	4.33
8(PSS)	70.38	20.85	3.92	4.86	68.21	24.17	3.35	4.28
9(PAH)	72.71	18.77	3.57	4.94	70.04	21.98	3.26	4.72
10(PSS)	71.06	20.17	3.99	4.78	68.87	23.02	3.56	4.55
11(PAH)	71.67	19.43	3.83	5.07	70.28	21.49	3.34	4.89
12(PSS)	70.56	19.83	4.30	5.31	69.27	22.20	3.71	4.82
13(PAH)	71.11	19.44	4.04	5.40	70.04	20.97	3.72	5.27
14(PSS)	69.26	21.51	4.11	5.12	69.61	21.41	3.96	5.02
15(PAH)	71.36	19.01	4.01	5.62	70.05	20.68	3.84	5.44
16(PSS)	69.57	21.22	4.19	5.02	69.26	21.34	4.17	5.23
18(PSS)	71.01	19.69	4.25	5.06	68.66	21.19	4.58	5.57
19(PAH)	71.74	18.72	4.06	5.48	69.40	20.34	4.29	5.97
20(PSS)	70.40	20.10	4.38	5.12	68.21	21.42	4.74	5.63
21(PAH)	72.18	18.17	4.10	5.55	69.89	19.80	4.35	5.96
22(PSS)	68.97	20.81	4.66	5.57	69.30	20.77	4.63	5.31

Table B.10. Carbonyl C_{1s} intensity (expressed as the percentage of total carbon intensity) versus the number of layers in the multilayer assembly.

	PET, case[a]		PET, case[b]		PET, case[c]		PET-CO_2^-		PET-NH_3^+	
Layer#	15 deg	75 deg	15 deg	75 deg	15 deg	75 deg	15 deg	75 deg	15 deg	75 deg
0	20	20	20	20	20	20	20	20		
1	9.13	12.04	16.6	16.23	16.6	16.23	12.54	13.53	10.66	14.34
2	5.17	9.17			11.62	15.35	10.17	12.24	5.19	8.37
3	3.65	7.04	8.39	10.84	10.55	14.37	8.51	9.86	4.43	6.79
4	0	4.9	5.07	9.27	8.89	12.05	6.31	8.05	3.04	5.24
5		2.81	3.64	8.77	8.61	11.37	6.08	7.72	3.21	5.28
6		4.15	4.72	7.06	5.9	9.4	3.84	6.04	1.03	4.80
7		0	0	5.38	5.33	8.43	3.64	5.34	1.45	3.96
8				3.59	4.4	8.49	2.31	5.14	1.03	4.30
9				1.84	4.12	8.34	1.11	3.20	1.33	3.91
10					3.24	6.59	0	1.46	0	3.95
11				1.07	2.23	5.34		1.04		2.80
12				0	2.65	5.7		0		2.69
13					2.04	5.72				1.24
14					1.99	4.84				2.48
15					0	3.18				2.30
16						3.73				2.20
17						4.48				0
18						2.45				0
19						2.52				
20						2.59				
21						1.74				
22						1.53				
23						1.88				
24						0				

[a]: $MnCl_2$ added to both PAH and PSS solutions, [b]: $MnCl_2$ added to only PSS solution, [c]: no salt added.

Table B.11. Advancing (θ_A) and receding (θ_R) water contact angles versus the number of layers in the multilayer assembly.

	PET, case [a]		PET, case [b]		PET, case [c]		$PET-CO_2^-$		$PET-NH_3^+$	
Layer#	θ_A	θ_R	θ_A	θ_R	θ_A	θ_R	θ_A	θ_R	θ_A	θ_R
0	77	55	77	55	77	55	62	16	77	55
1	81	26	80	39	80	39	73	26	73	17
2	44	16	66	16	73	29	67	20	50	12
3	70	22	65	15	75	22			60	24
4	42	17	53	12	68	20	62	17	49	14
5	70	21	62	12	69	19	70	18	59	23
6	43	16			59	14	58	20	50	16
7	70	24	59	16	53	17	62	18	60	19
8	44	15			54	14	52	17	49	14
9	69	20			47	17	62	18	61	20
10	44	17			54	17	53	15	50	16
11	69	20			47	20	63	18	60	18
12			46	12	53	14	53	16	50	15
13					46	15			59	18
14					52	14	52	17		
15			60	16	45	17	64	18		
16			46	18	54	15	52	17		
17			59	17			65	19		
18			47	14	53	18				
19					47	16				
20					52	17				

[a]: $MnCl_2$ added to both PAH and PSS solutions, [b]: $MnCl_2$ added to only PSS solution, [c]: no salt added.

Table B.12. Contact angle of buffered aqueous solutions on PET with layers (1M $MnCl_2$ added to PSS solution only).

PAH is the top layer:

pH	layer1		layer3		layer5		layer7	
	θ_A	θ_R	θ_A	θ_R	θ_A	θ_R	θ_A	θ_R
2.1	80	32	63	14	62	19	56	19
4	79	44	62	14	59	14	55	14
6	80	39	65	15	62	12	59	16
8	79	44	63	14	60	13	55	16
10	79	34	62	18	61	17	55	15
12	78	31	59	17	54	14	52	14
12.6	78	32	55	19	45	12	46	15
13	80	34	54	16	41	13	43	15

PSS is the top layer:

pH	layer2		layer4	
	θ_A	θ_R	θ_A	θ_R
2.1	67	17	54	14
4	68	18	52	15
6	66	16	53	12
8	65	15	52	13
10	66	18	52	14
12	70	14	56	14
12.6	67	17	55	16

APPENDIX C

ADDITIONAL DATA TABLES FOR CHAPTER 3

Table C.1. Adsorption isotherm (XPS atomic composition data) of $C_{60}(C_6F_{13})_{5.2}$ in 6.5 K PS after drying at r.t. for 24 h followed by annealing at 110 °C for 24 h.

Conc. (M)	15 deg %C	%O	%F	75 deg %C	%O	%F
0	99.52	0.48	0	99.47	0.53	0
0.01	92.64	4.08	3.28	98.40	1.22	0.39
0.02	90.26	3.03	6.71	94.03	2.61	3.36
0.04	80.10	3.07	16.83	94.08	1.77	4.15
0.08	59.21	1.71	39.07	75.25	1.64	23.11
0.1	53.32	1.14	45.54	62.71	1.13	36.15
0.2	47.47	0.85	51.68	56.75	0.97	42.28
0.4	49.27	1.91	48.82	50.40	1.41	48.19
0.8	47.40	1.15	51.45	47.05	1.11	51.84
1	50.34		49.66	54.39		45.61

Table C.2. Adsorption isotherm (water and hexadecane contact angles) of $C_{60}(C_6F_{13})_{5.2}$ in 6.5 K PS after drying at r.t. for 24 h followed by annealing at 110 °C for 24 h.

Conc. (M)	$\theta_A(H_2O)$ (deg)	θ_R (H_2O) (deg)	θ_A ($C_{16}H_{34}$) (deg)	θ_R ($C_{16}H_{34}$) (deg)
0	94	79	13	10
0.01	91	82	13	7
0.02	93	81	16	9
0.04	99	83	20	12
0.08	116	83	65	20
0.1	120	86	69	21
0.2	120	87	69	22
0.4	122	87	69	23
0.8	121	86	69	22
1	116	83	67	24

Table C.3. Annealing kinetics (water and hexadecane contact angles) of 10 w/w % of C_{60} in 6.5 K PS at r.t..

Time (day)	$\theta_A(H_2O)$ (deg)	θ_R (H2O) (deg)	$\theta_A(C_{16}H_{34})$ (deg)	$\theta_R(C_{16}H_{34})$ (deg)
1	92	70	11	7
2	95	76	11	7
3	95	74	11	8
4	95	74	12	8
5	96	76	12	8
6	96	74	12	8
8	95	74	13	10

Table C.4. Annealing kinetics (water and hexadecane contact angles) of 10 w/w % of C_{60} in 6.5 K PS at 110 °C.

Time. (day)	$\theta_A(H_2O)$ (deg)	$\theta_R(H_2O)$ (deg)	$\theta_A(C_{16}H_{34})$ (deg)	$\theta_R(C_{16}H_{34})$ (deg)
1	93	73	14	10
2	93	76	13	8
3	93	77	13	9
4	94	81	14	8
5	94	83	12	7
6	94	80	14	8
8	93	78	13	9

Table C.5. Adsorption kinetics (XPS atomic composition data) of 1 w/w % of $C_{60}(C_6F_{13})_{5.2}$ in 6.5 K PS at r.t..

Time (day)	15 deg %C	%O	%F	75 deg %C	%O	%F
1	50.34		49.66	54.39		45.61
2	50.98		49.02	54.35		45.65
3	48.86		51.14	54.01		45.99
4	49.11		50.89	54.15		45.85
5	49.35		50.65	54.28		45.72
6	50.54		49.46	54.00		46.00
7	50.36		49.64	54.04		45.96
8	49.82		50.18	54.58		45.42
9	50.11	1.96	47.93	53.88	0.50	45.62
10	50.08	1.38	48.53	53.86	0.53	45.61

Table C.6. Adsorption kinetics (water and hexadecane contact angles) of 1 w/w % of $C_{60}(C_6F_{13})_{5.2}$ in 6.5 K PS at r.t..

Time. (day)	$\theta_A(H_2O)$ (deg)	θ_R (H_2O) (deg)	θ_A ($C_{16}H_{34}$) (deg)	θ_R ($C_{16}H_{34}$) (deg)
1	114	85	66	22
2	116	83	68	22
3	117	83	69	23
4	117	84	69	22
5	117	83	68	23
6	116	82	69	23
7	116	84	69	22
8	117	82	68	23
9	117	83	68	22
10	117	83	68	22

Table C.7. Adsorption kinetics (XPS atomic composition data) of 1 w/w % of $C_{60}(C_6F_{13})_{5.2}$ in 6.5 K PS after drying at r.t. for 24 h followed by annealing at 110 °C.

Time (day)	15 deg %C	%O	%F	75 deg %C	%O	%F
0	50.34		49.66	54.39		45.61
1	50.66		49.34	55.60		44.40
2	51.86		48.14	57.98		42.02
3	50.81	1.61	47.58	56.50	0.70	42.80
4	51.70	1.35	46.95	56.42	0.75	42.84
5	51.04	1.30	47.66	57.15	0.50	42.35
6	52.33	1.38	46.30	60.00	0.65	39.35

Table C.8. Adsorption kinetics (water and hexadecane contact angles) of 1 w/w % of $C_{60}(C_6F_{13})_{5.2}$ in 6.5 K PS after drying at r.t. for 24 h followed by annealing at 110 °C.

Time. (day)	$\theta_A(H_2O)$ (deg)	θ_R (H_2O) (deg)	θ_A ($C_{16}H_{34}$) (deg)	θ_R ($C_{16}H_{34}$) (deg)
0	118	81	68	23
1	116	83	67	24
2	116	82	68	21
3	117	82	68	23
4	117	82	68	23
5	117	82	68	22
6	118	83	68	22

Table C.9. Surface reconstruction study (XPS atomic composition data) of 2.5 w/v % of 6.5 K PS/toluene solution spin-cast three times at 2000 rpm over a composite film containing 1 w/w % of $C_{60}(C_6F_{13})_{5.2}$ in 6.5 K PS after drying at r.t. for 24 h followed by annealing at 110 °C.

Time (day)	15 deg %C	%O	%F	75 deg %C	%O	%F
0	92.16	1.96	5.88	96.60	0.37	3.03
1	75.45	1.07	23.48	86.56	0.44	13.00
3	67.90	2.51	29.59	82.47	0.40	17.13
4	73.54	1.31	25.15	85.73	0.54	13.72
5	72.64	1.13	26.23	86.36	0.43	13.20
6	72.39	1.24	26.36	84.23	0.37	15.40
10	68.25	2.25	29.50	82.29	0.50	17.21
14	73.54	1.57	24.89	84.43	0.57	15.00

Table C.10. Surface reconstruction study (water and hexadecane contact angles) of 2.5 w/v % of 6.5 K PS/toluene solution spin-cast three times at 2000 rpm over a composite film containing 1 w/w % of $C_{60}(C_6F_{13})_{5.2}$ in 6.5 K PS after drying at r.t. for 24 h followed by annealing at 110 °C.

Time. (day)	$\theta_A(H_2O)$ (deg)	θ_R (H_2O) (deg)	θ_A ($C_{16}H_{34}$) (deg)	θ_R ($C_{16}H_{34}$) (deg)
0	92	83	26	10
1	103	83	52	13
3	109	88	50	13
4	107	86	48	13
5	108	88	50	12
6	110	88	52	12
10	108	79	52	12
14	107	85	51	13

Table C.11. Surface reconstruction study (XPS atomic composition data) of 2.5 w/v % of 6.5 K PS/toluene solution spin-cast once at 2000 rpm over a composite film containing 1 w/w % of $C_{60}(C_6F_{13})_{5.2}$ in 6.5 K PS after drying at r.t. for 24 h followed by annealing at 110 °C.

Time (day)	15 deg %C	%O	%F	75 deg %C	%O	%F
0	66.46	1.27	32.27	83.33	0.55	16.12
1	61.07	0.92	38.02	80.10	0.50	19.40
3	60.35	0.85	38.80	76.60	0.44	22.96
4	57.06	0.74	42.19	74.76	0.34	24.90
6	56.85	0.88	42.27	74.63	0.41	24.96
10	55.88	1.05	43.07	72.00	0.49	27.51
14	56.28	2.08	41.64	71.16	0.57	28.28

Table C.12. Surface reconstruction study (water and hexadecane contact angles) of 2.5 w/v % of 6.5 K PS/toluene solution spin-cast once at 2000 rpm over a composite film containing 1 w/w % of $C_{60}(C_6F_{13})_{5.2}$ in 6.5 K PS after drying at r.t. for 24 h followed by annealing at 110 °C.

Time. (day)	$\theta_A(H_2O)$ (deg)	θ_R (H_2O) (deg)	θ_A ($C_{16}H_{34}$) (deg)	θ_R ($C_{16}H_{34}$) (deg)
0	105	85	42	15
1	110	84	55	15
3	115	85	52	16
4	117	87	61	18
6	117	87	60	16
10	117	88	60	17
14	117	88	64	17

Table C.13. Surface reconstruction study (XPS atomic composition data) of 2.5 w/v % of 62 K PS/toluene solution spin-cast three times at 2000 rpm over a composite film containing 1 w/w % of $C_{60}(C_6F_{13})_{5.2}$ in 6.5 K PS after drying at r.t. for 24 h followed by annealing at 110 °C.

Time (day)	15 deg %C	%O	%F	75 deg %C	%O	%F
0	91.19	1.89	6.92	96.34	0.35	3.31
1	85.11	1.38	13.52	89.43	0.54	10.03
2	73.55	1.33	25.12	87.54	0.46	11.99
3	76.83	2.47	20.70	87.63	0.55	11.82
5	69.19	1.04	29.78	84.24	0.48	15.27
8	70.16	2.48	27.36	82.73	0.81	16.45
11	69.42	1.36	29.23	82.27	0.75	16.98
14	67.93	2.31	29.76	80.04	0.74	19.22

Table C.14. Surface reconstruction study (water and hexadecane contact angles) of 2.5 w/v % of 62 K PS/toluene solution spin-cast three times at 2000 rpm over a composite film containing 1 w/w % of $C_{60}(C_6F_{13})_{5.2}$ in 6.5 K PS after drying at r.t. for 24 h followed by annealing at 110 °C.

Time. (day)	$\theta_A(H_2O)$ (deg)	$\theta_R(H_2O)$ (deg)	$\theta_A(C_{16}H_{34})$ (deg)	$\theta_R(C_{16}H_{34})$ (deg)
0	94	84	26	10
1	99	85	40	12
2	101	85	46	12
3	109	82	51	12
5	104	84	45	13
8	110	86	50	12
14	108	87	44	12

Table C.15. Surface reconstruction study (XPS atomic composition data) of 2.5 w/v % of 62 K PS/toluene solution spin-cast once at 2000 rpm over a composite film containing 1 w/w % of $C_{60}(C_6F_{13})_{5.2}$ in 6.5 K PS after drying at r.t. for 24 h followed by annealing at 110 °C.

Time (day)	15 deg %C	%O	%F	75 deg %C	%O	%F
0	71.89	0.77	27.33	87.25	0.28	12.47
2	59.84	0.85	39.31	77.17	0.48	22.35
5	59.41	1.38	39.21	77.72	0.54	21.74
7	61.99	1.78	36.23	78.18	0.66	21.16
9	59.59	0.68	39.73	76.35	0.52	23.13
11	61.91	1.06	37.04	78.04	0.67	21.28
14	58.30	1.37	40.33	74.04	0.49	25.47

Table C.16. Surface reconstruction study (water and hexadecane contact angles) of 2.5 w/v % of 62 K/PS toluene solution spin-cast once at 2000 rpm over a composite film containing 1 w/w % of $C_{60}(C_6F_{13})_{5.2}$ in 6.5 K PS after drying at r.t. for 24 h followed by annealing at 110 °C.

Time. (day)	$\theta_A(H_2O)$ (deg)	θ_R (H_2O) (deg)	θ_A ($C_{16}H_{34}$) (deg)	θ_R ($C_{16}H_{34}$) (deg)
0	97	82	43	14
2	106	83	56	15
5	114	85	60	16
7	115	87	60	15
11	115	87	59	16
14	117	86	59	15

Table C.17. Surface reconstruction study (XPS atomic composition data) of 2.5 w/v % of 148 K PS/toluene solution spin-cast three times at 2000 rpm over a composite film containing 1 w/w % of $C_{60}(C_6F_{13})_{5.2}$ in 6.5 K PS after drying at r.t. for 24 h followed by annealing at 110 °C.

Time (day)	15 deg %C	%O	%F	75 deg %C	%O	%F
0	90.23	2.10	7.67	96.03	0.37	3.60
1	82.03	1.48	16.50	92.60	0.46	6.94
3	81.89	2.03	16.08	91.83	0.48	7.69
4	83.46	3.26	13.28	94.62	0.66	4.72
5	83.11	1.98	14.90	93.34	0.40	6.26
6	82.66	2.06	15.28	93.03	0.40	6.57

Table C.18. Surface reconstruction study (water and hexadecane contact angles) of 2.5 w/v % of 148 K PS/toluene solution spin-cast three times at 2000 rpm over a composite film containing 1 w/w % of $C_{60}(C_6F_{13})_{5.2}$ in 6.5 K PS after drying at r.t. for 24 h followed by annealing at 110 °C.

Time. (day)	$\theta_A(H_2O)$ (deg)	θ_R (H_2O) (deg)	θ_A ($C_{16}H_{34}$) (deg)	θ_R ($C_{16}H_{34}$) (deg)
0	92	82	27	13
1	94	85	29	13
3	98	85	37	14
4	98	84	36	13
5	98	85	37	13
6	95	86	33	13

Table C.19. Surface reconstruction study (XPS atomic composition data) of 2.5 w/v % of 498 K PS/toluene solution spin-cast three times at 2000 rpm over a composite film containing 1 w/w % of $C_{60}(C_6F_{13})_{5.2}$ in 6.5 K PS after drying at r.t. for 24 h followed by annealing at 110 °C.

Time (day)	15 deg %C	%O	%F	75 deg %C	%O	%F
0	90.55	1.55	7.91	96.19	0.37	3.43
1	90.78	1.16	8.95	96.18	0.40	3.42
3	91.85	1.27	6.88	96.98	0.36	2.66
4	89.06	2.23	8.71	95.52	0.49	3.99
5	90.72	1.38	7.89	95.52	0.80	3.67
6	88.89	2.56	8.55	95.88	0.59	3.53

Table C.20. Surface reconstruction study (water and hexadecane contact angles) of 2.5 w/v % of 498 K PS/toluene solution spin-cast three times at 2000 rpm over a composite film containing 1 w/w % of $C_{60}(C_6F_{13})_{5.2}$ in 6.5 K PS after drying at r.t. for 24 h followed by annealing at 110 °C.

Time. (day)	$\theta_A(H_2O)$ (deg)	$\theta_R(H_2O)$ (deg)	$\theta_A(C_{16}H_{34})$ (deg)	$\theta_R(C_{16}H_{34})$ (deg)
0	91	83	25	11
1	93	85	23	12
3	91	83	21	12
4	92	84	23	12
6	92	84	22	11

Table C.21. XPS atomic composition data of film samples containing PS spin-cast three times over 1 w/w % of $C_{60}(C_6F_{13})_{5.2}$ and 6.5 K PS composite: effect of molecular weight on diffusion of $C_{60}(C_6F_{13})_{5.2}$ through PS matrix after spin-casting.

M.W.	15 deg			75 deg		
	%C	%O	%F	%C	%O	%F
6500	67.90	2.51	29.59	82.47	0.40	17.13
62000	69.19	1.04	29.78	84.24	0.48	15.27
148000	82.03	1.48	16.50	92.60	0.46	6.94
498000	90.55	1.55	7.91	96.19	0.37	3.43

Table C.22. Surface reconstruction study (XPS atomic composition data) of free-standing 498 K PS film (2.5 w/v % of PS solution in toluene, spin-cast on a clean glass slide at 2000 rpm) transferred over a composite film containing 1 w/w % of $C_{60}(C_6F_{13})_{5.2}$ in 6.5 K PS after drying at r.t. for 24 h followed by annealing at 110 °C.

Time (day)	15 deg %C	%O	%F	75 deg %C	%O	%F
0	99.52	0.48	0	99.47	0.53	0
1	93.99	2.99	3.03	98.54	0.24	1.22
3	90.45	1.84	7.71	96.95	0.48	2.57
4	89.41	2.10	8.49	95.91	0.85	3.24
5	91.96	1.74	6.30	97.13	0.64	2.23
6	89.72	2.75	7.53	97.03	0.51	2.46

Table C.23. Surface reconstruction study (water and hexadecane contact angles) of free-standing 498 K PS film (2.5 w/v % of PS solution in toluene, spin-cast on a clean glass slide at 2000 rpm) transferred over a composite film containing 1 w/w % of $C_{60}(C_6F_{13})_{5.2}$ in 6.5 K PS after drying at r.t. for 24 h followed by annealing at 110 °C.

Time. (day)	$\theta_A(H_2O)$ (deg)	$\theta_R(H_2O)$ (deg)	$\theta_A(C_{16}H_{34})$ (deg)	$\theta_R(C_{16}H_{34})$ (deg)
0	89	82	10	6
1	93	85	20	9
3	92	83	22	11
4	92	81	21	11
5	93	81	21	11

APPENDIX D

ABBREVIATIONS

ATR IR	attenuated total reflectance infrared
mm	mmHg
GPC	gel permeation chromatography
PAH	poly(allylamine hydrochloride)
PDI	polydispersity index (M_w / M_n)
PET	poly(ethylene terephthalate)
PET-CO_2^-	hydrolyzed PET
PET-OH/-COOH	hydrolyzed PET
PET-OH^G	glycolyzed PET (transesterification with ethylene glycol)
PET-OH^R	reduced PET
PET-NH_3^+	PET reacted with PAH at high pH
PS	polystyrene
PSS	poly(sodium styrenesulfonate)
SEM	scanning electron microscopy
TGA	thermogravimetric analysis
XPS	x-ray photoelectron spectroscopy

BIBLIOGRAPHY

Anastasiadis, S. H.; Gancarz, I.; Koberstein, J. T. *Macromolecules* **1988**, *21*, 2980.

Andrade, J. D. *Surface and Interfacial Aspects of Biomedical Polymers, Surface Chemistry and Physics;* Plenum Press: New York, 1985; Vol. 1.

Arenolz, E.; Heitz, J.; Wagner, M.; Baeuerle, D.; Hibst, H.; Hagemeyer, A. *Appl. Surf. Sci.* **1993**, *69*, 16.

Arnett, E.M. *Prog. Phys. Org. Chem.* **1963**, *1*, 223.

Ashley, J.C. *IEEE Trans. Nucl. Sci.* **1980**, *NS-27*, 1454.

Ashley, J.C. *J. Electron Spectroscopy* **1982**, *28*, 177.

Ashley, J.C.; Tung, C.J. *Surf. Interfac. Anal.* **1982**, *4*, 52.

Ashley, J.C.; Williams, M.W. *Rad. Res.* **1980**, *81*, 364.

Avny, Y.; Reubenfeld, L. *J. Appl. Polym. Sci.* **1986**, *32*, 4009.

Baliga, S.; Wong, W. T. *J. Polym. Sci.: Polym. Chem.*, **1989**, *27*, 2071.

Bates, F. S. *Science* **1991**, *251*, 898.

Bausch, J. W. et al. *J. Am. Chem. Soc.* **1991**, *113*, 3205.

Bee, T. G.; McCarthy, T. J. *Macromolecules*, **1992**, *25*, 2093.

Bee, T. G., Ph.D. dissertation, University of Massachusetts, 1993.

Bening, R. C.; McCarthy, T. J. *Macromolecules* **1990**, *23*, 2648.

Bensnoin, J.-M.; Choi, K.Y. *J. Macromol. Sci. Rev., Macromol. Chem. and Phys.* **1989**, *C29*, 55.

Bertrand, P.; DePuydt, Y.; Beuken, J. M.; Lutgen, P.; Feyder, G. *Nucl. Instrum. Methods Phys. Res., Sect. B.* **1987**, *B19-20*, 887.

Birkett, P. R.; Hitchcock, P. W.; Kroto, H. W.; Taylor, R.; Walton, D. R. M. *Nature* **1992**, *357*, 479.

Blaakmeer, J.; Böhmer, M. R.; Cohen Stuart, M. A.; Fleer, G. J. *Macromolecules* **1990**, *23*, 2301.

Broseta, D.; Fredrickson, G. H.; Helfand, E.; Leibler, L. *Macromolecules* **1990**, *23*, 132.

Brown, H.C.; McDaniel, D.H.; Hflinger, O. In *Determination of Organic Structures by Physical Methods*; Braude, E.A., Nachod, F.C., Eds; Academic Press: New York, 1955; p 567.

Bùi, L. N.; Thompson, M.; McKeown, N. B.; Romaschin, A. D.; Kalman, P. G. *Analyst* **1993**, *118*, 463.

Campanelli, J. R.; Kamal, M. R.; Cooper, D. G. *J. Appl. Polym. Sci.* **1994**, *54*, 1731.

Chen, J. Y.; Ou, C. F.; Hu, Y. C.; Lin, C. C. *J. Appl. Polym. Sci.* **1991**, *42*, 1501.

Chen, W.; Franchina, N. L.; Viviano, K.; McCarthy, T. J. *Polym. Mat. Sci. Eng.* **1996**, *75*, 44.

Chiang, L. Y.; Wang, L.-Y.; Swirczewski, J. W.; Soled S.; Cameron, S. *J. Org. Chem.* **1994**, *59*, 3960.

Clark, D.T.; Adams, D.B.; Dilks, A.; Peeling, J.; Thomas, H.R. *J. Electron Spectroscopy* **1976**, *8*, 51.

Clark, D. T.; Feast, W. J. "Polymer Surfaces"; Wiley-Interscience: New York, 1978.

Clark, D. T.; Peeling, J.; O'Malley, J. J. *J. Polym. Sci., Polym. Chem.* **1976**, *14*, 543.

Clark, D.T.; Thomas, H.R. J. *Polym. Sci., Polym. Chem. Ed.* **1977**, *15*, 2843.

Clark, D.T.; Thomas, H.R.; Shuttleworth, D. *J. Polym. Sci., Polym. Lett. Ed.* **1978**, *16*, 465.

Collin, R. J. U.S. Pat. 2,955,954, **1964**.

Cooper, T. M.; Campbell, A. L.; Crane, R. L. *Langmuir*, **1995**, *11*, 2713.

Cosgrove, T.; Obey, T. M.; Vincent, B. *J. Colloid Interface Sci.* **1986**, *111(2)*, 409.

Costello, C. A.; McCarthy, T. J. *Macromolecules*, **1987**, *20*, 2819.

Costello, C. A.; McCarthy, T. J. *Macromolecules*, **1990**, *23*, 2648.

Creton, C.; Kramer, E. J.; Hadziioannou, G. *Macromolecules* **1991**, *24*, 1846.

Cross, E. M.; McCarthy, T. J. *Macromolecules*, **1990**, *23*, 3916.

Dave, J.; Kumar, R.; Srivastava, H. C. *J. Appl. Polym. Sci.* **1987**, *33*, 455.

Decher, G.; Hong, J. D.; Schmitt, J. *Thin Solid Films* **1992**, *210/211*, 831.

Desai, N. P.; Hubbell, J. A. *Macromolecules* **1992**, *25*, 226.

Dias, A. J.; McCarthy, T. J. *Macromolecules*, **1984**, *17*, 2529.

Dias, A. J.; McCarthy, T. J. *Macromolecules*, **1985**, *18*, 1826.

Dias, A. J.; McCarthy, T. J. *Macromolecules*, **1985**, *20*, 2068.

Fagan, P. J.; Krusic, P. J.; McEwen, C. N.; Lazar, J.; Parker, D. H.; Herron, N.; Wasserman, E. *Science* **1993**, *262*, 404.

Feast, W. J.; Munro, H. S.; Richards, R. W. "Polymer Surfaces and Interfaces"; John Wiley and Sons: New York, 1993.

Ferreira, M; Cheung, J. H.; Rubner, M. F. *Thin Solid Film* **1994**, *244*, 806.

Ferreira, M.; Rubner, M. F. *Macromolecules* **1995**, *28*, 7107.

Fleer, G. J.; Lyklema, J. In *Adsorption from Solution at the Solid/Liquid Interface*; Parfitt, G. D., Rochester, C. H., Eds.; Academic Press: New York/London, 1983; p 153.

Fleming, R. M.; Hessen, B.; Siegrist, T.; Kortan, A. R.; March, P.; Rycko, R.; Dabbagh, G.; Haddon, R. C. In *Fullerenes: Synthesis, Properties, and Chemistry of Large Carbon Clusters*; Hammond, G. S.; Kuck, V. J., eds.; Am. Chem. Soc. Sym. Ser. 481, 1992; p 25.

Fou, A. C.; Rubner, M. F. *Macromolecules* **1995**, *28*, 7115.

Franchina, N. L.; McCarthy, T. J. *Macromolecules*, **1991**, *24*, 3045.

Franchina, N. L. *Ph.D. Dissertation*, Univeristy of Massachuestts at Amherst, 1993.

Gagnon, D. R.; McCarthy, T. J. *J. Appl. Polym. Sci.* **1984**, *29*, 4335.

Gaines, G. L., Jr. *Macromolecules* **1979**, *12*, 1011.

Gaines, G. L., Jr.; Bender, G. W. *Macromolecules* **1972**, *5*, 82.

Gann, R. G. In *Kirk-Othmer Encyclopedia of Chemical Technology*, 4th ed.;John Wiley and Sons: New York, 1993; Vol. 10; p 930.

Green, P. F.; Christensen, T. M.; Russell, T. P. *Macromolecules* **1991**, *24*, 252.

Green, P. F.; Christensen, T. M.; Russell, T. P.; Jérôme, R. *Macromolecules* **1989**, *22*, 2189.

Green, P. F.; Russell, T. P. *Macromolecules* **1991**, *24*, 2931.

Hall, S.M.; Andrade, J.D.; Ma, S.M.; King, R.N. *J. Electron Spectroscopy* **1979**, *17*, 181.

Hammond, P. T.; Whitesides, G. M. *Macromolecules* **1995**, *28*, 7569.

Hariharan, A.; Kumar, S. K.; Russell, T. P. *Macromolecules* **1990**, *23*, 3584.

Hariharan, A.; Kumar, S. K.; Russell, T. P. *Macromolecules* **1991**, *24*, 4909.

Harrick, N. J. Internal Reflection Spectroscopy, Wiley Interscience: New York, 1967.

Holloway, J. H. et al. *J. Chem. Soc., Chem. Commun.* **1991**, 966.

Iyengar, D. R.; Brennan, J. V.; McCarthy, T. J. *Macromolecules*, **1991**, *24*, 5886.

Jarvis, N. L.; Fox, R. B.; Zisman, W. A. *Adv. Chem. Ser.* **1964**, *43*, 317.

Keller, S. W.; Kim, H. N.; Mallouk, T. E. *J. Am. Chem. Soc.* **1994**, *116*, 8817.

Kleinfeld, E. R.; Ferguson, G. S. *Science* **1994**, *265*, 370.

Koberstein, J. T. In *Encyclopedia of Polymer Science and Engineering*, 2nd ed.; Mark, H. F.; Bikales, N. M.; Overberger, C. G.; Menges, G.; Kroschwitz, J. I., eds.; John Wiley & Sons: New York, 1989; Vol. 8, p237.

Kolb, B. U.; Patton, P. A.; McCarthy, T. J. *Macromolecules*, **1990**, *23*, 366.

Krätschmer, W.; Lamb, L. D.; Fostiropoulos, K.; Huffman, D. R. *Nature* **1990**, *347*, 354.

Kroto, H. W.; Heath, J. R.; O'Brien, S. C; Curl, R. F.; Smalley, R. E. *Nature* **1985**, *318*, 162.

Kumar, S. K.; Vacatello, M.; Yoon, D. Y. *Macromolecules* **1990**, *23*, 2189.

Kumar, S. K.; Russell, T. P. *Macromolecules* **1991**, *24*, 3816.

Lee, K.-W.; McCarthy, T. J. *Macromolecules*, **1988**, *21*, 2318.

Lee, K.-W.; McCarthy, T. J. *Macromolecules*, **1988**, *21*, 3353.

LeGrand, D. G.; Gaines, G. L., Jr. *Polym. Prepr. (Am. Chem. Soc., Div. Polym. Chem.)* **1970**, *11*, 442.

Leväsalmi, J.-M.; McCarthy, T. J. *Polym. Prepr. (Am. Chem. Soc. Div. Polym. Chem.)* **1996**, *37(1)*, 457.

Leväsalmi, J.-M.; McCarthy, T. J. *Macromolecules*, **1997**, *30*, 1752.

Lvov, Y.; Decher, G.; Mohwald, H. *Langmuir* **1993**, *9*, 481.

Lvov, Y.; Decher, G.; Sukhorukov, G. *Macromolecules*, **1993**, *26*, 5396.

Lvov, Y.; Haas, H.; Decher, G.; Möhwald, H. *J. Phys. Chem.* **1993**, *97*, 12835.

Lvov, Y.; Haas, H.; Decher, G.; Möhwald, H. *Langmuir,*. **1994**, *10*, 4232.

Mallouk, T. E et al. *J. Am. Chem. Soc.* **1993**, *115*, 11855.

Mao, G.; Tsao, Y.; Tirrell, M.; Davis, H. T. *Langmuir* **1993**, 3461.

Marchand-Brynaert, J.; Deldime, M; Dupont, I.; Dewez, J.-L.; Schneider, Y.-J. *J. Coll. Interfac. Sci.* **1995**, *173*, 236.

Marra, J.; van der Schee, H. A.; Fleer, G. J.; Lyklema, J. In *Adsorption from Solution*; Ottewill, R. H., Rochester, C. H., Eds.; Academic Press: New York, 1983;

Ohsawa, Y.; Saji, T. *J. Chem. Soc., Chem. Commun.* **1992**, 781.

Olah, G. A. et al. *J. Am. Chem. Soc.* **1991**, *113*, 9385.

O'Malley, J. J.; Thomas, H. R.; Lee, G. M. *Macromolecules* **1979**, *12*, 996.

Papenhuijzen, J.; Fleer, G. J.; Bijsterbosch, B. H. *J. Colloid Interface Sci.* **1985**, *104*, 530.

Papenhuijzen, J.; van der Schee, H. A.; Fleer, G. J. *J. Colloid Interface Sci.* **1985**, *104*, 540.

Phuvanartrukus, V.; McCarthy, T. J. Manuscript in Preparation.

Robinson, R.A. In *CRC Handbook of Chemistry and Physics*, 67th ed.; Weast, R.C., Astle, M.L., Beyer, W.H. Eds; CRC Press, Inc: Boca Raton, Florida, 1986; D144-D145.

Ruoff, R. S.; Tse, D. S.; Malhorta, R.; Lorents, D. C. *J. Phys. Chem.* **1993**, *97*, 3379.

Russell, T. P. Personal communication.

Schmitt, R. L.; Gardella, J. A., Jr.; Magill, J. H.; Salvati, L., Jr.; Chin, R.L. *Macromolecules* **1985**, *18*, 2675.

Schmitt, R. L.; Gardella, J. A., Jr.; Salvati, L., Jr. *Macromolecules* **1986**, *19*, 648.

Schmitt, R. L.; Gardella, J. A., Jr.; Salvati, L., Jr. *Macromolecules* **1989**, *22*, 4489.

Shoichet, M. S.; McCarthy, T. J. *Macromolecules*, **1991**, *24*, 1441.

Shoichet, M. S.; McCarthy, T. J. *Macromolecules*, **1991**, *24*, 982.

Shull, K. R.; Kramer, E. J.; Bates, F. S.; Rosedale, J. H. *Macromolecules* **1991**, *24*, 1383.

Shull, K. R.; Kramer, E. J.; Hadziioanou, G.; Tang, W. *Macromolecules* **1990**, *23*, 4780.

Shull, K. R.; Winey, K. I.; Thomas, E. L.; Kramer, E. J. *Macromolecules* **1991**, *24*, 2748.

Sivaraman, N.; Dhamodaran, R.; Kaliappan, I.; Srinivasan, T. G.; Rao, P. R. V.; Mathews, C. K. *J. Org. Chem.* **1992**, *57*, 6077.

Solbrig, C. M.; Obendorf, S. K. *J. Appl. Polym. Sci.: Appl. Polym. Sym.*, **1991**, *47*, 437.

Solbrig, C. M. *Dissertation Abstracts International* **1991**, *51, 12*, 5899-B.

Srivens, W. A.; Tour, J. M. *J. Chem. Soc., Chem. Commun.* **1993**, 1207.

Stockton, W. B.; Rubner, M. F. *Polym. Prepr. (Am. Chem. Soc.: Div. Polym. Chem.)* **1994**, *35*, 319.

Strobel, M.; Lyons, C. S.; Strobel, J. M.; Kapaun, R. S. *J. Adhes. Sci. Technol.* **1992**, *6*, 429.

Swalen, J. D.; Allara, D. L.; Andrade, J. D.; Chandross, E. A.; Garoff, A.; Israelachvili, J.; McCarthy, T. J.; Murray, R.; Pease, R. F.; Rabolt, J. F.; Wynne, K. J.; Yu, H. *Langmuir* **1987**, *3*, 932.

Taylor, R.; Walton, D. R. M. *Nature* **1993**, *363*, 685.

Tebbe, F. N. et al. *J. Am. Chem. Soc.* **1991**, *113*, 9900.

Tebbe, F. N. et al. *Science* **1992**, *256*, 822.

Theodorou, D. N. *Macromolecules* **1988**, *21*, 1391.

Theodorou, D. N. *Macromolecules* **1988**, *21*, 1400.

Theodorou, D. N. *Macromolecules* **1988**, *21*, 1411.

Theodorou, D. N. *Macromolecules* **1988**, *21*, 1422.

Thomas, H. R.; O'Malley, J. J. *Macromolecules* **1979**, *12*, 323.

Thomas, H. R.; O'Malley, J. J. *Macromolecules* **1981**, *14*, 1316.

Torstensson, M.; Ranby, B.; Hult, A. *Macromolecules* **1990**, *23*, 126.

van der Schee, H. A.; Lyklema, J. *J. Phys. Chem.* **1984**, *88*, 6661.

Viviano, K. *Ph.D. Dissertation*, University of Massachusetts at Amherst, 1994.

Wang, J.; Feng, D.; Wang, H.; Rembold, M.; Fritz, T. *J. Appl. Polym. Sci.* **1993**, *50*, 585.

Ward, W.; McCarthy, T. J. In *Encyclopedia of Polymer Science and Engineering*, 2nd ed; Mark, H. F., Bikales, N. M.,Overberger, C. G., Menges, G.,Kroschwitz, J. I., Eds.; John Wiley and Sons: New York, 1989; suppl. vol., p 674.

Werner, E.; Janocha, S.; Hopper, M. J.; Mackenzie, K. J. In *Encyclopedia of Polymer Science and Engineering*, 2nd ed; Mark, H. F., Bikales, N. M., Overberger, C. G., Menges, G., Kroschwitz, J. I., Eds.; John Wiley and Sons: New York, 1989; Vol 12, p 193.

Xie, Q.; Perez-Cordero, E.; Echegoyen, L. *J. Am. Chem. Soc.* **1992**, *114*, 3978.

Xu, G.-F.; Bergbreiter, D. E.; Letton, A. *Chem. Mater.* **1992**, *4*, 1240.

Xue, J.; Wilkie, C. A. *J. Polym. Sci.: Part A: Polym. Chem.* **1995**, *33*, 1019

Yao, Z. P.; Rånby, B. *J. Appl. Polym. Sci.* **1990**, *41*, 1459.

Zhou, F.; Jehoulet, C.; Bard, A. J. *J. Am. Chem. Soc.* **1992**, *114*, 11004.

Zisman, W. A. *Adv. Chem. Ser.* **1964**, *43*, 1.